DNA-based coatings in implantology

utilization of the structural properties of the DNA-molecule to modulate cell and tissue response

Jeroen van den Beucken

Colofon

Thesis Raboud University Nijmegen Medical Center, with summary in Dutch.

DNA-based coatings in implantology: utilization of the structural properties of the DNA-molecule to modulate cell and tissue response.
Jeroen Johannes Jacobus Paulus van den Beucken, Nijmegen, 2007.

ISBN 978-90-9021550-1

Cover design Anneke Peeters
Printing Print Partners Ipskamp BV, Enschede

DNA-based coatings in implantology

utilization of the structural properties of the DNA-molecule to modulate cell and tissue response

Een wetenschappelijke proeve op het gebied van de Medische Wetenschappen

Proefschrift

ter verkrijging van de graad van doctor
aan de Radboud Universiteit Nijmegen
op gezag van Rector Magnificus, prof. dr. C.W.P.M. Blom,
volgens besluit van het College van Decanen
in het openbaar te verdedigen op donderdag 15 maart 2007,
om 15.30 uur precies

door

Jeroen Johannes Jacobus Paulus van den Beucken

geboren op 21 maart 1975
te Kessel-Eik (L)

Promotores	Prof. dr. J.A. Jansen Prof. dr. R.J.M. Nolte
Co-promotores	Dr. X.F. Walboomers Dr. N.A.J.M. Sommerdijk
Manuscriptcommissie	Prof. dr. R.P. Bleichrodt Prof. dr. V. Everts Dr. J.W. von den Hoff

Paranimfen	S.M.J.W. van den Beucken (Saskia) T.H.A. Bon (Yvonne)

DNA-based coatings in implantology

utilization of the structural properties of the DNA-molecule to modulate cell and tissue response

An academic essay in the field of Medical Sciences

Doctoral thesis

to obtain the degree of doctor
from Radboud University Nijmegen
on the authority of the Rector Magnificus, prof. dr. C.W.P.M. Blom,
according to the decision of the Council of Deans
to be defended in public on Thursday March 15, 2007
at precisely 15.30 hours

by

Jeroen Johannes Jacobus Paulus van den Beucken

born in Kessel-Eik (L)
on March 21, 1975

Supervisors	Prof. dr. J.A. Jansen Prof. dr. R.J.M. Nolte
Co-supervisors	Dr. X.F. Walboomers Dr. N.A.J.M. Sommerdijk
Doctoral thesis committee	Prof. dr. R.P. Bleichrodt Prof. dr. V. Everts Dr. J.W. von den Hoff
Ushers	Ms. S.M.J.W. van den Beucken (Saskia) Ms. T.H.A. Bon (Yvonne)

CONTENTS

1

GENERAL INTRODUCTION

partly adapted from

JJJP van den Beucken, XF Walboomers, JA Jansen. Implants and prostheses, in Biomedical Nanotechnology (NH Malsch, ed.), CRC Press, Taylor & Francis Group, Boca Raton, US, 2005

I INTRODUCTION

The importance of prostheses and implants in medicine is growing. Due to increasing life expectancy, mankind will need a growing number of such synthetic devices to overcome the problems associated with deteriorating or failing body parts. Examples of implants are orthopedic joint prostheses, cardiovascular devices, dental implants, and others. An implant does not have to be located completely inside the body; skin-penetrating devices such as catheters for the infusion of fluids must be regarded as implants as well (see Table 1.1). Furthermore, the expected increase in the use of implants arises not only from medical perspectives, which make certain devices necessary. Also, the flourishing prosperity of the past few decades has meant that the use of implants for aesthetic reasons has become substantial. Implants are made of biomaterials that have a common property: biocompatibility. Although biocompatibility is a difficult term to define, it is strongly related to the success of an implanted device in fulfilling its intended function [1]. This implies that a biomaterial used for the manufacturing of a prosthesis or implant and subsequently classified as biocompatible cannot necessarily be used for the manufacturing of implants with different functions. For instance, biomaterials with properties that resist the adhesion of biomolecules and cells may be classified biocompatible when used for the production of cardiovascular devices. However, the classification may not be legitimate for the use of such a biomaterial to manufacture artificial joints.

TABLE 1.1: APPLICATIONS OF SYNTHETIC AND MODIFIED NATURAL MATERIALS IN REPARATIVE MEDICINE

Material	Application	Tissue response
Titanium (alloys)	Joint prostheses, oral implants, fixation plates, pacemakers, heart valves	Inert
Calcium phosphate ceramic(s)	Joint prostheses, oral implants, bone replacement, middle ear replacement	Bioactive
Alumina	Joint prostheses, oral implants	Inert
Carbon	Heart valves	Inert
Polytetrafluoroethylene (PTFE)	Joint prostheses, tendon and ligament replacement, artificial blood vessels, heart valves	Inert
Poly(methylmethacrylate) (PMMA)	Eye lenses, bone cement	Tolerant
Poly(dimethylsiloxane) (PDMS)	Brest prostheses, catheters, facial reconstruction, tympanic tubes	Unknown
Poly)urethane) (PU)	Breast prostheses, artificial blood vessels, skin replacements	Inert
Poly(lactic acid) (PLA)	Bone fixation plates, bone screws	Inert
Poly(glycolic acid) (PGA)	Sutures, tissue membranes	Inert

Unfortunately, the classification of a biomaterial device as biocompatible does not necessarily imply its acceptance by its host. Most commonly, synthetic devices are recognized by their hosts as non-natural and regarded as intrusions of foreign bodies [2]. For that reason, the possibility exists that although a biomaterial device is classified biocompatible, the coexistence of minor side effects of the implantation cannot be excluded. Although the potential side effects may not be detrimental to the functionality of the implanted device, these still can have consequences that are not desirable. Generally, the placement (via surgical procedures) of, and subsequent habituation (host reaction) to a synthetic device can be categorized as the establishment of a symbiosis of living and non-living materials. This symbiosis is characterized by contact of biological (e.g. biomolecules) with non-biological compounds (e.g. molecules that constitute the biomaterial device). For a proper comprehension of the interactions between implants and their biological surroundings, and possibilities to modulate these responses, these issues are addressed in sections II and III, respectively. In section IV, the rationale of using deoxyribonucleic acid (DNA) as a biomaterial coating is described, as well as the methods to fabricate DNA-based coatings.

II BIOLOGICAL PROCESSES

In this section, biological processes that arise at the implant surface or in the direct vicinity of an inserted implant are described. These processes include wound healing, the role of macrophages, biomaterial interface processes, and the foreign body reaction.

A. Wound Healing Processes

The introduction of an implant into a living organism is commonly associated with surgical intervention. As noted earlier, an implant can be regarded as the intrusion of a foreign body that incontrovertibly initiates a response of the body toward the intruder through specific reactions arising from both the introduced material and the tissue damage or injury caused by the surgical procedure. In general, the response consists of wound healing processes that have the ultimate aim of healing the affected tissues, preferably without permanent damage. While this phenomenon, also known as '*restitutio ad integrum*', is feasible for human and animal fetuses, wound healing produces scar formation in adult humans and higher vertebrates [3]. Evidently, fibroproliferative responses rather than tissue regeneration control the repair of soft tissues. At this point, a striking difference exists between healing processes in soft tissues such as skin and hard tissues such as bone. While soft tissue healing is reparative, regenerative healing after wounding is feasible in hard tissues [4]. This means that the formation of scar tissue is absent in healing of hard tissues. Although its appearance is radiographically different, healed hard tissue will eventually return to its pre-injury state [5] and possess the same or even improved characteristics compared with the original tissue. The biology behind the processes of soft and hard tissue healing has been studied extensively and several excellent reviews on this subject have been published [4;6-13]. Although not all mysteries have been revealed yet, it is already evident that the healing processes involve a tight and regulated collaboration of specific cell types and their signaling products [14;15]. The wound healing processes preceded by thrombus formation are roughly divided into three overlapping phases: (1) Inflammation, (2) repair, and (3) tissue remodeling [4;6;7].

1. Thrombus Formation

Prior to the initiation of the healing processes, fluids containing blood constituents surround the newly implanted biomaterial. These fluids originate from the disruption and increased permeability of blood vessels and the subsequent extravasation of blood constituents, all of which are consequences of tissue injury. Through changes in the environment, several components of the blood including platelets and the surrounding or even adjacent tissues become activated, thereby initiating the blood coagulation cascade [10]. The activation of platelets results in increasing adhesiveness. This enables platelets to aggregate and form a plug to close perforations of damaged vessels and thus limit blood loss. The coagulation cascade also involves polymerization of fibrin. Activated platelets and strands of polymerized fibrin together form a fibrous clot that serves as a matrix for subsequent migration of a variety of cells into the area of injury. The recruitment of cells to the area of injury is at least partially orchestrated through the release of certain biologically active substances by platelets [16] and endothelial cells [17]. The migratory cells include those that are important to the inflammatory response, the formation of new tissue, and the tissue remodeling processes.

2. Inflammatory Phase

Inflammation is a physiological response of tissue resulting from detrimental physical, chemical, or immunological stimuli or from infection [18]. The inflammatory response is initiated as a reaction to the release of vasodilators, chemo-attractants, and other mediators, including platelet-derived growth factor (PDGF) and various isoforms of the tumor growth factor-beta (TGF-β) family by platelets [19] and activation of the complement cascade within the coagulating fluid surrounding the implanted biomaterial [7]. The release of these substances is responsible for the recruitment of inflammatory and other cells (chemotaxis), the development of new blood vessels (angiogenesis), and overall cell regulation at the site of injury. The response consists of non-specific defense mechanisms carried out by

cells and non-cellular components of the circulating blood (granulocytes, monocytes, and the complement system) as well as resident inflammatory cells (macrophages and mast cells) that collectively try to eliminate intruders. If necessary, specific immune responses such as the production of antibodies by B-lymphocytes and/or the activation of cytotoxic T lymphocytes can be initiated.

3. Reparative Phase

The formation of new tissue requires the activation and/or proliferation of distinct cell types, resulting in the replacement of lost or damaged tissue. In soft tissue healing, extremely important cells related to new tissue formation are fibroblasts and endothelial cells that are capable of new extracellular matrix formation and angiogenesis, respectively. The provisional extracellular matrix is important as a scaffold for the migration of cells into the damaged area. Additionally, the extracellular matrix and its components contain signals for the differentiation and stimulation of cells, mainly via receptor–ligand interactions. Through the development of new blood vessels, nutrients and oxygen become available for proliferating cells that replace the tissue at the damaged area. In hard tissue healing, the process of ossification (bone formation) is important and two types assure new bone formation: intra-membranous and endochondral ossification [4]. Intra-membranous ossification is carried out by osteoprogenitor cells present in the cambium layer of the periosteum. Endochondral ossification occurs at and overlies the defect site and undifferentiated mesenchymal cells attracted from tissues surrounding the defect (e.g., soft tissues and periosteum) become committed cartilage-producing cells [13] under influence of local production and release of mediators, including growth factors. The mineralization of the cartilage tissue leads to bone formation.

4. Tissue Remodeling

Tissue remodeling involves the transition of newly formed, immature tissue into mature tissue. In contradistinction to the relatively short duration of both the inflammatory and reparative phases, the remodeling phase may last for several years. The general process of soft tissue remodeling involves rapid synthesis and degradation of connective tissue proteins [20]. The degradation of these extracellular matrix (ECM) proteins is accomplished through the actions of matrix metalloproteinases (MMPs) [21]. The common outcome of soft tissue remodeling is scar formation, which results mainly from an imbalance between the stimulation of collagen synthesis and degradation of extracellular collagen. Remodeling in hard tissues involves bone resorption by osteoclasts, followed by the synthesis of new bone matrix and its mineralization by osteoblasts. The remodeling process in hard tissues is subject to mechanical forces acting upon it (Wolff's law [22]). In contrast with soft tissue remodeling, hard tissue remodeling is devoid of scarring. Furthermore, healed hard tissue is able to resume its original configuration.

B. Macrophages

Several cell types are involved in the biological processes that occur after the implantation of a biomaterial. The interplay among these cells is extremely important because inadequate cellular responses could directly or indirectly impede the functionality of the implanted device. Cells respond to stimuli mostly via receptors on their surfaces. Via these receptors, cells can recognize a large variety of ligands including soluble mediators secreted by other cells (cytokines), molecules present on the surfaces of adjacent cells, and distinct patterns in molecules of ECM proteins. Due to their early appearance at an implantation site, their longevity, and the large number of cytokines they can produce and secrete, macrophages are generally considered the most important cell type in the vicinity of a newly-implanted device [23]. Macrophages perform multiple functions at a site of implantation ranging from phagocytosis of cell debris and potential pathogens via initiation of an inflammatory reaction to orchestration of the processes necessary to heal the damaged tissue resulting from the surgical procedure.

C. Biomaterial Interface Processes

Although an implant is subject to cellular biological processes upon introduction, as described above, the initial contact of implant and host relies on non-cellular interactions. A newly introduced implant is surrounded by an aqueous liquid. The water molecules in the direct vicinity of an implant can substantially alter the appearance of the biomaterial surface for the biological environment [24]. The abundance of water molecules within this liquid means that water is the primary molecule involved in the first series of interactions of a biomaterial surface interface with its in vivo surroundings. An important parameter is the free energy of a biomaterial surface reflected by its water wettability. Biomaterial surfaces are often categorized as hydrophobic or hydrophilic. A related parameter of biomaterial surfaces is cell adhesion. Although some authors assert the existence of a correlation between surface free energy and cell adhesion [25;26], others impugn this correlation [27] or even postulate the inverse [28]. The water molecules in the direct vicinity of the biomaterial surface will form a water monolayer or bi-layer in which the arrangement of the water molecules depends on the surface properties at the atomic scale and completely differs from that of liquid water [24]. Subsequent to interface interactions with water molecules, a biomaterial surface will first encounter ions and then the proteins present within the surrounding liquid. In the monolayer or bi-layer of water molecules, natural ions (e.g., Na^+ and Cl^-) are incorporated as hydrated ions [29]. The surface properties of the biomaterial determine the type, amount, and conformational state of the adsorbed proteins [30;31]. Thus, the spectrum of adsorbed proteins will not necessarily reflect the amounts and ratios of the proteins within the surrounding liquid [32;33]. Additionally, denaturation of the adsorbed proteins may occur. As a result, biologically important sites may become inaccessible or nonfunctional, limiting interactions with counter-receptors present on cellular membranes. Finally, living cells will become involved. The presence of a wide variety of membrane-bound receptors on the surfaces of cells enables them to adhere to adsorbed proteins on the biomaterial surface. Because the interaction of cells with the biomaterial surface does not rely on direct contact between cells and biomaterial, but merely on an indirect interaction mediated by adsorbed proteins, it has been suggested that the biomaterial is not what causes unwanted responses [34]. The non-specific layer of proteins adsorbed on the biomaterial surface immediately after implantation is recognized by the host as a foreign or unnatural material. This assumption seems plausible because such an adsorbed mixture of proteins with random orientations and conformational states presents a divergence from natural, intentionally arranged protein layers.

D. Foreign Body Reaction

The cumulative effects of all separate contributive processes that occur at the biomaterial interface results in one of the following outcomes of implantation: (1) integration, (2) extrusion, (3) resorption, or (4) encapsulation. Although integration of the biomaterial device is the most favorable outcome, the number of cases in which true bio-integration is achieved is limited [35]. Most frequently, true bio-integration occurs after implantation of compatible biomaterials such as titanium coated with hydroxyapatite (HA) into bone tissue [36;37]. Implantation of biomaterials into soft tissues usually results in one of the other three outcomes. Extrusion occurs when an implanted device is in direct contact with epithelial tissue. The epithelium will form a pocket continuous with the adjacent epithelial membrane that subsequently dissipates the implant. In the case of external epithelium, the implant will be externalized from the host. Resorption of the implant can occur when an implant is made of degradable material. After complete resorption, only a collapsed scar will remain at the implantation site. In most cases, implanted biomaterials in soft tissues become encapsulated by a process known as the foreign body reaction [2;38] (Figure 1) The capsule commonly consists of a relatively hypo-cellular membrane with a high collagen content [39]. Adjacent to this collageneous membrane, a layer of myofibroblasts is occasionally observed. Furthermore, foreign body giant cells (FBGCs; i.e. fused macrophages) are frequently observed in the space between implant and capsule [40;41]. In general, the organization of cells and matrix surrounding an implant is built up in such a way that a barrier between the foreign material and the body is created and this structure more or less isolates the implant from the body. The capsule,

including FBGCs, surrounding the implant may persist for the lifetime of the implant. However, it is not yet clear whether FBGCs present at the biomaterial surface remain activated during the lifetime of the implant or become quiescent [38]. Since encapsulated implants can perform their functions for many years, the isolation of an implant in a collageneous capsule is not necessarily an unwanted phenomenon. It may even help the body live in symbiosis with a synthetic device, although the establishment of genuine symbiosis in this respect may be arguable. Unfortunately, the presence of myofibroblasts within the capsule may lead to contraction and thus cause pain and/or implant failure. Furthermore, the formation of a capsule, either or not associated with wearing of the biomaterial, may result in loosening.

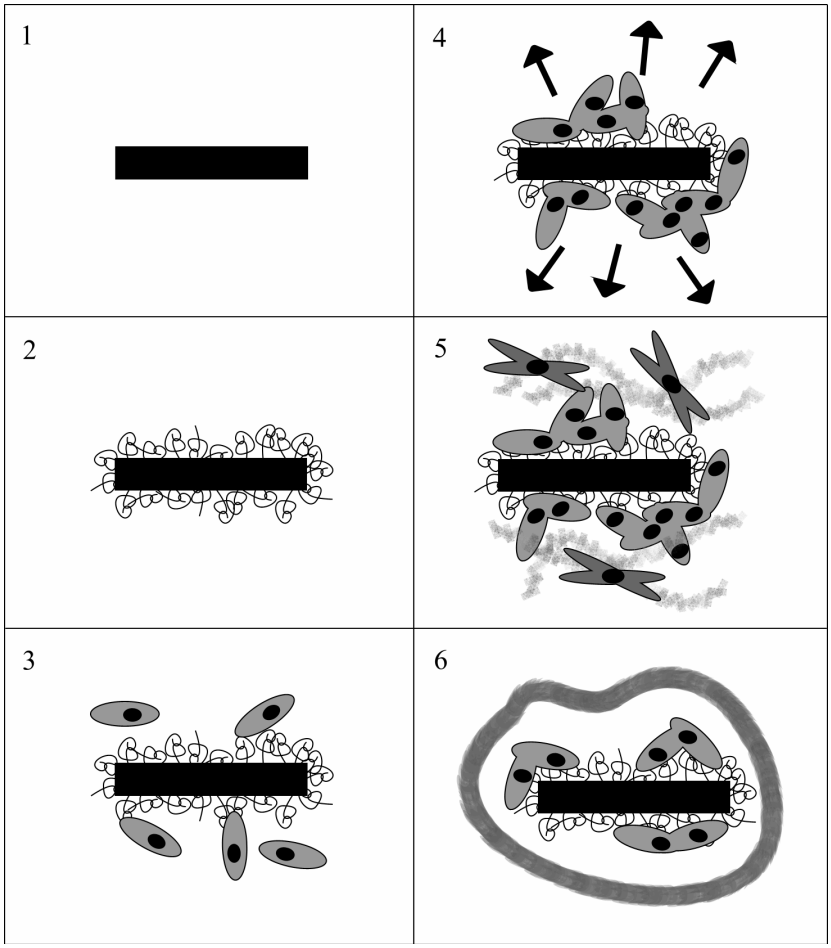

Figure 1: Foreign body reaction. The introduction of an implant (1) into a recipient leads to the adsorption of proteins in all possible configurations on the surface (2). Subsequently, cells (including macrophages) will attach to the implant surface via cell surface receptors that recognize corresponding ligands in the adsorbed protein layer (3). Attached cells secrete a wide variety of signal molecules that influence the behavior of perceptive cells (4) that become activated and start to produce extracellular matrix (5). Finally, the implant becomes enclosed in a fibrous capsule that isolates the implant from the body (6).

III BIOMATERIALS

A. Introduction

Biomaterials are substances used for the production of devices that interact with biological systems, which are known as medical devices. This definition inherently suggests that biomaterials can be widely used. For example, biomaterials are used for cell cultures in laboratories, for the production of diagnostic devices, for extracorporeal apparatus (heart–lung machines), and many other applications. The use of biomaterials for the production of implants is the focus of this section.

The use of biomaterials in medicine is not a novel concept. As early as 2000 years ago, dental implants made of gold or iron were used [42]. However, the practical use of implants in that era is not comparable to their present use. The increasing demands for safe and reliable implants have resulted in the evolution of biomaterials science as a distinct discipline. In addition to the somewhat old-fashioned biomaterials such as stainless steel, a high number of novel, mostly polymeric, biomaterials are now available and can be categorized as depicted in Figure 2.

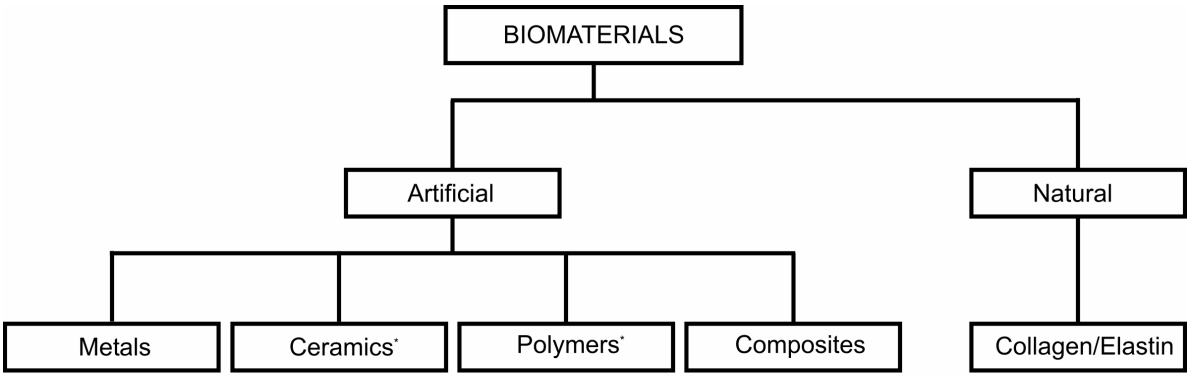

Figure 2: Classification of biomaterials

B. Properties of Biomaterials

In order to function appropriately, biomaterials must possess properties that allow them to be used successfully for their intended applications. In view of this, it is logical to distinguish bulk properties from surface properties. Bulk properties (together with the design) determine the (mechanical) strength of an implant, whereas the surface properties are important in view of the eventual interactions of an implant with biological systems.

1. Bulk Properties

Bulk properties of materials are determined by the organization of the atoms of which the materials are built and the forces by which the atoms are kept together (inter-atomic forces). Several types of inter-atomic forces are known, including ionic bonding, covalent bonding, and metallic bonding [43]. The mechanical properties of a biomaterial must be adjusted to its intended function; otherwise the implant is likely to fail. For example, if a device intended for the fixation of a bone fracture lacks the required strength, it may break, making the device unsuitable for this function. Hence, the intrinsic properties of biomaterials may be appropriate for a certain application, but play a role in the failure of an implant made from the same material and used for another application. Regarding specific requirements from a mechanical view, three intrinsic properties of materials are especially important: elastic modulus, yield stress, and ultimate stress [44]. Together, these three parameters determine the stiffness, deformability, and strength of a material. Another important bulk property of a biomaterial is fatigue — the "process by which structures fail as a result of cyclic stresses that may be much less than the ultimate tensile stress [43]." Such cyclic stresses are common at many locations in the human body, such as in a pumping heart (artificial heart valves), in the mouth (tooth prostheses), and in joints (artificial hips/knees).

2. Surface Properties

In addition to intrinsic (bulk) properties of biomaterials, surface properties are also important to the success of an implant. Since the interaction of a synthetic device and biological system takes place at the biomaterial–tissue interface, it is evident that the surface properties of a biomaterial are pivotal for the regulation of implant integration. Several factors determine the surface characteristics of a material, including composition, roughness, release of ions, charge, and energy [45]. Obviously, the interaction of biological constituents with the surface of a biomaterial device must not cause any detrimental effects to the surrounding viable cells, tissues, and organs. For that reason, the surface molecules of a biomaterial should not be toxic, carcinogenic, pyrogenic, cytotoxic, or antigenic to living cells in any way. If materials containing one or more of these characteristics are excluded, the reactions of body tissues to an implant surface still depend on the surface properties of the biomaterial in question.

One commonly assessed property for biomaterial surface characterization is surface energy. As will be discussed later, this parameter may be an important factor in the establishment of cell adhesion to biomaterial surfaces. However, other factors that are probably important in monitoring the adhesion of cells to biomaterial surfaces are cell type and presence of adhesive proteins [46]. Interaction of biological systems with biomaterial surfaces can be desirable to enhance the integration of the biomaterial in the body. In contrast, also the generation of non-interacting surfaces can be an aim in designing implants. In synthetic vascular grafts, for example, the deposition of biological material (bio-fouling or bio-adhesion) is undesirable because it may lead to occlusion of blood vessels. Furthermore, control over bio-adhesion may eventually result in the generation of biomaterial surfaces that encourage adhesion of host cells but discourage adhesion of infectious bacteria — a common cause of implant failure [47;48].
Processes of a biological nature can affect the integrity of biomaterials. Upon implantation, a biomaterial is subject to interactions with the constituents of the biological environment and may be subject to biodegradation, a process in which components of the biological environment (or host) attack the biomaterial. Metals are inherently susceptible to corrosion — an electrochemical process in which oxidative and reductive reactions take place [49]. Due to such reactions, the integrity of a metal may be affected by the formation of metal ions from the solid metal, resulting in degradation. For ceramics, the extent to which the biological environment is capable of degradation is dependent on the chemical structure of the biomaterial. Increased knowledge in biomaterial science has resulted in the production of both polymeric and ceramic biomaterials whose degradation rates can be controlled. This has presented opportunities to generate and use biomaterial devices that in time can be replaced by native tissues.

C. Modifications of the biomaterial surface

From the previous descriptions of interfacial biological processes and biomaterial properties, it is evident that the placement of an implant into a living organism causes specific reactions of the biological environment. Since the biological environment recognizes the implant surface and not the bulk material, attempts to modulate biological responses have been focused at biomaterial surface modifications. The ultimate aim of biomaterial surface modifications is to gain control over biological responses against biomaterials, and hence increase implant functionality, performance, and longevity. Roughly, biomaterial surface modifications can be divided in (i) topographical modifications, (ii) biomaterial coatings, and (iii) incorporation of biologically active compounds at the biomaterial surface.

(i) Surface topography

The topography of biomaterial surfaces has been a major topic in biomaterials science in the past decade, and can be divided in texture (regular features) and roughness (random features). Surface topography can be of great importance with respect to area enlargement. An increase in surface area may provide greater potential for tissue integration (mechanical interlocking). Excellent reviews on this topic evidence a general consensus that topographical textures indeed influence cell behavior [50-54]. An enormous diversity of textural cues was used: grooves, pits, ridges, cliffs, tunnels, steps, waves wells, tubes nodes pillars, pores, spheres, and cylinders. Researchers used many different cell types in studies to examine the effects of microscale textured topography on the behavior of primary isolated cells or immortalized cell lines, including fibroblasts, macrophages, epithelial cells, leukocytes, neuronal cells, endothelial cells, and osteoblasts.
Unfortunately, the precise biological effects of microscale topographies remain unclear – various research groups have obtained contradictory results. Parker et al. [55] found no favorable effects of surface texturing on capsule formation around subcutaneous implants, but *in vivo* studies by others indicated that grooved implant surfaces produced beneficial effects on tissues surrounding the implant [52]. In the latter studies, grooved textures appeared to encourage tissue organization and showed a reduction in fibrous capsule formation as compared to smooth implant surfaces.

Although the technology for creating textured topographical cues with nanoscale dimensions on biomaterial surfaces is a novelty, several studies have demonstrated the substantial effect these cues can exert on cell behavior. The effect on cell behavior of grooves with nanoscale dimensions has been a subject of interest in many *in vitro* studies [56-59]. Regarding the effects of grooves with nanoscale dimensions, the findings generally indicate that cells become oriented and elongate along the surface groves. Furthermore, the activity of cells on nanotopographically modified substrates is increased compared to activity on smooth control substrates. This is demonstrated by higher proliferation rates and enhanced spreading of fibroblasts [60], increased phagocytic activity of macrophages [59], and a notable up-regulation of gene expression related to cell signaling, proliferation, and the production of cytoskeleton and ECM protein [61].

(ii) Biomaterial coatings

While synthetic surfaces lack specific signals cells can recognize, naturally-derived materials may possess numerous signals involved in a wide variety of biological processes. In view of this characteristic, modulation of a biomaterial surface with naturally occurring components of ECM proteins containing such signals has become a common modality. The effect of the immobilization of specific peptide sequences, especially the sequence arginine-glycine-aspartic acid (abbreviated as RGD), onto the surfaces of materials has been studied for biomaterials intended for implantation in both soft and hard tissues. Excellent reviews dealing with this topic [62;63] outline proven applications and promising potential for the future.

TABLE 1.2: APPLICATION OF IMMOBILIZED PEPTIDES ONTO BIOMATERIALS

Peptide	ECM molecule source	Application
RGD	Multiple ECM molecules, e.g. fibronectin, vitronectin, laminin, collagen, and thrombospondin	Enhance bone and cartilage tissue formation *in vitro* and *in vivo*; regulate neurite outgrowth *in vitro* and *in vivo*; promote myoblast adhesion, proliferation, and differentiation; enhance endothelial cell adhesion and proliferation
IKVAV YIGSR RNIAEIIKDI	Laminin	Regulate neurite outgrowth *in vitro* and *in vivo*
Recombinant fibronectin fragment ($FNIII_{7-10}$)	Fibronectin	Promote formation of focal contacts in preosteoblasts
Ac-GCRDGPQGIWGQDRCG	Common MMP substrates, e.g. collagen, fibronectin, and laminin	Encourage cell-mediated proteolytic degradation, remodeling, and bone regeneration *in vivo*

Biomaterial surfaces and matrices endowed with peptides for tissue engineering have been shown to enhance cellular behavior substantially (Table 1.2). Beneficial effects of such surfaces haven been demonstrated for cell types with different functions and originating from both soft and hard tissues, i.e. connective tissue (fibroblasts), muscle tissue (myoblasts and smooth muscle cells), bone (osteoblasts), and cartilage (chondrocytes).

Especially for hard tissue implants, calcium phosphate-coatings are widely used. It is evident that calcium phosphate coatings improve the biological performance of endosseous implants [64-66] due to the capacity of these materials to form a direct bond with bone tissue without an intervening fibrous tissue layer. Concomitantly, the use of calcium phosphate ceramics as a coating onto material with appropriate mechanical properties allows their use at load-bearing sites, since their brittleness hinders their use as a bulk material for load-bearing applications.

(iii) Biologically active compounds

Biologically active compounds, such as growth factors, cytokines, and antibiotics, can be used to add a degree of functionalization to a biomaterial surface (coating). As such, functionalized implant surfaces

can provide drug availability in therapeutic concentrations directly at the intended target site for prolonged time. An overview of the advantages of local drug release over systemic drug therapy is presented in Table 1.3.

TABLE 1.3: ADVANTAGES OF LOCAL DRUG RELEASE OVER SYSTEMIC DRUG THERAPY

1	Lower dose required
2	Greater control over toxicity and bioavailability of dose
3	Less susceptibility to promoting antibiotic resistance
4	Extended duration of release
5	Possibilities to combine local and systemic drugs with different kinetics
6	Controlled release from functionalized surfaces directly to the site
7	Avoidance of systemic drug exposure
8	Direct mitigation of implant-centered infection

Exploiting the opportunities of functionalized implant surfaces, several targets have been addressed, including biomedical device-related infections, therapeutic angiogenesis, and bone formation.
The functionalization of implant surfaces with antimicrobial compounds (antibiotics) is a straightforward method to minimize the risk of implant-associated infections. As discussed previously, implant-associated infections are a common cause of implant failure [67;68]. Consequently, several approaches have been explored experimentally, and already several implants are commercially available, primarily focused at minimizing catheter-related bloodstream infections (reviewed in Wu and Grainger [69]).
Therapeutic angiogenesis is a pivotal element to achieve regrowth of, or engineer new tissue. Especially for tissue engineering, in which an artificial body part eventually will be replaced by native tissues, a proper supply of nutrients and oxygen and removal of waste products is needed. Additionally, if the tissue engineering construct consists of a combination of scaffold and cells, a delay in the development of the vascular network could result in loss of the cells within the tissue engineering construct. Although vascular endothelial growth factor (VEGF) is generally recognized as the most potent angiogenic factor, current approaches utilize mixed growth factor formulations (VEGF plus basic fibroblast growth factor [bFGF], platelet-derived growth factor [PDGF], or angiopoietin 1) as these would not only induce de novo formation of capillaries, but as well stabilize and maturate these capillaries [70].
For bone implants, including oral and orthopedic implants, it is essential to become directly-bonded to the native bone tissue. The process of osseo-integration can be accelerated using osteoinductive factors, including members of the bone morphogenetic proteins (BMPs; especially BMP-2 and BMP-7) and transforming growth factor beta (TGF-β). *In vivo* , these compounds have been demonstrated to effectively accelerate the formation of new bone tissue, and thus more rapid healing of bone defects and integration of bone implants [71-73].
For all of these biologically-active compounds it is important that their availability is such that they can exert their therapeutic function. In view of this, improper delivery of these compounds could result in, for instance, only short-term efficacy (overdose) or microbial resistance (underdose).

IV DEOXYRIBONUCLEIC ACID (DNA) FOR BIOMATERIAL PURPOSES

Deoxyribonucleic acid (DNA) represents the origin of life, as it is the repository of genetic information. The genetic information is allocated into genes, which via the process of transcription can be converted to ribonucleic acid (RNA), and, after further processing, can be translated into proteins. Although the genetic material of organisms usually is contained within DNA, several species, mainly viruses, use RNA as the main encoding molecule. Since the discovery of the three-dimensional structure of DNA by Watson and Crick in 1953 and its function, selective interference with the source of biological information became available.

Structure of DNA

Deoxyribonucleic acid (DNA) molecules are composed of a polymeric conformation of a large number of deoxyribonucleotides, which consist of a sugar, a phosphate group, and a nitrogenous base [74](Figure 3).

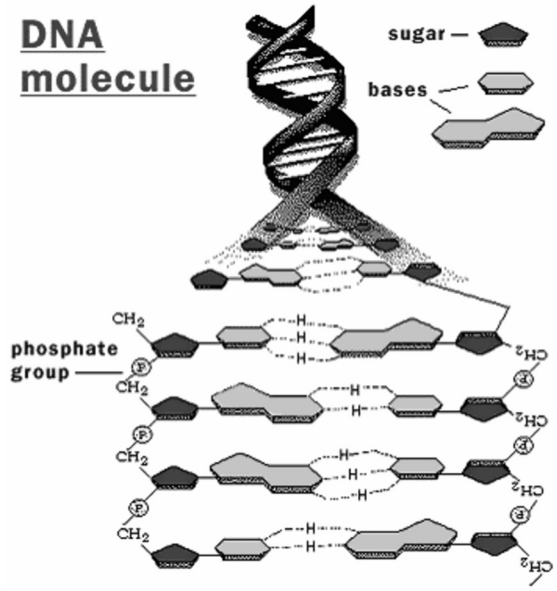

Figure 3: Structure of the DNA molecule.
The DNA molecule consists of a double helical sugar/phosphate backbone, with centrally located bases. Pairing of the bases (adenine, a; thymine, t; guanine, g; and cytosine, c) is restricted to form base-pairs (a-t, c-g), which form hydrogen bonds that hold the two strands together.

In these deoxynucleotide units, the sugar component is represented by deoxyribose. The nitrogenous bases used in DNA molecules are derivatives of purine (i.e. adenine and guanine) or pyrimidine (i.e. thymine and cytosine). In the three-dimensional structure of DNA, two polymers of nucleotides form helical polynucleotide chains which run in opposite directions and are coiled around a common axis, with a sugar-phosphate backbone and a base-centre, resulting in the typical double-helical configuration of DNA. In this configuration, the diameter of the helix is 20 Å (= 2 x 10^{-9} m), whereas adjacent bases are separated by 3.4 Å (= 3.4 x 10^{-10} m) along the axis and related by a rotation of 36 degrees [74]. Together, this makes that the double-helical structure repeats after 10 deoxynucleotides at intervals of 34 Å (= 3.4 x 10^{-9} m). Through the intra-helical positioning of the bases, the two chains are held together by hydrogen bounds which are formed between distinct pairs of opposite bases. In this respect, the pairing of bases is restricted to adenine-thymine (two hydrogen bonds) and guanine-cytosine (three hydrogen bonds). Although the pairing of the bases is restricted to the mentioned base-pairs, this does not implicate a restriction in the sequence of base-pairs, as this sequence of the base-pairs in DNA is responsible for the unique genetic information of each individual.

DNA-helices can have three conformational states, i.e. an A-, B-, or Z-form. Both the A- and B-form are right-handed double helices, with the difference that in the A-form, the rise per base pair is smaller, and the helix diameter is broader. Consequently, DNA in the A-form contains more base-pairs per turn of the helix, and thus forms a more concise style. On the contrary, the helices of the Z-form of DNA are left-handed, and the diameter of the helix is smaller than that of the B-form. Although under physiologic conditions nearly all DNA is in the B-form, transformation into the A- or Z-form can occur under specific conditions [74]. The A-form appears when the relative humidity is reduced below approximately 75%, and the Z-form can be adopted by short oligonucleotides that have sequences of alternating pyrimidines and purines.

The unraveling of the genetic information encoded within the DNA, and the increased knowledge on genetic deficiencies related to pathological disorders have undoubtedly had their impact on 'modern' medicine and science, resulting in the development of an independent scientific discipline called 'genomics'.

Possibilities and limitations of DNA as a coating material

Although predominantly associated with genetics, DNA also represents an interesting natural polymeric molecule that can be used for purposes other than transfer of genetic information. Several properties of the DNA molecule, which derive from its stereochemical structure, may be beneficial in implantology. As a natural, non-proteinic polymer, DNA is suggested to be non- or low-immunogenic [75;76]. Consequently, possible immune responses upon implantation of DNA-coated biomaterial devices, will be not specifically directed against the coating, and are expected to be low. Secondly, the structure of DNA allows interactions of DNA with molecules via either intercalation of groove-binding [77-79]. This opens the applicability of DNA as a tissue-engineering scaffold and/or drug-delivery system, in which cells surrounding the DNA-coated implant can be influenced. Amongst potential molecules that can be applied for loading a DNA-coated implant are growth factors, immuno-regulatory molecules, and antibiotics. Finally, the high content of phosphate groups in DNA might be contributive for bone formation. As it is demonstrated that phosphate groups have a high affinity for calcium ions [80], and bone bonding to a polymeric material modified by surface graft polymerization of a phosphate-containing monomer is firm [81], the polymeric, phosphate-containing DNA molecule might be an interesting candidate for a novel bone substitution material.

Although the idea seems compelling, the application of DNA as a coating material necessitates solutions for some intrinsic properties of DNA. The major problem of using DNA in an in vivo situation is its solubility in aqueous solutions, hampering coating applications without modifications. Furthermore, extracellular DNA is easily degraded by DNases [82], which are ubiquitously present endogenously.

In addition to these issues concerning the generation of a DNA-based coating, also safety issues are involved in the application of DNA for biomedical coating purposes. These safety issues include the risks of transfection and consequences of potential impurities of the DNA. To minimize these risks, the research described in this thesis was performed using specially prepared DNA from Nichiro Corporation (Japan). This DNA, derived from waist products of salmons for the food industry, is of vertebrate origin, randomly cut into molecules of approximately 300 base pairs, and purified to obtain extremely pure material. Consequently, this DNA shares the homogeneity of vertebrate DNA, is unlikely to contain encoding regions due to the limited size of the molecules, and minimizes immune responses directed against potential protein impurities.

Method for the generation of DNA-based coatings

To overcome the aforementioned problems of solubility and degradation, a method for the fabrication of stable coatings containing DNA was required. In this respect, an interesting technique is electrostatic self-assembly (ESA), also known as layer-by-layer (LbL) assembly. This technique was developed by Decher and co-workers in 1992 [83;84] and is based on the electrostatic interactions between positively-(cationic) and negatively-charged (anionic) polyelectrolytes. These interactions can be used to build up polyelectrolyte multilayers (PEMs), as schematically depicted in Figure 4. PEM build up is achieved by alternate immersion of a substrate in aqueous solutions of cationic and anionic polyelectrolytes. Each immersion step allows the adsorption of a layer of polyelectrolytes that reverses the charge at the interface with the solution. This reversed surface charge prevents further polyelectrolyte adsorption and overcompensates the original surface charge. In the subsequent immersion step in an aqueous solution of an oppositely-charged polyelectrolyte, the original surface charge is restored by the adsorption of a next layer of polyelectrolytes, which makes the surface ready for further assembly. To remove excess free polyelectrolytes, the surface is rinsed with pure water after each adsorption step. Repetitive adsorption cycles of cationic and anionic polyelectrolytes allow tailoring of PEM thickness.

A major advantage of this technique is that it can be employed for many substrate materials, irrespective of their geometry. Additionally, the wide range of available polyelectrolytes allows the selection of specific polyelectrolytes with desired properties. Consequently, the ESA-technique represents a simple technique for surface modification that allows tailoring of surface properties of both two- and three-dimensional supports.

Previously, multilayered coatings with DNA as the anionic component have been generated using the ESA-technique [85-92]. These studies indicate the possibility to generate multilayered DNA-coatings but are not conclusive regarding coating characteristics. Furthermore, these studies do not suggest the use of multilayered DNA-coatings for biomaterial purposes.

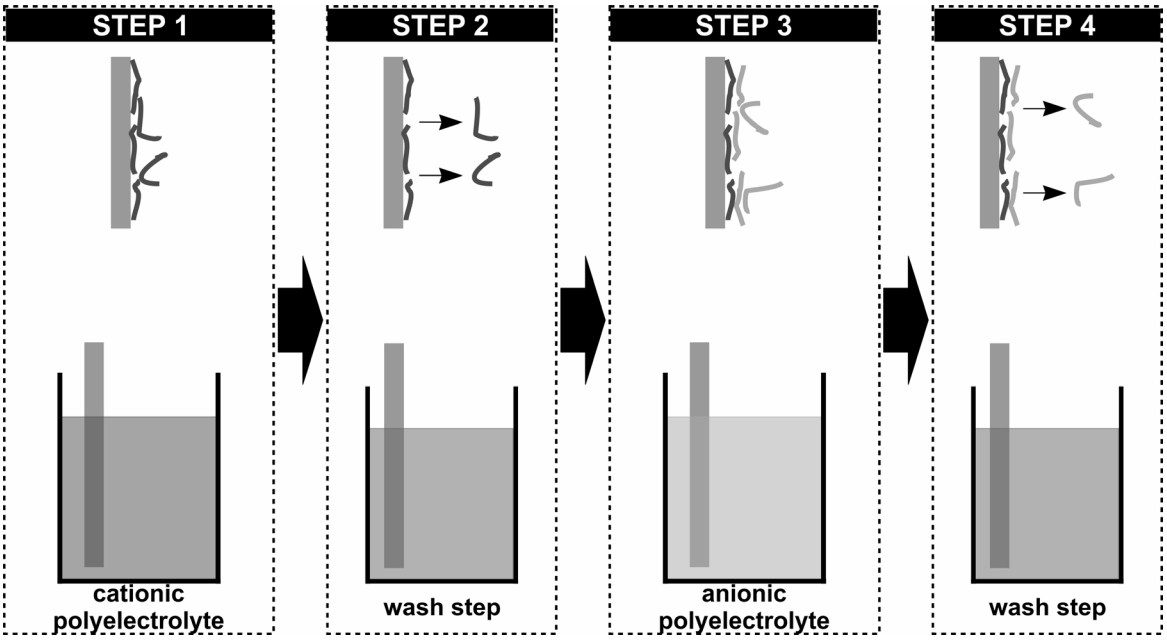

Figure 4: Schematic representation of the electrostatic self-assembly technique. The build up of a multilayered structure is achieved by the successive immersion of a substrate in aqueous solutions of a cationic polyelectrolyte (step 1) and a cationic electrolyte (step 3) with intermediate wash steps (steps 2 & 4). During these wash steps, loosely-bound polyelectrolytes are removed from the adsorbed polyelectrolyte layer. Repetition of steps 1-4 results in a multilayered coating with an accordingly number of double-layers.

V OBJECTIVE & HYPOTHESES

In view of the structural properties of the (vertebrate) DNA-molecule, a collaborative project between Laboratory for Macromolecular & Organic Chemistry (Eindhoven University of Technology) and the Department of Periodontology & Biomaterials (Radboud University Nijmegen Medical Center) was initiated to consider the use of DNA for biomaterial coating purposes. The hypothesis behind this bewildering intention is that the structural properties of the DNA-molecule (within a DNA-based coating) beneficially affect several facets of the interaction between implant and surrounding tissue(s), including the inflammatory response and mineral deposition. Additionally, it is hypothesized that DNA-based coatings can be used as a drug-delivery vehicle to modulate cell and tissue responses using factors with desired biological activity (e.g. growth factors, antibiotics, cytokines, etc).

The research described in this thesis was part of this project. More specifically, the subaims of this project were to:

- fabricate and characterize DNA-based coatings;
- evaluate cytological and histological responses to DNA-based coatings;
- evaluate inflammatory responses to DNA-based coatings *in vitro* using macrophage models;
- evaluate the effect of DNA-based coatings on the deposition of calcium phosphates, and the behavior of bone-forming cells;
- evaluate the possibilities to functionalize DNA-based coatings with the osteoinductive factor BMP-2;
- evaluate the effect of VEGF-functionalized DNA-based coatings on the angiogenic response of endothelial cells and implant-surrounding tissue(s).

VI REFERENCES

1. Anderson, J. M., B. Bevacqua, A. N. Cranin, L. M. Graham , A. S. Hoffman, M. Klein, J. B. Kowalski, R. F. Morrissey, S. A. Obstbaum, B. D. Ratner, F. J. Schoen, A. Sirakian, and D. Whittlesey. 1996. Implants and devices. In *Biomaterials Science: An introduction to materials in medicine*. B. D. Ratner, A. S. Hoffman, F. J. Schoen, and J. E. Lemons, eds. Academic Press, Inc., London, UK.

2. Ratner, B. D. 2001. Replacing and renewing: synthetic materials, biomimetics, and tissue engineering in implant dentistry. *J Dent Educ* 65:1340-7.

3. Liu, W., Y. Cao, and M. T. Longaker. 2001. Gene therapy of scarring: a lesson learned from fetal scarless wound healing. *Yonsei Med J* 42:634-45.

4. Webb, J. C. J. and Tricker, J. 2000. Bone biology: A review of fracture healing. Curr Orthop 14, 457-463.

5. Glowacki, J. 1998. Angiogenesis in fracture repair. *Clin Orthop*S82-9.

6. Harding, K. G., H. L. Morris, and G. K. Patel. 2002. Science, medicine and the future: healing chronic wounds. *BMJ* 324:160-3.

7. Singer, A. J. and R. A. Clark. 1999. Cutaneous wound healing. *N Engl J Med* 341:738-46.

8. Bello, Y. M. and T. J. Phillips. 2000. Recent advances in wound healing. *JAMA* 283:716-8.

9. Clark, R. A. 2001. Fibrin and wound healing. *Ann N Y Acad Sci* 936:355-67.

10. Hart, J. 2002. Inflammation. 1: Its role in the healing of acute wounds. *J Wound Care* 11:205-9.

11. Hart, J. 2002. Inflammation. 2: Its role in the healing of chronic wounds. *J Wound Care* 11:245-9.

12. Wong, M. E., J. O. Hollinger, and G. J. Pinero. 1996. Integrated processes responsible for soft tissue healing. *Oral Surg Oral Med Oral Pathol Oral Radiol Endod* 82:475-92.

13. Hollinger, J. and M. E. Wong. 1996. The integrated processes of hard tissue regeneration with special emphasis on fracture healing. *Oral Surg Oral Med Oral Pathol Oral Radiol Endod* 82:594-606.

14. Gerstenfeld, L. C., D. M. Cullinane, G. L. Barnes, D. T. Graves, and T. A. Einhorn. 2003. Fracture healing as a post-natal developmental process: Molecular, spatial, and temporal aspects of its regulation. *J Cell Biochem* 88:873-84.

15. Werner, S. and R. Grose. 2003. Regulation of wound healing by growth factors and cytokines. *Physiol Rev* 83:835-70.

16. Baj-Krzyworzeka, M., M. Majka, D. Pratico, J. Ratajczak, G. Vilaire, J. Kijowski, R. Reca, A. Janowska-Wieczorek, and M. Z. Ratajczak. 2002. Platelet-derived microparticles stimulate proliferation, survival, adhesion, and chemotaxis of hematopoietic cells. *Exp Hematol* 30:450-9.

17. Mackay, C. R. 2001. Chemokines: immunology's high impact factors. *Nat Immunol* 2:95-101.

18. Janeway, C. A., P. Travers, M. Walport, and J. Capra. 1999. *Immunobiology: the immune system in health and disease*. Elsevier Science Ltd/Garland Publishing, London, UK.

19. Einhorn, T. A. 1998. The cell and molecular biology of fracture healing. *Clin Orthop*S7-21.

20. Mutsaers, S. E., J. E. Bishop, G. McGrouther, and G. J. Laurent. 1997. Mechanisms of tissue repair: from wound healing to fibrosis. *Int J Biochem Cell Biol* 29:5-17.

21. Visse, R. and H. Nagase. 2003. Matrix metalloproteinases and tissue inhibitors of metalloproteinases: structure, function, and biochemistry. *Circ Res* 92:827-39.

22. Chamay, A. and P. Tschantz. 1972. Mechanical influences in bone remodeling. Experimental research on Wolff's law. *J Biomech* 5:173-80.

23. Thomsen, P. and C. Gretzer. 2001. Macrophage interactions with modified material surfaces. *Curr Opin Sol State Mat Sci* 5:163-176.

24. Vogler, E. A. 1998. Structure and reactivity of water at biomaterial surfaces. *Adv Colloid Interface Sci* 74:69-117.

25. Hallab, N. J., K. J. Bundy, K. O'Connor, R. L. Moses, and J. J. Jacobs. 2001. Evaluation of metallic and polymeric biomaterial surface energy and surface roughness characteristics for directed cell adhesion. *Tissue Eng* 7:55-71.

26. Walboomers, X. F., H. J. Croes, L. A. Ginsel, and J. A. Jansen. 1999. Contact guidance of rat fibroblasts on various implant materials. *J Biomed Mater Res* 47:204-12.

27. Jansen, J. A., J. P. van der Waerden, and K. de Groot. 1989. Effect of surface treatments on attachment and growth of epithelial cells. *Biomaterials* 10:604-8.

28. Horbett, T. A. and M. B. Schay. 1988. Correlations between mouse 3T3 cell spreading and serum fibronectin adsorption on glass and hydroxyethylmethacrylate-ethylmethacrylate copolymers. *J Biomed Mater Res* 22:763-793.

29. Kasemo, B. and J. Gold. 1999. Implant surfaces and interface processes. *Adv Dent Res* 13:8-20.

30. Horbett, T. A. 1999. The role of adsorbed adhesion proteins in cellular recognition of biomaterials. *BMES Bull* 23:5-9.

31. Horbett, T. A. and L. A. Klumb. 1996. Cell culturing : surface aspects and considerations. In *Interfacial phenomena and bioproducts*. W. P. Brash JL, ed. Marcel Dekker, New York, USA.

32. Steele, J. G., B. A. Dalton, G. Johnson, and P. A. Underwood. 1995. Adsorption of fibronectin and vitronectin onto Primaria and tissue culture polystyrene and relationship to the mechanism of initial attachment of human vein endothelial cells and BHK-21 fibroblasts. *Biomaterials* 16:1057-67.

33. Steele, J. G., G. Johnson, C. McFarland, B. A. Dalton, T. R. Gengenbach, R. C. Chatelier, P. A. Underwood, and H. J. Griesser. 1994. Roles of serum vitronectin and fibronectin in initial attachment of human vein endothelial cells and dermal fibroblasts on oxygen- and nitrogen-containing surfaces made by radiofrequency plasmas. *J Biomater Sci Polym Ed* 6:511-32.

34. Ratner, B. D. 2002. Reducing capsular thickness and enhancing angiogenesis around implant drug release systems. *J Control Release* 78:211-8.

35. Seare, W. J. Jr. 2000. Alloplasts and biointegration . *J Endourol* 14:9-17.

36. Ducheyne, P., L. L. Hench, A. Kagan 2nd, M. Martens, A. Bursens, and J. C. Mulier. 1980. Effect of hydroxyapatite impregnation on skeletal bonding of porous coated implants. *J Biomed Mater Res* 14:225-37.

37. Geesink, R. G., K. de Groot, and C. P. Klein. 1988. Bonding of bone to apatite-coated implants. *J Bone Joint Surg Br* 70:17-22.

38. Anderson, J. M. Biological responses to materials. 2001. Annu Rev Mater Res 31, 81-110.

39. van Diest, P. J., W. H. Beekman, and J. J. Hage. 1998. Pathology of silicone leakage from breast implants. *J Clin Pathol* 51:493-7.

40. Anderson, J. M. 2000. Multinucleated giant cells. *Curr Opin Hematol* 7:40-7.

41. Zhao, Q., N. Topham, J. M. Anderson, A. Hiltner, G. Lodoen, and C. R. Payet. 1991. Foreign-body giant cells and polyurethane biostability: in vivo correlation of cell adhesion and surface cracking. *J Biomed Mater Res* 25:177-83.

42. Crubezy, E., P. Murail, L. Girard, and J. P. Bernadou. 1998. False teeth of the Roman world. *Nature* 391:29.

43. Cooke, F. W. 1996. Bulk properties of materials. In *Biomaterials Science: An introduction to materials in medicine*. B. D. Ratner, A. S. Hoffman, F. J. Schoen, and J. E. Lemons, eds. Academic Press, Inc., London, UK.

44. Black, J. 1992. *Biological performance of materials: fundamentals of biocompatibility*. Marcel Dekker, Inc, New York.

45. Lacefield, W. R. 1999. Materials characteristics of uncoated/ceramic-coated implant materials. *Adv Dent Res* 13:21-6.

46. Schakenraad, J. M. 1996. Cells: their surfaces and interactions with materials. In *Biomaterials Sciences: an introduction to materials in medicine*. B. D. Ratner, A. S. Hoffman, F. J. Schoen, and J. E. Lemons, eds. Academic Press, Inc., London, UK.

47. Cordero, J., L. Munuera, and M. D. Folgueira. 1996. The influence of the chemical composition and surface of the implant on infection. *Injury* 27 Suppl 3:SC34-7.

48. Bauer, T. W. and J. Schils. 1999. The pathology of total joint arthroplasty.II. Mechanisms of implant failure. *Skeletal Radiol* 28:483-97.

49. Williams, D. F. and R. L. Williams. 1996. Degradative effects of the biological environment on metals and ceramics. In *Biomaterials Science: an introduction to materials in medicine*. B. D. Ratner, A. S. Hoffman, F. J. Schoen, and J. E. Lemons, eds. Academic Press, Inc., London, UK.

50. Curtis, A. and C. Wilkinson. 1997. Topographical control of cells. *Biomaterials* 18:1573-83.

51. Ito, Y. 1999. Surface micropatterning to regulate cell functions. *Biomaterials* 20:2333-42.

52. Brunette, D. M. and B. Chehroudi. 1999. The effects of the surface topography of micromachined titanium substrata on cell behavior in vitro and in vivo. *J Biomech Eng* 121 :49-57.

53. Singhvi, R., A. Kumar, G. P. Lopez, G. N. Stephanopoulos, D. I. Wang, G. M. Whitesides, and D. E. Ingber. 1994. Engineering cell shape and function. *Science* 264:696-8.

54. Walboomers X.F. and Jansen, J. A. Cell and tissue behavior on micro-grooved surfaces. Odontology 89, 2-11. 2001.

55. Parker, J. A., X. F. Walboomers, J. W. Von den Hoff, J. C. Maltha, and J. A. Jansen. 2002. Soft-tissue response to silicone and poly-L-lactic acid implants with a periodic or random surface micropattern. *J Biomed Mater Res* 61:91-8.

56. den Braber, E. T., J. E. de Ruijter, L. A. Ginsel, A. F. von Recum, and J. A. Jansen. 1996. Quantitative analysis of fibroblast morphology on microgrooved surfaces with various groove and ridge dimensions. *Biomaterials* 17:2037-44.

57. Rajnicek, A., S. Britland, and C. McCaig. 1997. Contact guidance of CNS neurites on grooved quartz: influence of groove dimensions, neuronal age and cell type. *J Cell Sci* 110 (Pt 23):2905-13.

58. Clark, P., P. Connolly, A. S. Curtis, J. A. Dow, and C. D. Wilkinson. 1991. Cell guidance by ultrafine topography in vitro. *J Cell Sci* 99 (Pt 1):73-7.

59. Wojciak-Stothard, B., A. Curtis, W. Monaghan, K. MacDonald, and C. Wilkinson. 1996. Guidance and activation of murine macrophages by nanometric scale topography. *Exp Cell Res* 223:426-35.

60. Dalby, M. J., M. O. Riehle, H. J. Johnstone, S. Affrossman, and A. S. Curtis. 2002. Polymer-Demixed Nanotopography: Control of Fibroblast Spreading and Proliferation. *Tissue Eng* 8:1099-1108.

61. Dalby, M. J. , S. J. Yarwood, M. O. Riehle, H. J. Johnstone , S. Affrossman, and A. S. Curtis. 2002. Increasing fibroblast response to materials using nanotopography: morphological and genetic measurements of cell response to 13-nm-high polymer demixed islands. *Exp Cell Res* 276:1-9.

62. Hersel, U., C. Dahmen, and H. Kessler. 2003. RGD modified polymers: biomaterials for stimulated cell adhesion and beyond. *Biomaterials* 24:4385-415.

63. LeBaron, R. G. and K. A. Athanasiou. 2000. Extracellular matrix cell adhesion peptides: functional applications in orthopedic materials. *Tissue Eng* 6:85-103.

64. Dorozhkin, S. V. and M. Epple. 2002. Biological and medical significance of calcium phosphates . *Angew Chem Int Ed* 41:3130-3146.

65. Lacefield, W. R. 1999. Materials characteristics of uncoated/ceramic-coated implant materials. *Adv Dent Res* 13:21-6.

66. Kokubo, T., H. M. Kim, and M. Kawashita. 2003. Novel bioactive materials with different mechanical properties. *Biomaterials* 24:2161-75.

67. Cordero, J., L. Munuera, and M. D. Folgueira. 1996. The influence of the chemical composition and surface of the implant on infection. *Injury* 27 Suppl 3:SC34-7.

68. Bauer, T. W. and J. Schils. 1999. The pathology of total joint arthroplasty.II. Mechanisms of implant failure. *Skeletal Radiol* 28:483-97.

69. Wu, P. and D. W. Grainger. 2006. Drug/device combinations for local drug therapies and infection prophylaxis. *Biomaterials* 27:2450-67.

70. Zisch, A. H., M. P. Lutolf, and J. A. Hubbell. 2003. Biopolymeric delivery matrices for angiogenic growth factors. *Cardiovasc Pathol* 12:295-310.

71. Ruhe, P. Q., H. C. Kroese-Deutman, J. G. Wolke, P. H. Spauwen, and J. A. Jansen. 2004. Bone inductive properties of rhBMP-2 loaded porous calcium phosphate cement implants in cranial defects in rabbits. *Biomaterials* 25:2123-32.

72. Jansen, J. A., J. W. Vehof, P. Q. Ruhe, H. Kroeze-Deutman, Y. Kuboki, H. Takita, E. L. Hedberg, and A. G. Mikos. 2005. Growth factor-loaded scaffolds for bone engineering. *J Control Release* 101:127-36.

73. Vehof, J. W., J. P. Fisher, D. Dean, J. P. van der Waerden, P. H. Spauwen, A. G. Mikos, and J. A. Jansen. 2002. Bone formation in transforming growth factor beta-1-coated porous poly(propylene fumarate) scaffolds. *J Biomed Mater Res* 60:241-51.

74. Stryer, L. 1995. *Biochemistry*. W.H. Freeman and Company, New York, USA.

75. Yamamoto, S., T. Yamamoto, S. Shimada, E. Kuramoto, O. Yano, T. Kataoka, and T. Tokunaga. 1992. DNA from bacteria, but not from vertebrates, induces interferons, activates natural killer cells and inhibits tumor growth. *Microbiol Immunol* 36:983-97.

76. McMichael, A. J. 1992. Antigens and MHC systems. In *Oxford textbook of pathology*. J. O. D. McGee, P. G. Isaacson, and N. A. Wright, eds. Oxford University Press, Oxford, UK.

77. Werner, M. H., A. M. Gronenborn, and G. M. Clore. 1996. Intercalation, DNA kinking, and the control of transcription. *Science* 271:778-84.

78. Wilson, W. D. 1996. Reversible interactions of nucleic acids with small molecules. In *Nucleic acids in chemistry and biology*. G. M. Blackburn and M. J. Gait, eds. Oxford University Press, Oxford, UK.

79. Goldman, A. and T. Glumoff. 1996. Interaction of proteins with nucleic acids. In *Nucleic acids in chemistry and biology*. G. M. Blackburn GM, ed.

80. Kamei, S., N. Tomita, S. Tamai, K. Kato, and Y. Ikada. 1997. Histologic and mechanical evaluation for bone bonding of polymer surfaces grafted with a phosphate-containing polymer. *J Biomed Mater Res* 37:384-93.

81. Tretinnikov, O. N., K. Kato, and Y. Ikada. 1994. In vitro hydroxyapatite deposition onto a film surface-grated with organophosphate polymer. *J Biomed Mater Res* 28:1365-73.

82. Wiethoff, C. M. and C. R. Middaugh. 2003. Barriers to nonviral gene delivery. *J Pharm Sci* 92:203-17.

83. Decher, G., Hong, J. D., and Schmitt, J. 1992. Buildup of ultrathin multilayer films by a self-assembly process: III. Consecutively alternating adsorption of anionic an cationic polyelectrolytes on charged surfaces. Thin Solid Films 210-211, 831-835.

84. Decher G. 1997. Fuzzy Nanoassemblies: Toward Layered Polymeric Multicomposites. Science 277, 1232-1237.

85. Pei, R., X. Cui, X. Yang, and E. Wang. 2001. Assembly of alternating polycation and DNA multilayer films by electrostatic layer-by-layer adsorption. *Biomacromolecules* 2:463-8.

86. Sastry, M., M. Rao, and K. N. Ganesh. 2002. Electrostatic assembly of nanoparticles and biomacromolecules. *Acc Chem Res* 35:847-55.

87. Luo, L., J. Liu, Z. Wang, X. Yang, S. Dong, and E. Wang. 2001. Fabrication of layer-by-layer deposited multilayer films containing DNA and its interaction with methyl green. *Biophys Chem* 94:11-22.

88. Sukhorukov, G. B., M. M. Montrel, A. I. Petrov, L. I. Shabarchina, and B. I. Sukhorukov. 1996. Multilayer films containing immobilized nucleic acids. Their structure and possibilities in biosensor applications. *Biosens Bioelectron* 11:913-22.

89. Sukhorukov G.B. , Mohwald H. , Decher G. , and Lvov Y.M. 1996. Assembly of polyelectrolyte multilayer films by consecutively alternating adsorption of polynucleotides and polycations. Thin Solid Films 284-285, 220-223.

90. Lvov Y. , Decher G. , and Sukhorukov G. 1993. Assembly of thin films by means of successive deposition of alternate

layers of DNA and Poly(allylamine). Macromolecules 26, 5396-5399.

91. Chen X. , Lang J. , and Liu M. 2002. Layer-by-layer assembly of DNA-dye complex films. Thin Solid Films 409, 227-232.

92. Zhou, Y. and Li, Y. 2004. Layer-by-Layer Self-Assembly of Multilayer Films Containing DNA and Eu^{3+}: Their Characteristics and Interactions with Small Molecules. Langmuir 20, 7208-7214.

93. Boontheekul T. and Mooney D.J. 2003. Protein-based signaling systems in tissue engineering. Curr Opin Biotechnol 14, 559-565.

2

FABRICATION, CHARACTERIZATION, AND BIOLOGICAL ASSESSMENT OF MULTILAYERED DNA-COATINGS FOR BIOMATERIAL PURPOSES

JJJP van den Beucken, MRJ Vos, PC Thüne, T Hayakawa, T Fukushima, Y Okahata, XF Walboomers NAJM Sommerdijk, RJM Nolte, JA Jansen

Biomaterials 27 (2006);691-701

I INTRODUCTION

In implantology, a wide variety of materials are used to generate biomedical devices with satisfactory properties. Although bulk properties of materials largely determine their suitability for a given application, the biological response is mainly determined at the biomaterial surface, via the interactions with components of the biological surroundings [1;2].

Modifications of the biomaterial surface have been a major research topic in the past decades. In view of this, an intriguing novel coating material for biomaterials is deoxyribonucleic acid (DNA), the repository of (individual-specific) genetic information. Irrespective of its genetic information, the structural properties of DNA give this unique, natural compound potential for use as a biomaterial coating. The specific build-up of the DNA molecule may ensure a versatile use at various implantation sites. The molecular structure of DNA in vertebrate species is homogenous [3;4], and the non- or low-immunogenic properties of DNA (compared to other biological antigens like proteins and sugars) may limit both innate and acquired immune responses [3;5;6]. Additionally, DNA can incorporate other molecules via groove-binding and intercalation [7;8]. This creates opportunities to specifically deliver desired biological mediators in the direct vicinity of the implantation site. Finally, the high phosphate content in DNA might, via the high affinity of phosphate for calcium ions [9;10], beneficially affect the deposition of calcium in the bone formation process. The use of DNA as a functional biomaterial, instead as a carrier for its genetic information, has already been suggested [11;12], and pioneering efforts have resulted in the fabrication of DNA-containing bulk (bio)material [13], which demonstrated to cause no adverse reactions upon subcutaneous implantation in the backs of rats.

The application of DNA as a coating material, however, is hampered by (a) its easy nucleolytic degradation, and (b) its solubility in aqueous solutions. The use of the previously mentioned DNA-containing bulk material [13] resulted in easily detaching coatings on various substrates. Therefore other methods to obtain stable DNA-containing coatings for biomaterial purposes have to be explored. One applicable technique could be electrostatic self-assembly (ESA), also known as layer by layer (LbL) assembly. Via this technique, polyelectrolyte multilayers (PEMs) can be generated through the alternated progressive adsorption of oppositely-charged polyelectrolytes via electrostatic interactions [14].

The ESA technique has been applied successfully using DNA as a polyanionic building block [15-22]. Interestingly, electrostatic interactions with positively charged polyelectrolytes have demonstrated to protect DNA from degradation by nucleolytic activity [23]. Furthermore, the method of fabrication (i.e. under immersion in aqueous solutions) inherently evidences the water insolubility of PEMs. Even immersion of PEMs in high ionic solutions (i.e. exceeding those in physiological conditions) does not cause dissociation of the PEM structure. Instead, changes in the ionic content of the polyelectrolyte solutions in the fabrication process are one of the means to modulate PEM properties, including layer thickness [14;24].

Irrespective of the progress made so far, the use of DNA-containing multilayered coatings in the biomaterials field still requires their complete characterization. Whereas the build-up mechanism of PEMs has been described previously, information on the morphological properties is scarce. Additionally, the hypothesized beneficial properties of DNA necessitate the quantification of the amount of DNA immobilized in the coatings. Therefore, the aim of this study was to fabricate and characterize two types of multilayered DNA-coatings, which differ in the type of cationic polyelectrolyte used, and assess their effects on cell behavior using *in vitro*-experiments.

II MATERIALS & METHODS

Materials

Polyanionic DNA (± 300 bp/molecule; sodium salt) was kindly provided by Nichiro Corporation (Yokosuka-shi, Kanagawa prefecture, Japan). Potential protein impurities in the DNA were checked using the BCA protein assay (Pierce, Rockford, Illinois, USA) and measured to be below 0.20% w/w (data not shown). Polycationic polyelectrolytes poly(allylamine hydrochloride) (PAH; MW ~70000) and poly-D-lysine (PDL; MW 30000 – 70000) were purchased from Sigma (Sigma-Aldrich Chemie B.V., Zwijndrecht, the Netherlands). All materials were used without further purification. The monomeric structures of the cationic polyelectrolytes used are presented in Figure 1.

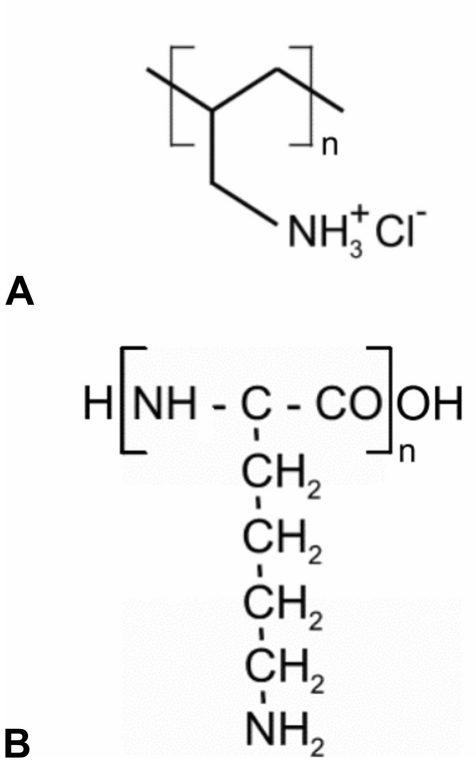

Figure 1: Molecular structure of (A) poly(allylamine hydrochloride) (PAH) and (B) poly-D-lysine (PDL).

Substrate preparation and cleaning

Three types of substrates were used:

1. Quartz substrates (45 x 12 mm; Hellma Benelux B.V., Rijswijk, the Netherlands) were used for UV-vis spectrophotometry, contact angle measurements, FTIR spectroscopy, and XPS;
2. Silicon substrates (1 x 1 cm; Wafernet GmbH, Eching, Germany) were coated with a 50 nm thick titanium layer, using the RF magnetron sputter technique. The titanium sputtering process (duration 5 min., pressure ~5 x 10^{-4} mbar) was performed with the silicon substrates attached to a rotating sample holder. Titanium-sputtered silicon substrates were used for XPS, contact angle measurements, and AFM;
3. Disc-shaped titanium substrates (12 mm diameter, 2 mm thickness; commercially-pure titanium, as-machined) were used to determine the incorporation of radiolabeled DNA into each double-layer.

Quartz substrates were cleaned in Piranha solution (H_2O_2 (30% aqueous solution) / H_2SO_4 – 3:7 v/v) to completely remove all traces of organic materials at the surface, and increase the hydrophilicity of the surface. *(caution: Piranha solution is an extremely corrosive mixture)*. Subsequently, the substrates were thoroughly rinsed with ultra-pure water from a Millipore system (resistivity ≥ 18.2 MΩ·cm; Millipore B.V., Amsterdam, the Netherlands) and dried using a pressurized air stream.

Titanium-sputtered silicon substrates and titanium discs were cleaned ultrasonically using consecutively nitric acid (10% v/v), acetone, and isopropanol. Between each cleaning step, the substrates were rinsed with ultra-pure water. After the last cleaning step, the substrates were dried in air.

Generation of multilayered DNA-coatings

Multilayered DNA-coatings were generated using the ESA technique, as described by Luo et al. [17] with few modifications. The cleaned substrates were immersed in an aqueous solution of either PDL (0.1 mg/ml) or PAH (1 mg/ml) for 30 minutes, allowing sufficient time for the adsorption of the first cationic polyelectrolyte layer onto the substrates. Subsequently, the substrates were washed in ultra-pure water (5 minutes, continuous water flow) and dried using a pressurized air stream. Thereafter, the substrates were alternately immersed in an anionic aqueous DNA solution (1 mg/ml) and the respective cationic polyelectrolyte solution for 7 minutes each, with intermediate washing in ultra-pure water (5 minutes, continuous water flow) and drying using a pressurized air stream. The build-up of the multilayered DNA-coatings was continued until a total of 5 double-layers was reached. These were designated either $[PDL/DNA]_5$ or $[PAH/DNA]_5$) (the denotation of coatings is restricted to indicating the number of double-layers, i.e. ½ represents only the cationic part of the double-layer).

Characterization

UV-Vis spectrophotometry

The progressive build-up of the multilayered DNA-coatings onto quartz substrates was monitored using a Shimadzu multi-spec UV-Vis spectrophotometer (Shimadzu Germany, Duisburg, Germany), equipped with a diode-array detector. Measurements were taken after each successive layer. Growth of the multilayered DNA-coatings was studied via the incremental increase at 260 nm, the absorbance maximum of the nucleic base chromophores. All measurements were replicated in a separate second run.

Atomic Force Microscopy (AFM)

The morphology of non-coated titanium-sputtered silicon, partial ($[PDL/DNA]_{½}$ and $[PAH/DNA]_{½}$; $[PDL/DNA]_2$ and $[PAH/DNA]_2$; $[PDL/DNA]_{3½}$ and $[PAH/DNA]_{3½}$) and complete ($[PDL/DNA]_5$ and $[PAH/DNA]_5$) multilayered DNA-coatings was analyzed using a Nanoscope IIIa AFM set-up (Digital Instruments, Buffalo, NY, USA). All scans were made in contact mode, using a Si_3N_4-tip. Typical scan sizes were between 0.5 x 0.5 μm^2 and 5 x 5 μm^2. To detect potential damaging effects of the probe to the multilayered DNA-coatings, scans of the samples were always made with increasing scan size. Image analysis software (WSxM free software, downloadable at http://www.nanotec.es) was used to generate micrographs and quantitatively compare surface roughness, using Root-Mean-Square (RMS) calculations, a roughness denotation based on the standard deviations of the z-value (vertical direction).

X-ray photospectroscopy (XPS)

XPS measurements were performed using a non-monochromized VG-Escalab 200 spectrometer equipped with an aluminum anode (Al KR; 1486.6 eV) operating at 510 VA with a background pressure of 2 x 10^{-9} mbar. Spectra were acquired at 0° and 60° with respect to the surface normal, after the adsorption of 1, 3½, and 5 double-layers of [PDL/DNA] or [PAH/DNA] onto titanium-sputtered silicon substrates. As a reference, the spectrum of a dropcast (pure) DNA film was included. The (I_{P2p} / I_{N1s}) (ratio of integrated intensities) of the experimental substrates were used to calculate the fraction of DNA (x_{DNA}) within the top (5 - 10 nm) of the measured sample, according to Formula 1:

$$I_{P2p} / I_{N1s} = x_{DNA} \left(I_{P2p} / I_{N1s-DNA} \right) \quad (1)$$

As the stoichiometric carbon/nitrogen ratios for DNA, PDL, and PAH are similar, no extra correction was necessary.

Contact Angle measurements
The progressive build-up of the multilayered DNA-coatings on quartz and titanium-sputtered silicon substrates was monitored using contact angle measurements on a Drop Shape Analysis System DSA10 (Krüss GmbH, Hamburg, Germany). Four measurements per substrate were taken using the sessile drop method. All measurements were replicated in a separate second run.

Fourier transform infrared spectroscopy (FTIR)
Infrared spectra of the multilayered DNA-coatings on quartz substrates were obtained using Fourier transform infrared spectroscopy (Perkin Elmer Instruments, Bucks, England, UK). The infrared spectrum of DNA (as sodium salt) was obtained using the KBr-pellet method (0.4 % w/w DNA in KBr).

Build-up of multilayered DNA-coatings with radiolabeled DNA
The amount of DNA immobilized into the multilayered coatings was determined using radiolabeled DNA. In brief, DNA was radiolabeled using ^{32}P-postlabeling through the T4-kinase enzyme. Non-bound label was removed via 2 successive filtrations using Sephadex®-50 columns. The efficiency of labeling was 34%. Radiolabeled DNA was added to an aqueous DNA solution with a final concentration of 1 mg/ml. Concentrations of the aqueous solutions of the cationic polyelectrolytes were as described above. Multilayered coatings were fabricated as described above onto disc-shaped glass and titanium substrates. After the completion of 1, 2, 3, 4, and 5 double-layers, substrates were taken out of the fabrication process, immersed in scintillation fluid, and counted using a liquid scintillation counter. For comparison, samples containing 100 (l of the initial aqueous DNA solution (1 mg/ml) were counted. All experimental and control samples were present in 3-fold.

Biological assessment
Mutagenicity assay
The mutagenicity of the chemicals used to build up the multilayered DNA-coatings was assessed using the Muta-ChromoplateTM basic kit (version 3.1; Environmental Biodetection Products Inc., Brampton, Ontario, Canada), according to the instructions of the manufacturer. This kit is based on the most generally used and validated bacterial reverse-mutation test, known as the 'Ames Test'. Briefly, a mutant strain of Salmonella typhimurium (TA100), carrying a mutation in the operon coding for histidine biosynthesis, was exposed to 2 concentrations of the chemicals used for the build up of the multilayered DNA-coatings (DNA and PAH: 250 and 2500 μg/ml; PDL: 25 and 250 μg/ml). After an incubation period of five days at 37°C, the number of positive wells for each condition was recorded and scored against the results of the background (negative control). Sodium azide (NaN_3; 5 μg/ml), a direct-acting mutagen, was used as a positive control.

Cell culture and seeding
Biological experiments were performed using DNA-coatings generated on disc-shaped titanium substrates and non-coated titanium control substrates. All substrates were sterilized using a UV-irradiation treatment (254 nm; 4 hrs).
Rat dermal fibroblasts (RDF) were obtained from the ventral skin of male Wistar rats, using a standard procedure as described previously [25], after which cells were cryo-preserved. Before the initiation of an experiment, cells were thawed and cultured in culture medium (α-MEM (Gibco), supplemented with 10% v/v fetal calf serum (FCS) and gentamicin (50 μg/ml)). All assays were performed with cells of the 4th or 5th culture passage. Prior to the assays, cells were detached using trypsin/EDTA (0.25% w/v trypsin/0.02% EDTA) and concentrated by centrifugation at 1500 rpm for 5 min. Subsequently, cells were resuspended in culture medium and counted using a Coulter® counter (Beckman Coulter Inc.,

Fullerton, CA, USA). For all *in vitro* assays, cells were seeded at 1 x 10^4 cells/cm^2 into 24-well plates (Greiner Bio-One BV, Alphen aan de Rijn, the Netherlands).

Cell proliferation

At 1, 3, 7, and 10 days after seeding, the medium was aspirated and the cell layer was washed twice with PBS. Subsequently, substrates with attached cells were transferred into fresh wells and incubated with 0.5 ml trypsin/EDTA. After detachment of the cells, 0.5 ml culture medium was added. The cell suspension was diluted using Coulter® Isotone II diluent (Beckman Coulter Inc.) and cell numbers were counted using a Coulter® counter. The experiment was performed 3 times, with at each time point 3 samples per condition (n=3).

Cell viability

Cell viability was assessed using a commercially available cytotoxicity assay, according to the instructions of the manufacturer (Promega Corporation, Madison, WI, USA). The test is based on the conversion of a tetrazolium salt ([3-(4,5-dimethylthiazol-2-yl)-2,5-diphenyltetrazoliumbromide], MTT) into a formazan product. Briefly, at 3 days after cell seeding on the experimental substrates, 150 µl dye solution was added to each well, and cells were incubated at 37 °C for 4 hours. Subsequently, 1 ml of solubilization/stop solution was added to each well, and the cells were incubated for another hour (at room temperature). Finally, the contents of the wells were mixed thoroughly using a pipette and the absorbance at 570 nm wavelength was read using a spectrophotometer. Measured absorbance values were corrected for cell numbers using parallel samples, from which the cell number was determined using a Coulter® counter. Normalization of the data was performed to the results of the non-coated control substrates.

Cell morphology

To study cell morphology, cell cultured on the experimental substrates for 3 days were washed twice with PBS. Subsequently, cell fixation was carried out for 15 min. in 2% glutaraldehyde in 0.1 M sodium cacodylate buffered solution. Then, samples were rinsed twice with cacodylate buffered solution and dehydrated using a graded series of ethanol. Finally, samples were dried using with tetramethylsilane. The samples were sputter coated with gold, and examined using a JEOL 6310 SEM.

Statistical analysis

Statistical analyses were performed using GraphPad Instat, version 3.0 (GraphPad Software, San Diego, CA, USA). Statistical comparisons for RMS-values within one type of coating were performed using an ANOVA-test, combined with a post-hoc Tukey-Kramer Multiple Comparisons Test. Statistical comparisons between the two types of coatings were performed using an unpaired *t*-test. The results of the biological assays were analyzed using an unpaired *t*-test.

III RESULTS

Characterization

UV-Vis photospectrometry

The build-up of multilayered DNA-coatings on quartz substrates via UV-Vis spectrophotometry could be easily monitored using the nucleic base chromophores in DNA (absorbance maximum at 260 nm). As illustrated in Figure 2 (A and B), both multilayered DNA-coatings showed an increase in UV-absorbance spectrum with every successively added double-layer. The UV-absorbance of [PDL/DNA] double-layers was higher compared to that of [PAH/DNA] double-layers. When peak values at 260 nm were plotted against the number of double-layers (Figures 3A and 3B), a linear increase with every added double-layer became apparent for both types of coatings (Figures 3A en 3B).

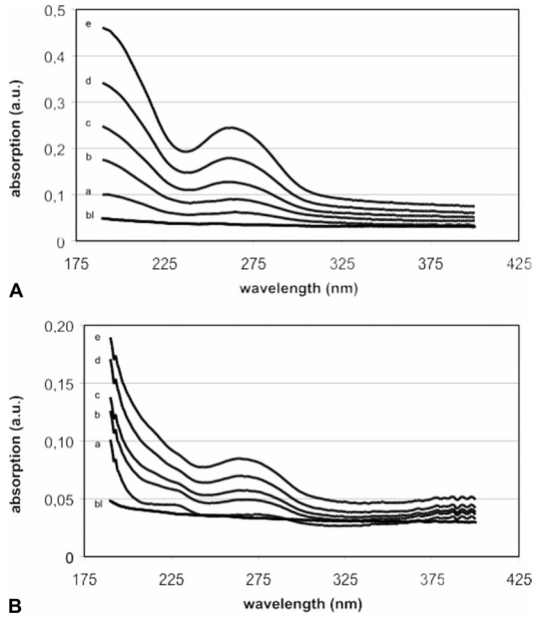

Figure 2: UV-absorption spectra of (A) [PDL/DNA]-multilayer coatings, and (B) [PAH/DNA]-multilayer coatings. The UV-absorption spectra were monitored using quartz substrates after the deposition of 0 (bl), 1 (a), 2 (b), 3 (c), 4 (d), and 5 (e) double-layers.

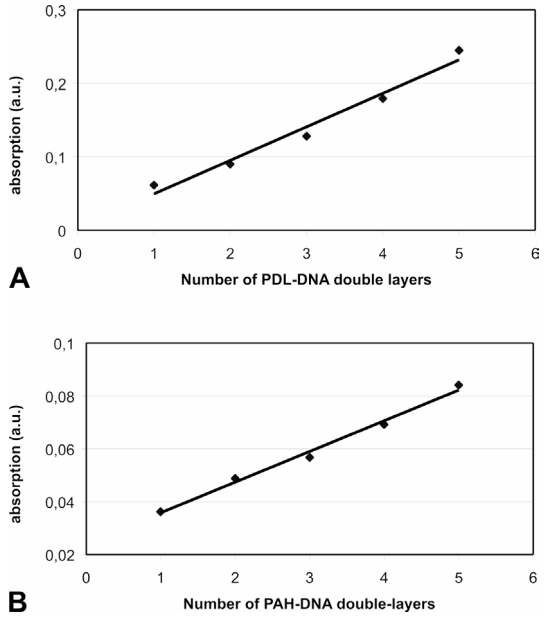

Figure 3: Plots of the absorbance at 260 nm (A_{260}) against the number of (A) [PDL/DNA]-double-layers, and (B) [PAH/DNA]-double-layers.

Atomic Force Microscopy

The surface morphology of partial and complete multilayered DNA-coatings on titanium-sputtered silicon substrates was studied using AFM. The forces of the cantilever on the coatings during contact mode scanning were well below the threshold causing damage to the coatings, as evidenced by the absence of damage on AFM-images with increasing scan size.

Figure 4 shows the AFM height images of (partial and complete) multilayered DNA-coatings of both [PDL/DNA] (Figure 4A-E) and [PAH/DNA] (Figure 4F-J) double-layers. For both types of coating, the AFM height images showed an optical increase in surface roughness. Further analysis of the surface roughness using RMS-values of both types of multilayered DNA-coatings showed significant increases with every step (i.e. 1½ double-layer) from $[PDL/DNA]_{1/2}$ and $[PAH/DNA]_2$ during the build-up of the coatings (Table 1). Furthermore, RMS-values of [PDL/DNA]-coatings were significantly lower than those of equivalent [PAH/DNA]-coatings after the deposition of 2 double-layers.

TABLE 1: DETERMINATION OF SURFACE ROUGHNESS (RMS (IN NM) ± STANDARD DEVIATION)

(Partial) coating	[PDL/DNA]	[PAH/DNA]
Control (Titanium-sputtered silicon)	1.64 ± 0.03	1.64 ± 0.03
$[double\text{-}layer]_{½}$	1.68 ± 0.27	1.99 ± 0.10
$[double\text{-}layer]_{2}$	2.40 ± 0.11*	1.96 ± 0.11
$[double\text{-}layer]_{3½}$	3.16 ± 0.17*	4.58 ± 0.96*
$[double\text{-}layer]_{5}$	5.49 ± 0.57*	8.32 ± 1.70*

*Asterisk indicates significantly increased surface roughness ($p<0.05$) compared to previous (partial) coating.

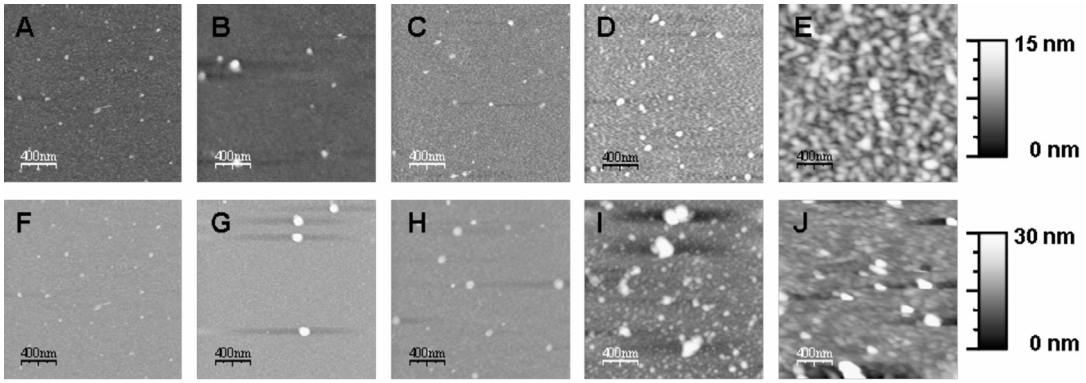

Figure 4: AFM height images of several stages during the build-up of a $[PDL/DNA]_5$ (A-E) and $[PAH/DNA]_5$ multilayered coating on titanium-sputtered silicon substrates. Images were taken after the adsorption of 0 (A and F), ½ (B and G), 2 (C and H), 3½ (D and I), and 5 (E and J) double-layers.

Typical differences in surface morphology between the two types of coatings included the spatial distribution of elevations, as well as their average height. Whereas $[PDL/DNA]_5$ showed a relatively homogenous morphological appearance with equally-spaced elevations of relatively low height

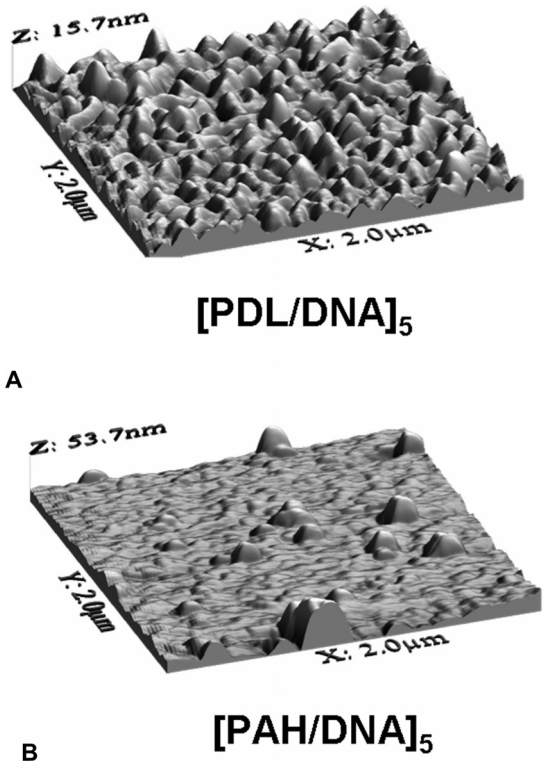

Figure 5: Three-dimensional images of the morphology of a $[PDL/DNA]_5$ and $[PAH/DNA]_5$ multilayered coating on titanium-sputtered silicon substrates.

(average 6 nm), $[PAH/DNA]_5$ showed randomly-distributed elevations of relatively large height (average 14 nm). To further illustrate these differences, 3D-image reconstructions of both complete multilayered DNA-coatings are presented in Figure 5.

X-ray photospectroscopy (XPS)

The XPS spectra of DNA (dropcast) and 1, 3½ , and 5 double-layers of [PDL/DNA] or [PAH/DNA] on titanium-sputtered silicon substrates are presented in Figure 6. The XPS spectrum of DNA (dropcast) showed the presence of magnesium (Mg), probably as a cationic counter ion, whereas almost no sodium (Na) or potassium (K) peaks could be detected. Correspondingly, XPS spectra of DNA-terminated [PDL/DNA]-coatings showed the presence of Mg-peaks. However, DNA-terminated [PAH/DNA]-coatings did not show the presence of Mg-peaks, nor did coatings terminated with a cationic layer (PDL or PAH). Furthermore, a distinct difference was observed regarding the presence of titanium (Ti) peaks. Whereas partial and complete [PAH/DNA]-coatings showed the presence of Ti-peaks, equivalent [PDL/DNA]-coatings did not.

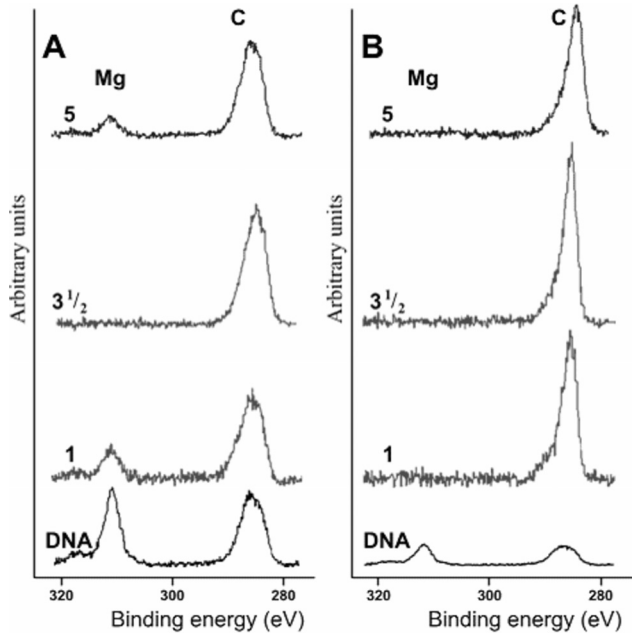

Figure 6: XPS spectra of dropcast DNA film and indicated number of double-layers for (A) [PDL/DNA] or (B) [PAH/DNA]. Scaling of the spectra is adjusted for constant integrated intensity of Phosphorus 2p emissions (not shown).

No angle dependency was observed regarding the phosphorus/nitrogen ratio (I_{P2p} / I_{N1s}) for the (dropcast) DNA film, as expected from a one-component film. Interestingly, (partial) [PDL/DNA]- and [PAH/DNA]-coatings also showed no angle dependency, implying a homogeneous distribution of DNA in the surface region of the coatings.

The amount of DNA in the top (5 - 10 nm) of the multilayered coatings was calculated using Formula 1 (see Materials & Methods section). Table 2 demonstrates that [PDL/DNA]-coatings display a higher DNA content in the DNA-terminated layers compared to [PAH/DNA]-coatings.

Contact angle measurements

Regardless of the substrate used (either quartz or titanium-sputtered silicon), the contact angles demonstrated to be higher after the adsorption of the positively-charged polymer (either PDL or PAH) than after the adsorption of the negatively-charged DNA (data not shown). When the build-up of both types of multilayered DNA-coatings progressed, the alternating behavior of the contact angles became more pronounced.

Fourier transform infrared spectroscopy (FTIR)

DNA exhibited its characteristic bands of base-pairs at 1602 cm^{-1} (adenine), 1650 cm^{-1} (thymine), 1684 cm^{-1} (guanine), and 1481 cm^{-1} (cytosine) [25]. For characterization, however, spectra with minimum wavelengths of 1250 cm^{-1} were used, since PDL and PAH do not have characteristic infrared spectral criterions below this wavelength.

Infrared spectral criterions of the DNA double helical structure can be observed in the 1250 – 950 cm^{-1} sugar-phosphate backbone vibration range (Figure 7; upper line). DNA showed its characteristic

absorption bands at 1235, 1088, 1063, and 963 cm^{-1}, which can be assigned to the antisymmetric stretching of the phosphate groups (ν_{as} 1235 cm^{-1}) [26], the symmetric stretching vibrations of the phosphate groups (ν_s 1088 & 1063 cm^{-1}) [18;19], and the CC stretching of the backbone (963 cm^{-1}) [26], respectively.

Both the $[PDL/DNA]_5$ (Figure 7; middle line) and $[PAH/DNA]_5$ (Figure 7; lower line) multilayered coatings showed the characteristic infrared absorption band at 1088 cm^{-1}, corresponding with the ν_s band. Furthermore, a frequency shift of the ν_{as} absorption band is visible for $[PDL/DNA]_5$ (1235 → 1213 cm^{-1}) and for $[PAH/DNA]_5$ (1235 → 1224 cm^{-1}).

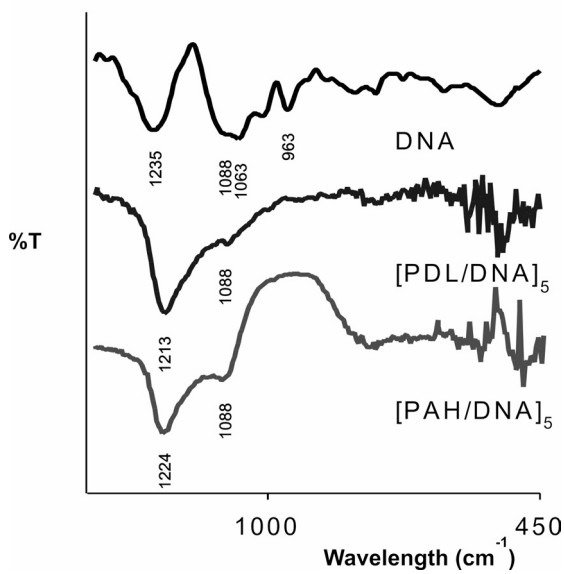

Figure 7: FTIR-spectra of DNA (upper line), $[PDL/DNA]_5$ (middle line), and $[PAH/DNA]_5$ (bottom line). Both types of multilayered DNA-coatings were build-up on quartz substrates.

DNA immobilization during the build-up of multilayered coatings

The amount of DNA (μg/substrate) immobilized into the multilayered DNA-coatings was analyzed using radiolabeled DNA. In Figure 8, the progressive immobilization of DNA into multilayered DNA-coatings titanium is represented. Results of the DNA-immobilization into multilayered DNA-coatings on glass substrates were also performed (data not shown). Whereas on glass substrates the amount of DNA immobilized in the first double-layer is higher for [PDL/DNA]-coatings than for [PAH/DNA]-coatings (33 vs. 20 μg/substrate, respectively), an equal amount of DNA (~20 μg/substrate) is immobilized into the first double-layer of both types of multilayered DNA-coatings on titanium substrates. After the generation of the first double-layer, both types of multilayered DNA-coatings immobilize a constant amount of DNA with each successively-adsorbed double-layer, irrespective of the substrate material (i.e. glass or titanium) onto which the multilayers are adsorbed. The amount of DNA immobilized into the multilayered DNA-coatings is approximately 9-10 μg DNA per double-layer (≈ 3 $\mu g/cm^2$).

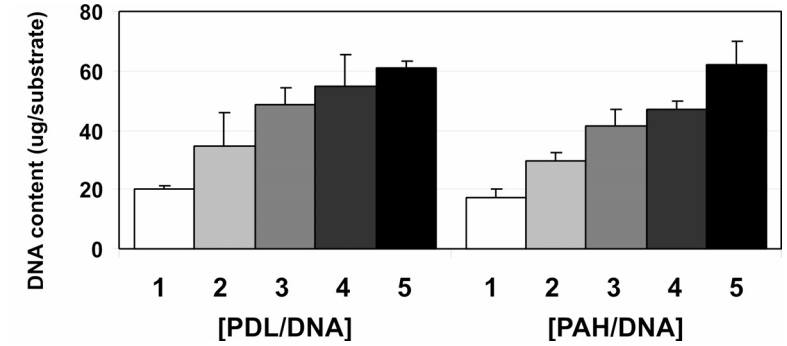

Figure 8: Immobilization of DNA into each double-layer during the build-up of $[PDL/DNA]_5$ and $[PAH/DNA]_5$ coatings on titanium substrates. Measurements were performed using radiolabeled DNA.

Biological assessment

Mutagenicity assay

Incubation of a mutant strain of *Salmonella typhimurium* (TA100) in selected concentrations of DNA (250 and 2500 μg/ml), PDL (25 and 250 μg/ml), or PAH (250 and 2500 μg/ml) did not show a significant increase in reverse-mutation ($p>0.05$; data not shown). Negative and positive controls showed a limited and an intensive increase in reverse-mutation, respectively.

Cell proliferation and viability

The results of a representative cell proliferation assay are presented in Figure 9. Compared to non-coated control substrates, significantly higher cell numbers ($p<0.05$) were observed at almost every assayed time point on both types of multilayered DNA-coatings. No differences in cell proliferation between the two types of multilayered DNA-coatings were observed.

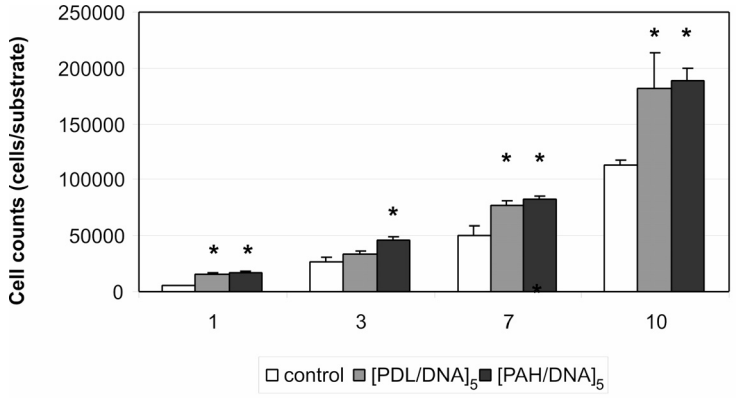

Figure 9: Proliferation of RDF cells on non-coated titanium controls, $[PDL/DNA]_5$-, and $[PAH/DNA]_5$-coated titanium substrates. Results are shown as mean ± SD. Asterisks indicate significant difference compared to non-coated control ($p<0.05$).

To assess potential effects of multilayered DNA-coatings on cell viability, the mitochondrial redox activity was assessed using a MTT-based assay. Neither of the two types of multilayered DNA-coatings significantly decreased mitochondrial redox activity of RDF cells after 3 days of culture (data not shown).

Cell morphology

The morphological appearance of the primary fibroblast cells, cultured on both types of multilayered DNA-coatings and non-coated titanium controls, was evaluated using scanning electron microscopy. Figure 10 presents representative images of these cells after a 3-day culture period. Although the native roughness of the as-machined titanium substrates does not allow a clear observation of completely spread cells, it becomes apparent from slightly elevated cells that both types of multilayered DNA-coatings do not alter the morphological appearance of the cells compared to non-coated titanium controls. In general, all cells had a typical fibroblast appearance with several (short) cellular extensions.

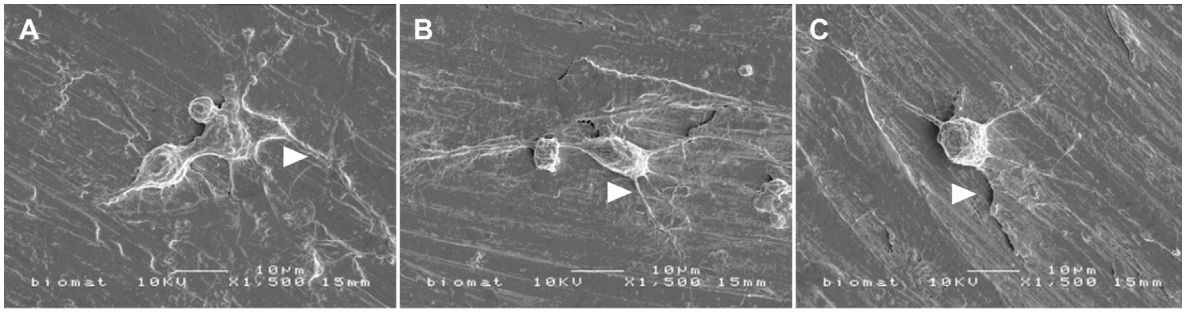

Figure 10: SEM images showing the morphology of RDF cells on (A) non-coated titanium controls, (B) $[PDL/DNA]_5$-, and (C) $[PAH/DNA]_5$-coated titanium substrates after 3 days of cell culture. Note the presence of multiple cellular extensions (arrowheads) of the fibroblasts on all types of substrates.

IV DISCUSSION

The aim of this study was to fabricate and characterize multilayered DNA-coatings, generated via the ESA-technique. The choice of DNA as the anionic building block relates to the structural properties of the DNA-molecule and their potential beneficial effects in implantology rather than to the encoded genetic information. As the cationic building blocks, either PDL or PAH was used.

Many researchers utilize a polyelectrolyte, which under neutral acidity is extremely charged (e.g. poly(ethyleneimine), PEI; or poly(styrenesulfonate), PSS) as the primary layer(s) onto the substrate of desire [15;19;20;22;27-31]. This is done to achieve optimal coverage of the oppositely-charged substrate. However, other researchers do not indicate this necessity [17;32-35]. To avoid potential detrimental effects of PEI on cellular behavior [27], and because the build-up of PEMs is well-acceptable without using extremely-charged polyelectrolytes as a primary layer, the use of polyelectrolytes for our two types of multilayered DNA-coatings was limited to the functional anionic polyelectrolyte DNA, and one specific cationic polyelectrolyte (either PDL or PAH).

The build-up of multilayered DNA-coatings has been demonstrated to be dependent on the type of cationic polyelectrolyte used. Linear build-up regimes have been demonstrated for PAH-containing coatings [14;21;36], whereas exponential build-up regimes were found for PLL-containing coatings [35;37]. Although the driving force for both growth regimes is essentially similar (i.e. the charge overcompensation with each deposited polyionic layer), the diffusive behavior of PLL throughout the coatings allows an exponential build-up, proportional to the amount of PLL that diffuses out of the coating during immersion in a polyanionic solution [37;38]. However, based on both the UV-spectrophotometry results and the results of the immobilization of radiolabeled DNA in our study, we conclude that the build-up regime for both our $[PDL/DNA]_5$ and $[PAH/DNA]_5$ coatings is linear, with typical incremental increases with each successively adsorbed double-layer of approximately 10 μg DNA on titanium substrates, respectively. Interestingly, a substrate-dependent difference in the amount of DNA immobilized in the first double-layer was found for multilayered DNA-coatings. Probably, these differences relate to the amount of cationic polyelectrolyte adsorbed in the primary adsorption layer and the inherent specific affinity of the used cationic polyelectrolytes for each type of substrate.

The structure of the DNA after immobilization into either the $[PDL/DNA]_5$ or $[PAH/DNA]_5$ coating remains unclear. The shift of the ν_{as} band from 1235 to 1213 cm^{-1} for $[PDL/DNA]_5$ coatings and from 1235 to 1224 cm^{-1} for [PAH/DNA]-coatings may reflect a change in the conformation from A to Z-form and from A to B-form, respectively [26]. Shifts of the ν_{as} band after complexation of DNA with cationic polyelectrolytes or ions have been observed frequently [18;19;39], and are explained by the interaction of the anionic phosphate groups of the DNA-molecules with cationic counterparts. Additionally, the relative humidity of multilayered DNA-coatings is an important factor determining the precise location of characteristic bands [19]. Nevertheless, the results of the FTIR spectroscopy clearly indicate the presence of double-helical DNA within both types of multilayered DNA-coating, as evidenced by the presence of the characteristic absorption band at 1088 cm^{-1} [19]. The biological relevance of DNA structure in the coatings remains to be determined.

AFM images of both types of multilayered DNA-coatings clearly demonstrate a nanoscale roughness for both $[PDL/DNA]_5$ and $[PAH/DNA]_5$. The difference in RMS-roughness calculation between equal numbers of [PDL/DNA]- and [PAH/DNA]-double-layers most probably also relates to the adsorption of the first cationic polyelectrolyte layer. The more homogenous $[PDL/DNA]_5$-coating (RMS = 5.49 nm) reflects a uniform adsorption of the primary PDL-layer, whereas for the $[PAH/DNA]_5$-coating (RMS = 8.32 nm) randomly-distributed elevations suggest a heterogeneous adsorption of the primary PAH-layer. This is further evidenced by the results of the contact angle measurements, which show a more pronounced alternating behavior after the adsorption of several double-layers.

XPS-data corroborate with the results of the AFM-measurements. The build-up of [PDL/DNA]-coatings is more homogeneously than that of [PAH/DNA]-coatings, reflected by the presence of Ti-peaks and the absence of Mg-peaks in the latter coatings. A less homogeneous DNA incorporation and/or an irregular build-up regime of the multilayer structure for [PAH/DNA]-coatings might explain these results.

Additionally, the absence of Mg-peaks in the DNA-terminated [PAH/DNA]-coatings might be an indication that in this case all counter ions of the DNA are exchanged by the positively-charged PAH-component, resulting in a decreased three-dimensional structure of the DNA-molecules. Hence, Ti-peaks might be present in [PAH/DNA]-coatings due to the limited thickness of these coatings. The absence of angle-dependent differences in the $^{P}/_{N}$-ratios for both types of coatings indicates a homogeneous distribution of the molecules in the top (5 - 10 nm) of the coatings. Therefore, the layers can be regarded as not completely separated, but partly mixed. This mixed character of PEMs has been described previously [14].

The mutagenicity assay demonstrated that the materials used to generate both types of multilayered DNA-coatings are non-mutagenic. Further biological assessment revealed that fibroblast cell proliferation was increased on both types of multilayered DNA-coatings compared to non-coated titanium controls. Although the reason remains unclear, the increased surface roughness [40-43] or an altered protein adsorption profile on both types of multilayered DNA-coatings might affect fibroblast cell proliferation. Nevertheless, we attribute the elevated cell growth to the presence of a multilayered DNA-coating, and not for instance to DNA release from the layers. In view of the studies performed by Kitamura et al. [44], who demonstrated that the addition of DNA to the culture medium significantly decreases the proliferation of fibroblast cells, this furthermore indicates the stability of the multilayered DNA-coatings. The metabolic activity of the fibroblast cells cultured on both types of multilayered DNA-coatings was not affected, indicating that both types of multilayered DNA-coatings are cytocompatible.

CONCLUSION

In conclusion, this study demonstrates the feasibility of the ESA-technique to fabricate multilayered DNA-coatings. UV-vis spectrophotometry, AFM, and contact angle measurements clearly indicated the progressive build-up of both [PDL/DNA]- and [PAH/DNA]-multilayers. Furthermore, AFM and XPS data showed a more uniform build-up and morphology of [PDL/DNA]-coatings compared to [PAH/DNA]-coatings. The DNA-immobilization into both types of multilayered DNA-coatings was linear, and approximated 3 $\mu g/cm^2$ into each double-layer, irrespective of cationic polyelectrolyte and substrate material. The surface morphology of both types of multilayered DNA-coatings showed elevations in the nanoscale range. Biological assessment demonstrated an increased proliferation of primary fibroblasts on both types of multilayered DNA-coatings compared to non-coated titanium controls. Cell viability and morphology were unaffected by the presence of either type of multilayered DNA-coating. Further biocompatibility and functionalization of the coatings produced here, will be assessed in subsequent cell culture and animal-implantation studies.

V ACKNOWLEDGEMENTS

We thank Dr. Bas Feddes (Dept. Peridodontology & Biomaterials, UMC St Radboud, Nijmegen) and Dr. Gerald Verhaegh for their help with the AFM analyses and the radiolabeled DNA-experiments, respectively. AFM imaging was performed in collaboration with the Microscopical Imaging Center of the Nijmegen Center for Molecular Life Sciences (NCMLS). Mr. Maichel van Riel (Control Laboratory, Central Animal Facility, Radboud University Nijmegen Medical Centre) is acknowledged for his assistance with performing the mutagenicity assay. This study was financially supported by the Dutch Technology Foundation STW, grant # NKG.5758.

VI REFERENCES

1. Kasemo, B. and J. Gold. 1999. Implant surfaces and interface processes. *Adv Dent Res* 13:8-20.
2. Castner D.G. and Ratner B.D. 2002. Biomedical surface science: Foundations to frontiers. *Surf Sci* 500:28-60.
3. Krieg, A. M. 2000. Immune effects and mechanisms of action of CpG motifs. *Vaccine* 19:618-22.
4. Stryer, L. 1995. *Biochemistry*. W.H. Freeman and Company, New York, USA.
5. Krieg, A. M., A. K. Yi, S. Matson, T. J. Waldschmidt, G. A. Bishop, R. Teasdale, G. A. Koretzky, and D. M. Klinman. 1995. CpG motifs in bacterial DNA trigger direct B-cell activation. *Nature* 374:546-9.
6. McMichael, A. J. 1992. Antigens and MHC systems. In *Oxford textbook of pathology*. J. O. D. McGee, P. G. Isaacson, and N. A. Wright, eds. Oxford University Press, Oxford, UK.
7. Werner, M. H. , A. M. Gronenborn, and G. M. Clore. 1996. Intercalation, DNA kinking, and the control of transcription. *Science* 271:778-84.
8. Wilson, W. D. 1996. Reversible interactions of nucleic acids with small molecules. In *Nucleic acids in chemistry and biology*. G. M. Blackburn and M. J. Gait, eds. Oxford University Press, Oxford, UK.
9. Tretinnikov, O. N., K. Kato, and Y. Ikada. 1994. In vitro hydroxyapatite deposition onto a film surface-grated with organophosphate polymer . *J Biomed Mater Res* 28:1365-73.
10. Kamei, S., N. Tomita, S. Tamai, K. Kato, and Y. Ikada. 1997. Histologic and mechanical evaluation for bone bonding of polymer surfaces grafted with a phosphate-containing polymer. *J Biomed Mater Res* 37:384-93.
11. Yamada, M., K. Kato, M. Nomizu, N. Sakairi, K. Ohkawa, H. Yamamoto, and N. Nishi. 2002. Preparation and characterization of DNA films induced by UV irradiation. *Chemistry* 8:1407-12.
12. Inoue, Y., T. Fukushima, T. Hayakawa, H. Takeuchi, H. Kaminishi, K. Miyazaki, and Y. Okahata. 2003. Antibacterial characteristics of newly developed amphiphilic lipids and DNA-lipid complexes against bacteria. *J Biomed Mater Res* 65A:203-8.
13. Fukushima, T., Y. Inoue, T. Hayakawa, K. Taniguchi, K. Miyazaki, and Y. Okahata. 2001. Preparation of and tissue response to DNA-lipid films. *J Dent Res* 80:1772-6.
14. Decher G. Fuzzy Nanoassemblies: Toward Layered Polymeric Multicomposites. Science 277, 1232-1237. 97.
15. Pei, R., X. Cui, X. Yang, and E. Wang. 2001. Assembly of alternating polycation and DNA multilayer films by electrostatic layer-by-layer adsorption. *Biomacromolecules* 2:463-8.
16. Sastry, M., M. Rao, and K. N. Ganesh. 2002. Electrostatic assembly of nanoparticles and biomacromolecules. *Acc Chem Res* 35:847-55.
17. Luo, L., J. Liu, Z. Wang, X. Yang, S. Dong, and E. Wang. 2001. Fabrication of layer-by-layer deposited multilayer films containing DNA and its interaction with methyl green. *Biophys Chem* 94:11-22.
18. Zhou, Y. and Y. Li. 2004. Studies of interaction between poly(allylamine hydrochloride) and double helix DNA by spectral methods. *Biophys Chem* 107:273-81.
19. Sukhorukov, G. B., M. M. Montrel, A. I. Petrov, L. I. Shabarchina, and B. I. Sukhorukov. 1996. Multilayer films containing immobilized nucleic acids. Their structure and possibilities in biosensor applications. *Biosens Bioelectron* 11:913-22.
20. Sukhorukov G.B. , Mohwald H. , Decher G. , and Lvov Y.M. Assembly of polyelectrolyte multilayer films by consecutively alternating adsorption of polynucleotides and polycations. Thin Solid Films 284-285, 220-223. 96.
21. Lvov Y. , Decher G. , and Sukhorukov G. Assembly of thin films by means of successive deposition of alternate layers of DNA and Poly(allylamine). Macromolecules 26, 5396-5399. 93.
22. Chen X. , Lang J. , and Liu M. Layer-by-layer assembly of DNA-dye complex films. Thin Solid Films 409, 227-232. 2002.
23. Hill, I. R., M. C. Garnett, F. Bignotti, and S. S. Davis. 2001. Determination of protection from serum nuclease activity by

DNA-polyelectrolyte complexes using an electrophoretic method. *Anal Biochem* 291:62-8.

24. Schonhoff M. Layered polyelectrolyte complexes: physics of formation and molecular properties. J Phys: Condens Matter 15, R1781-R1808. 2003.

25. Liu, W., Sun, S., Cao, Z., Zhang, X., Yao, K., Lu, W. W., and Luk, K. D. K. An investigation on the physicochemical properties of chitosan/DNA polyelectrolyte complexes. Biomaterials .

26. Banyay, M., Sarkar, M., and Graslund, A. A library of IR bands of nucleic acids in solution. Biophys Chem 104(2), 477-488. 2003.

27. Tryoen-Toth, P., D. Vautier, Y. Haikel, J. C. Voegel, P. Schaaf, J. Chluba, and J. Ogier. 2002. Viability, adhesion, and bone phenotype of osteoblast-like cells on polyelectrolyte multilayer films. *J Biomed Mater Res* 60:657-67.

28. Serrano, M. C., R. Pagani, M. Vallet-Regi, J. Pena, A. Ramila, I. Izquierdo, and M. T. Portoles. 2004. In vitro biocompatibility assessment of poly(epsilon-caprolactone) films using L929 mouse fibroblasts. *Biomaterials* 25:5603-11.

29. Zhu, H., J. Ji, and J. Shen. 2004. Construction of multilayer coating onto poly-(DL-lactide) to promote cytocompatibility. *Biomaterials* 25:109-17.

30. Boura, C., P. Menu, E. Payan, C. Picart, J. C. Voegel, S. Muller, and J. F. Stoltz. 2003. Endothelial cells grown on thin polyelectrolyte mutlilayered films: an evaluation of a new versatile surface modification. *Biomaterials* 24:3521-30.

31. Tedeschi, C., H. Mohwald, and S. Kirstein. 2001. Polarity of layer-by-layer deposited polyelectrolyte films as determined by pyrene fluorescence. *J Am Chem Soc* 123:954-60.

32. Richert, L., F. Boulmedais, P. Lavalle, J. Mutterer, E. Ferreux, G. Decher, P. Schaaf, J. C. Voegel, and C. Picart. 2004. Improvement of stability and cell adhesion properties of polyelectrolyte multilayer films by chemical cross-linking. *Biomacromolecules* 5:284-94.

33. Richert, L., P. Lavalle, D. Vautier, B. Senger, J. F. Stoltz, P. Schaaf, J. C. Voegel, and C. Picart. 2002. Cell interactions with polyelectrolyte multilayer films. *Biomacromolecules* 3:1170-8.

34. Shi, X., Sanedrin, R. J., and Zhou, F. Structural characterization of multilayered DNA and polylysine composite films: influence of ionic strength of DNA solutions on the extent of DNA incorporation. J Phys Chem B 106, 1173-1180. 2002.

35. Picart, C., Lavalle, Ph., Hubert, P., Cuisinier, F. J. G., Decher, G., Schaaf, P., and Voegel, J.-C. Buildup mechanism for poly(L-lysine)/Hyaluronic acid films onto a solid surface. Langmuir 17, 7414-7424. 2001.

36. Decher, G., Hong, J. D., and Schmitt, J. Buildup of ultrathin multilayer films by a self-assembly process: III. Consecutively alternating adsorption of anionic an cationic polyelectrolytes on charged surfaces. Thin Solid Films 210-211, 831-835. 92.

37. Picart, C., J. Mutterer, L. Richert, Y. Luo, G. D. Prestwich, P. Schaaf, J. C. Voegel, and P. Lavalle. 2002. Molecular basis for the explanation of the exponential growth of polyelectrolyte multilayers. *Proc Natl Acad Sci U S A* 99:12531-5.

38. Mendez Garza, J., Schaaf, P., Muller, S., Ball, V., Stoltz, J-F., Voegel, J-C., and Lavalle, P. Multicompartment Films Made of Alternate Polyelectrolyte Multilayers of Exponential and Linear Growth. Langmuir 20, 7298-7302. 2004.

39. Zhou, Y. and Li, Y. Layer-by-Layer Self-Assembly of Multilayer Films Containing DNA and Eu^{3+}: Their Characteristics and Interactions with Small Molecules. Langmuir 20, 7208-7214. 2004.

40. Flemming, R. G., C. J. Murphy, G. A. Abrams, S. L. Goodman, and P. F. Nealey. 1999. Effects of synthetic micro- and nano-structured surfaces on cell behavior. *Biomaterials* 20:573-88.

41. Thapa, A., D. C. Miller, T. J. Webster, and K. M. Haberstroh. 2003. Nano-structured polymers enhance bladder smooth muscle cell function. *Biomaterials* 24:2915-26.

42. Zhang, R. and P. X. Ma. 2000. Synthetic nano-fibrillar extracellular matrices with predesigned macroporous architectures. *J Biomed Mater Res* 52:430-8.

43. Teixeira, A. I., G. A. Abrams, P. J. Bertics, C. J. Murphy, and P. F. Nealey. 2003. Epithelial contact guidance on well-defined micro- and nanostructured substrates. *J Cell Sci* 116:1881-92.

44. Kitamura, H., N. Takemoto, M. Mizuno, Y. Kuboki, N. Sakairi, and N. Nishi. 1997. Suppression for the proliferation of fibroblasts by external DNA. *Int J Biol Macromol* 21:337-40.

3

CYTO- AND HISTOCOMPATIBILITY OF MULTILAYERED DNA-COATINGS ON TITANIUM

JJJP van den Beucken, XF Walboomers, MRJ Vos, NAJM Sommerdijk, RJM Nolte, JA Jansen

J Biomed Mater Res 77A (2006);202 – 211

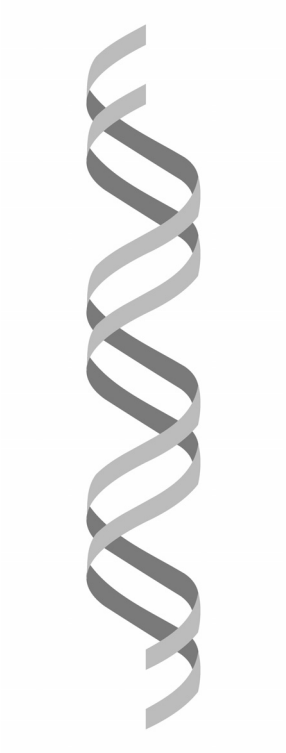

I INTRODUCTION

The control over cellular and tissue interactions with biomaterial surfaces is gaining importance. Currently, we observe an increase in the use of implants and prostheses. Moreover, the implants are placed more frequently in ageing patients suffering from all kinds of health problems, including metabolic disorders, vascular diseases, and diabetes. A frequently observed side-effect of such conditions is the interference with the healing response around implants [1]. Additionally, age-related delayed wound healing in senile recipients of implants might aggravate wound healing responses around implants [2]. Therefore, implant surfaces that evoke a controlled cellular and tissue response gain importance.

Titanium and its alloys are widely applied materials for the generation of implants. Especially for orthopedic and dental applications [3;4], titanium (or its alloys) is the material of choice due to its biomechanical properties. Also for soft tissue implants, titanium is used for the production of pacemakers and the anchorage of percutaneous devices [5;6].

A recently introduced idea to improve implant performance is the use of deoxyribonucleic acid (DNA) to coat implants. Due to the homogeneity of this molecule in vertebrate species, DNA can be regarded as non- or low immunogenic [7-9]. Furthermore, its capacity to incorporate other substances (e.g. cytokines, growth factors, and antibiotics) turns DNA into a potential drug-delivery vehicle. Finally, the high phosphate content in the DNA backbone might facilitate the deposition of calciumphosphates [10;11]. Together, these properties give DNA high potential as a versatile implant coating material that (a) reduces adverse immunological responses, (b) allows functionalization with desired substances and subsequent modulation of tissue responses, and (c) is applicable in both soft and hard tissues.

Recently, the fabrication and characterization of multilayered DNA-coatings for biomaterial purposes was reported [12]. These coatings were fabricated using the so-called electrostatic self-assembly (ESA) technique [13], which allows the build-up of a layered coating via the alternate adsorption of cationic polyelectrolytes (poly-D-lysine, PDL; poly(allylamine) hydrochloride, PAH) and anionic DNA. The fabricated multilayered DNA-coatings, consisting of 5 double-layers, were shown to have a nano-rough surface morphology and incorporated approximately 15 μg DNA/cm^2. Additionally, an Ames test-based assay demonstrated that the materials used to build up the multilayered DNA-coatings were non-mutagenic.

In view of the proposed beneficial properties of DNA, a first step towards the use of DNA as an implant coating material is to evaluate cell and tissue responses to non-functionalized, multilayered DNA-coatings. Therefore, the aim of this study was to evaluate the cyto- and histocompatibility of non-functionalized multilayered DNA-coatings on titanium. First, *in vitro* assays with primary fibroblasts were used to study cell proliferation and viability. Secondly, the soft tissue reaction to multilayered DNA-coatings was assessed when implanted subcutaneously in rats.

II MATERIALS & METHODS

Materials

Polyanionic DNA (± 300 bp/molecule; sodium salt) was kindly provided by Nichiro Corporation (Kawasaki-shi, Kanagawa prefecture, Japan). Potential protein impurities in the DNA were checked using the BCA protein assay (Pierce, Rockford, Illinois, USA) and measured to be below 0.20% w/w (data not shown). Polycationic polyelectrolytes poly(allylamine hydrochloride) (PAH; MW ~70000) and poly-D-lysine (PDL; MW 30000 – 70000) were purchased from Sigma (Sigma-Aldrich Chemie B.V., Zwijndrecht, the Netherlands). All materials were used without further purification.

Substrate preparation and cleaning

Titanium substrates were used for the build-up of multilayered DNA-coatings. For the *in vitro*-experiments, disc-shaped titanium substrates (12 mm diameter; commercially-pure titanium, as-machined) were used. For the *in vivo*-experiments, we used cylindrical titanium substrates (14 mm height, 4 mm diameter; commercially-pure titanium, as-machined). The surface roughness (Ra) of the

as-machined titanium was 0.3 μm, as determined using a universal surface tester (UST; Innowep, Wurzburg, Germany). Titanium substrates were cleaned ultrasonically using consecutively nitric acid (10% v/v), acetone, and isopropanol. Between each cleaning step, the substrates were rinsed with ultra-pure water. After the last cleaning step, the substrates were dried to air. After cleaning, prepared substrates were either directly sterilized (to serve as non-coated controls) or processed for DNA-coating.

Generation of multilayered DNA-coatings
Multilayered DNA-coatings were generated using the ESA technique, as described by Van den Beucken et al. [12]. Briefly, the cleaned substrates were immersed in an aqueous solution of either PDL (0.1 mg/ml) or PAH (1 mg/ml) for 30 minutes, allowing sufficient time for the adsorption of the first cationic polyelectrolyte layer onto the substrates. Subsequently, the substrates were washed in ultra-pure water (5 minutes, continuous water flow) and dried using a pressurized air stream. Thereafter, the substrates were alternately immersed in an anionic aqueous DNA solution (1 mg/ml) and the respective cationic polyelectrolyte solution for 7 minutes each, with intermediate washing in ultra-pure water (5 minutes, continuous water flow) and drying using a pressurized air stream. The build-up of the multilayered DNA-coatings was continued until a total of 5 double-layers were reached. These were designated either $[PDL/DNA]_5$ or $[PAH/DNA]_5$ (the number indicates the number of double-layers).

Substrate sterilization
All substrates, coated with either type of multilayered DNA-coating or non-coated control substrates, were sterilized using a UV-irradiation treatment (254 nm; 4 hrs).

In vitro experiments
Cell culture and seeding
Rat dermal fibroblasts (RDF) were obtained from the ventral skin of male Wistar rats, using a standard procedure as described previously [14], after which cells were cryo-preserved. Before the initiation of an experiment, cells were thawed and cultured in culture medium (α-MEM (Gibco), supplemented with 10% (v/v) fetal calf serum (FCS) and gentamycin (50 μg/ml)). All assays were performed with cells of the 4^{th} or 5^{th} culture passage.
Prior to the assays, cells were detached using trypsin/EDTA (0.25% w/v trypsin/0.02% EDTA) and concentrated by centrifugation at 1500 rpm for 5 min. Subsequently, cells were resuspended in culture medium and counted using a Coulter® counter (Beckman Coulter Inc., Fullerton, CA, USA). For all in vitro assays, cells were seeded at 1 x 10^4 cells/substrate into 24 well plates (Greiner Bio-One BV, Alphen aan de Rijn, the Netherlands).

Live/dead assay
To further study cell viability and cytotoxicity, cells cultured on the experimental substrates for 3 days were conducted in a Live/Dead® assay (Molecular Probes, Inc., Eugene, OR, USA), according to the instructions of the manufacturer. Briefly, cells were washed twice with PBS. Subsequently, cells were incubated in appropriate amounts of fluorescent dye for 45 min. at 37°C. Then, cells were rinsed twice with PBS and visualized using a fluorescence microscope (Leica Microsystems AG, Wetzlar, Germany), equipped with a digital camera.

Cell viability
Cell viability was assessed using a commercially available cytotoxicity assay, according to the instructions of the manufacturer (Promega Corporation, Madison, WI, USA). The test is based on the conversion of a tetrazolium salt ([3-(4,5-dimethylthiazol-2-yl)-2,5-diphenyltetrazoliumbromide], MTT) into a formazan product. Briefly, at 3 days after cell seeding on the experimental substrates (3 substrates per condition; n=3), 150 μl dye solution was added to each well, and cells were incubated at 37 °C for 4 hours. Subsequently, 1 ml of solubilization/stop solution was added to each well, and cells were

incubated for another hour (at room temperature). Finally, the contents of the wells were mixed thoroughly using a pipette and the absorbance at 570 nm wavelength was read using a spectrophotometer. Measured absorbance values were corrected for cell numbers, using parallel samples, from which the cell number was determined using a Coulter® Counter. Normalization of the data was performed to the results of the non-coated control substrates.

Cell proliferation

At 1, 3, 7, and 10 days after seeding, the medium was aspirated and the cell layer was washed twice with PBS. Subsequently, substrates with attached cells were transferred into fresh wells and incubated with 0.5 ml trypsin/EDTA. After detachment of the cells, 0.5 ml culture medium was added. The cell suspension was diluted using Coulter® Isotone II diluent (Beckman Coulter Inc., Fullerton, CA, USA) and cell numbers were counted using a Coulter® counter. A total of 3 independent runs were performed, in which at each time point, 3 substrates per condition were used (n=3).

In vivo experiment

Animals and implantation procedure

For implantation, male Wistar rats of 200-250 grams were used. The animals were housed in the central animal facility at the Radboud University Nijmegen Medical Center (Nijmegen, the Netherlands), observing all national guidelines for care and use of laboratory animals. The animals received chow and water *ad libitum*. Prior to the implantation procedure, approval was acquired from the Ethical Committee for animal experiments at the Radboud University Nijmegen.

The implantation procedure was performed under general anesthesia of O_2, N_2O, and isoflurane. The dorsal skin was shaved and disinfected using iodine. On each side of the vertebral column, paravertebral incisions of approximately 10 mm were made. Lateral to these incisions, subcutaneous pockets were created by blunt dissection with scissors. After insertion of the implants, the wounds were closed using skin staples (Agraves®, InstruVet C.V., Cuijk, the Netherlands). A total of 48 implants (16 non-coated controls, 16 $[PDL/DNA]_5$, and 16 $[PAH/DNA]_5$) were distributed over 24 animals (2 implants per animal) according to a Latin Square randomization scheme.

Implant retrieval and histological preparations

After each implantation period (either 4 or 12 weeks), tissue-covered titanium implants were retrieved. The specimens were fixed in 4% buffered paraformaldehyde for 20 hours. Subsequently, the specimens were divided in two groups. In the first group, the implants were removed from the tissue capsule through an apical incision using tweezers. The separated tissue capsules were embedded in paraffin, after which 6 μm sections were cut in a transversal direction using a Leica RM 2165 Microtome (Leica Microsystems, Rijswijk, the Netherlands). The sections were cut from at least three arbitrary regions perpendicular to the long axis of the tissue capsule (paraffin sections). Paraffin sections were stained with haematoxylin/eosin. To detect potential tissue remains on the implant surface, the implants were dehydrated in a graded series of ethanol, air dried, sputter-coated with gold, and investigated by SEM directly afterwards excision.

In the second group, the specimens (implants including surrounding tissues) were dehydrated in ethanol, and embedded in methylmethacrylate (MMA). After polymerization, thin transversal sections (10 μm thickness) were prepared with a modified diamond blade sawing microtome technique [15](MMA-sections). The MMA-sections were stained with methylene blue and basic fuchsin.

Immunohistochemistry

For the detection of myofibroblasts, also immunohistochemistry was performed on the paraffin-embedded sections for α-smooth muscle actin (α-SMA). Deparaffinated sections were treated with 3% H_2O_2 in PBS for 20 minutes to block endogenous peroxidase and rinsed in PBS at room temperature. Subsequently, the tissue sections were fixed with 4% Formalin and blocked with 5% BSA (Sigma) in PBS.

Then, tissue sections were incubated with monoclonal IgG2a mouse anti α-SMA (Sigma), 1:1600 for 1 hour. After washing with PBS, the tissue sections were incubated with biotinylated donkey anti-mouse secondary antibody (Jackson Laboratories, West Grove, PA), 1:500 for 1 hour. After another washing step with PBS, staining was performed with a biotin-streptavidin detection system (Vectra elite kit; Vector Laboratories, Burlingame, CA) for 45 minutes. Positive controls (blood vessel walls) and negative controls (1% BSA in PBS) were included.

TABLE 1: HISTOLOGICAL GRADING SCALE FOR CAPSULE QUALITY

Histological capsule quality	score
Capsule tissue is fibrous, not dense, resembling connective or fat tissue in the non-injured regions	4
Capsule tissue is fibrous but immature, showing fibroblasts and little collagen	3
Capsule tissue is granulous and dense, containing both fibroblasts and many inflammatory cells	2
Capsule tissue consists of masses of inflammatory cells with little or no signs of connective tissue organization	1
Cannot be evaluated because of infection or other factors not necessarily related to the material	0

TABLE 2: HISTOLOGICAL GRADING SCALE FOR CAPSULE THICKNESS

Histological capsule thickness	score
1 – 4 fibroblasts	4
5 – 9 fibroblasts	3
10 – 30 fibroblasts	2
> 30 fibroblasts	1
Not applicable	0

Histological evaluation

Histological evaluation on all sections was performed using a light microscope (Leica Microsystems AG, Wetzlar, Germany). For the analyses of haematoxylin/eosin stained sections (paraffin excluding implants), a refined histomorphometric grading scale was used (Tables 1 & 2) [16]. Three observers independently scored a total of 3 paraffin sections per retrieved specimen.

Statistical analysis

Statistical analysis on the data of the *in vitro* experiments was performed using a one-way ANOVA and a post-hoc Tukey's Studentized Range Test. The histomorphometrical data of the *in vivo* experiment were processed in a two-way ANOVA and a post-hoc Tukey's Studentized Range Test. Data shown represent means ± SD. Calculations were performed in GraphPad Instat, Version 3.05 (GraphPad Software, San Diego, CA, USA).

III RESULTS

In vitro experiments

Live/Dead assay

Generally, the primary RDF cells, cultured on both types of multilayered DNA-coatings and non-coated controls, demonstrated high numbers of live (green) cells and hardly any dead (red) cells were observed (Figure 1). No apparent difference in the number of dead (red) cells was observed between non-coated control samples and either type of multilayered DNA-coatings. On the other hand, an apparent higher number of live (green) cells were observed on both types of multilayered DNA-coatings compared to non-coated control samples.

Cell viability

To assess potential effects of multilayered DNA-coatings on cell viability, the mitochondrial activity was measured using a MTT-based assay. The capacity of the mitochondrial enzyme succinate dehydrogenase to reduce MTT is a measure to evaluate the metabolic activity of cells, as this enzyme is centrally involved in both oxidative phosphorylation and the tricarboxylic acid cycle [17]. In Figure 2, the normalized results of the MTT-based assay after 3 days of cell culture are presented, in which the normalized values are corrected for cell number. Neither type of multilayered DNA-coatings decreased

mitochondrial redox activity of RDF cells (after 3 days of culture) compared to non-coated controls ($p>0.05$).

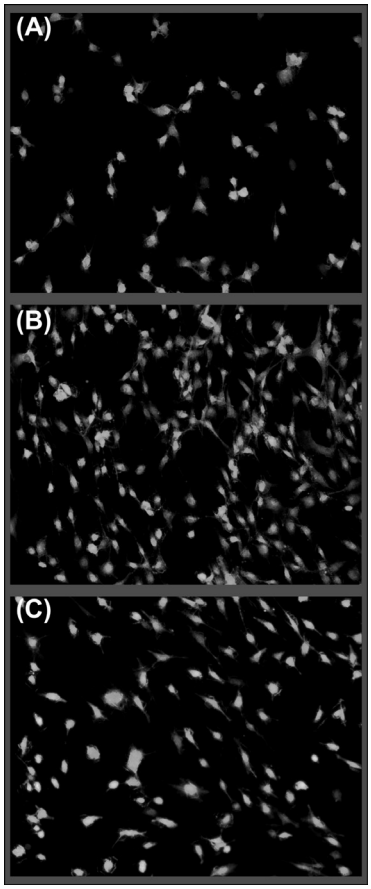

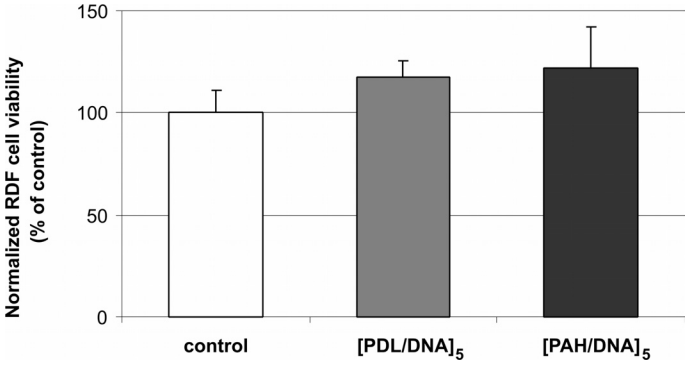

Figure 1(left): Representative fluorescence images of RDF cells, cultured for 3 days on (A) non-coated control substrates, (B) $[PDL/DNA]_5$, and (C) $\{PAH/DNA]_5$ fabricated on titanium substrates (original magnification 20x).

Figure 2 (top):Viability of RDF cells on multilayered DNA-coatings fabricated on titanium substrates.

Cell proliferation

The results of a representative proliferation experiment are presented in Figure 3. Proliferation of primary rat dermal fibroblasts (RDFs) was monitored on non-coated controls, $[PDL/DNA]_5$-coated, and $[PAH/DNA]_5$-coated titanium substrates. Compared to non-coated control titanium substrates, significantly higher cell numbers ($p<0.05$) were observed at almost every assayed time point on both types of multilayered DNA-coatings, corresponding with the results of the Live/Dead assay. No statistical significant differences ($p>0.05$) were found between the cell numbers on the $[PDL/DNA]_5$- and $[PAH/DNA]_5$-coated substrates.

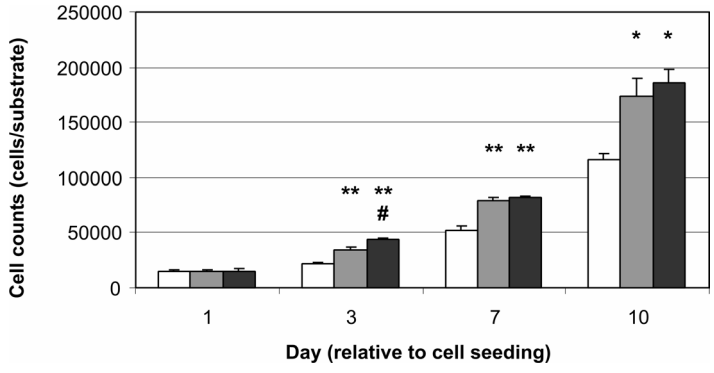

Figure 3: Proliferation of rat dermal fibroblast (RDF) cells on non-coated control substrates (white bars), $[PDL/DNA]_5$ (grey bars), and $[PAH/DNA]_5$ (black bars) fabricated on titanium substrates. Results are shown as means ± SD of triplicate wells for one representative experiment out of three. (*), significantly different from non-coated control substrates, $p < 0.01$. (**), significantly different from non-coated control substrates, $p < 0.001$. (#), significantly different from $[PDL/DNA]_5$-coated substrates, $p < 0.01$.

In vivo experiment

General observations

During the experiment, none of the 24 experimental animals showed any clinical signs of illness. Furthermore, none of the experimental animals showed wound complications after implantation. All 48 implants could be retrieved after the intended implantation periods. At implant retrieval, no macroscopic signs of inflammation or adverse tissue reactions could be observed. All implants were surrounded by a semi-transparent fibrous capsule.

SEM observation of excised implants

At each time point (4 and 12 weeks) after fixation of the retrieved specimens, implants were excised from the surrounding capsule tissue and prepared for scanning electron microscopic examination. The excised implants were only scarcely covered with biological compounds, which were not identifiable as cellular material (Figure 4) but as a proteinaceous-like deposits. No apparent differences in coverage with biological compounds were observed between non-coated titanium control implants and implants coated with either $[PDL/DNA]_5$ or $[PAH/DNA]_5$.

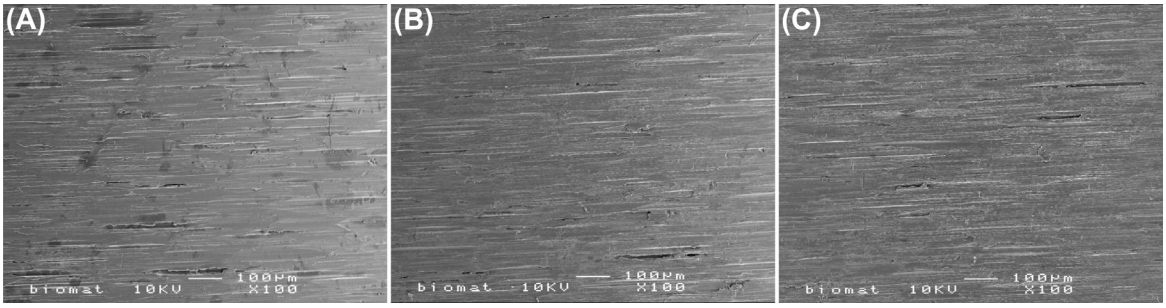

Figure 4: Representative electron microscopy images of an excised (A) non-coated control implant, (B) $[PDL/DNA]_5$, and (C) $[PAH/DNA]_5$, after 12 weeks of implantation.

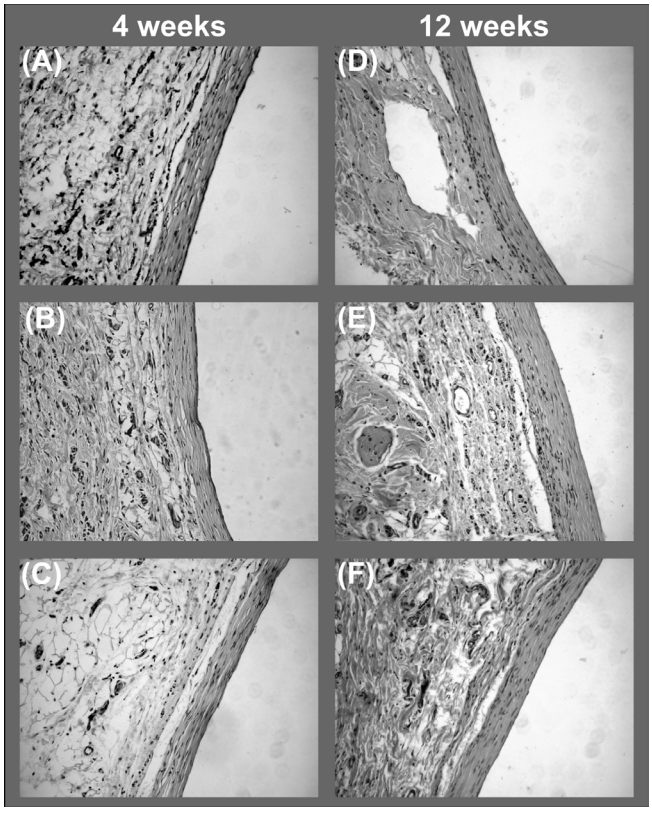

Figure 5: Light microscopic images of tissue capsule surrounding titanium control implants (A and D), $[PDL/DNA]_5$- (B and E), and $[PAH/DNA]_5$-coated titanium implants after implantation periods of 4 (A, B, and C) and 12 weeks (D, E, and F).

Descriptive histological evaluation

Gross evaluation of the sections of the implant surrounding tissue capsules after four weeks of implantation revealed a relatively uniform tissue response to all implants (Figure 5 A - C), except for one case, in which an inflammatory infiltrate was observed around a titanium control implant. All implants were encapsulated in a fibrous layer, consisting of fibrocytes, which could be clearly discerned from the original connective tissue. Especially at the implant side of the fibrous capsule, the fibrocytes had a flat appearance, indicating a matured capsule formation. The fibrocytes of the fibrous capsule surrounded the implants without intervening mono- or multinucleated phagocytotic cells at the implant surface. Similarly, after twelve weeks of implantation, all implants were surrounded by a relatively mature fibrous capsule without the presence of inflammatory cells at the implant interface (Figure 5 D - F).

No gross differences in tissue response were observed depending either on implant type (titanium control, $[PDL/DNA]_5$- or $[PAH/DNA]_5$-coated titanium) or implantation period (4 or 12 weeks).

Similarly, after twelve weeks of implantation, all implants were surrounded by a relatively mature fibrous capsule without the presence of inflammatory cells at the implant interface (Figure 5 D - F).

No gross differences in tissue response were observed depending either on implant type (titanium control, $[PDL/DNA]_5$- or $[PAH/DNA]_5$-coated titanium) or implantation period (4 or 12 weeks).

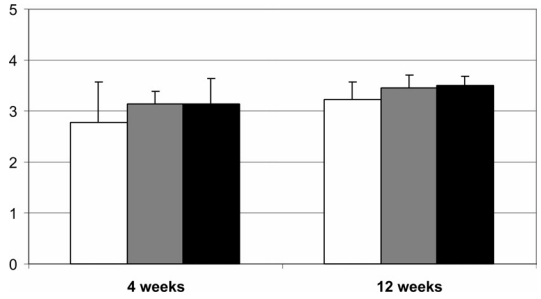

Figure 6: Histological quality of fibrous tissue capsules surrounding titanium control implants (white bars), $[PDL/DNA]_5$-coated (grey bars) or $[PAH/DNA]_5$-coated implants (black bars). Results represent the means ± SD of 4 implants per condition.

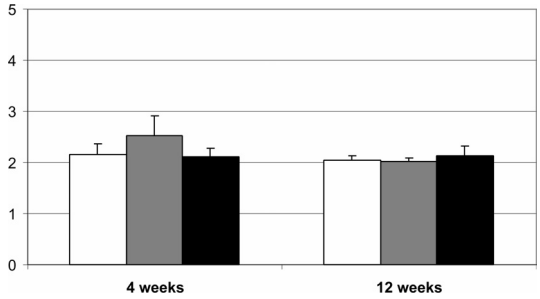

Figure 7: Thickness (number of fibroblast layers) of fibrous tissue capsules surrounding (A) glass and (B) titanium control implants (white bars), or $[PDL/DNA]_5$-coated (grey bars) or $[PAH/DNA]_5$-coated implants (black bars). Results represent the means ± SD of 4 implants per condition.

Histomorphometrical evaluation of implant surrounding capsules

The results of the histomorphometrical analyses are presented in Figure 6 and 7. Regarding capsule thickness, no significant implant type-dependent differences ($p>0.05$) in the number of fibroblast layers in the implant surrounding fibrous capsule were observed. The thickness of all fibroblast capsules was in the range of 5 – 30 after both implantation periods, regardless of the substrate type. No significant differences ($p>0.05$) in capsule quality were detected, neither dependent on type of implant (i.e.non-coated control, $[PDL/DNA]_5$, or $[PAH/DNA]_5$) nor on duration of implantation (i.e. 4 or 12 weeks).

Immunohistochemistry

To visualize the presence of myofibroblasts in the fibrous capsules surrounding the implants, paraffin sections were subjected to immunohistochemical techniques using a monoclonal antibody against α-SMA. Representative pictures of stained sections are presented in Figure 8. Gross evaluation of the α-SMA stained sections revealed a uniformous staining in the capsules, irrespective of substrate type and implantation period.

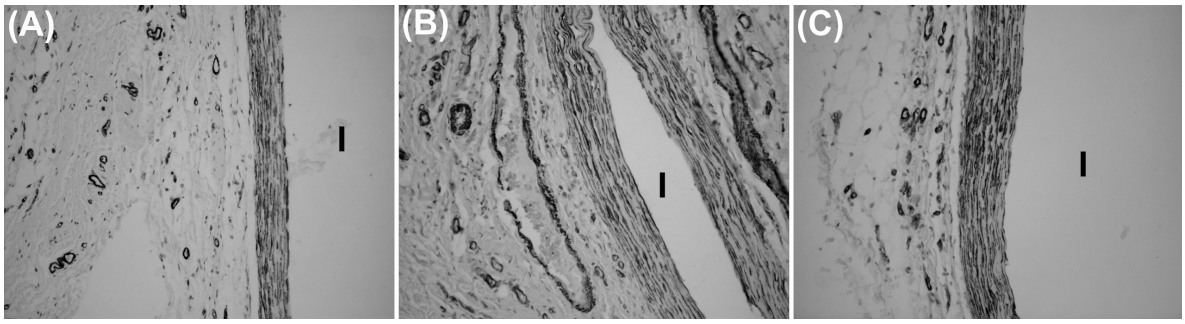

Figure 8:Representative immunohistochemical staining for α-SMA of the fibrous capsule surrounding (a) non-coated control, (b) $[PDL/DNA]_5$, and (c) $[PAH/DNA]_5$ after an implantation period of 12 weeks. I denotes the position of the implant.

IV DISCUSSION

This study was initiated to evaluate the cyto- and histocompatibility of multilayered DNA-coatings. Cytocompatibility of multilayered DNA-coatings was studied via *in vitro* experiments to determine cell proliferation and viability. Histocompatibility of multilayered DNA-coatings was evaluated using a rat model, in which the specimens were inserted subcutaneously for either 4 or 12 weeks, after which capsule quality and thickness were scored histomorphometrically. The results of the *in vitro* and *in vivo* experiments performed in this study indicated that multilayered DNA-coatings are cytocompatible as well as histocompatible.

A wide variety of polyelectrolytes, including cationic PDL and PAH, but not anionic DNA, have been used for the fabrication of polyelectrolyte multilayered coatings with the aim to modulate cell behavior. Various *in vitro* experiments with cells of many different origins, including endothelial [18;19], bone [20], neuronal [21;22], and cartilage tissue [23;24], and blood cells [25] have shown that polyelectrolyte multilayered coatings are a feasible means to modulate biomaterial surfaces. Although in most of these studies established cell lines were used, the *in vitro* experiments of the current study were performed using freshly isolated rat dermal fibroblasts. The difference between these cells and established cell lines is that in the latter cells the life-span and proliferative behavior are artificially affected. Although primary cell cultures also have drawbacks, including the induction of senescence-associated genetic alterations [26] after extensive culture generations and occasional variance in behavior partly attributed to donor-related origins, we assumed that freshly isolated fibroblasts are a more suitable model for evaluating cytocompatibility.

Regarding the sterilization of the substrates for the *in vitro* and the implants for the *in vivo* experiments in this study, the authors are aware of the effects of UV-light on DNA. However, as the DNA in the coatings is immobilized and not applied for its genetic information, potential cross-linking of the DNA is not considered as a negative effect on the coatings. Furthermore, previous research has demonstrated that the sterilization process does not change the infrared absorption spectra of DNA-coatings (unpublished data).

The *in vitro* proliferation assay demonstrated that the proliferation of RDF cells was significantly increased on both types of multilayered DNA-coatings. This observation, which was confirmed by fluorescence microscopy in the Live/Dead assay, might be explained by a number of phenomena. The presence of DNA in the outermost layer of both types of multilayered DNA-coatings might directly or via the adsorption of proteins influence cell behavior. Direct contact between DNA and fibroblasts via supplementation of DNA in the culture medium has been demonstrated to decrease proliferation [27]. On the other hand, DNA has a high affinity for collagen and affects collagen fibrillogenesis [28]. As collagen is a major extracellular matrix product produced by fibroblasts [29], the interaction of DNA with collagen could affect the cell environment. The increased proliferation of RDF cells on multilayered DNA-coatings in this study demonstrates that inhibiting effects on fibroblast proliferation of DNA in solution are reversed after immobilization of the DNA to the substrate surface using ESA.

Besides chemical modification of the surface, the fabrication of multilayered DNA-coatings has demonstrated to result in increased nanorough surface morphologies [12]. The influence of micro- and nanoscale topography on cell behavior has been studied intensively in the last few years using many different types of features [30-33]. Still, considerable debate is ongoing on the true effects of nanoscale topography on cell behavior, since results from several different research groups on this subject are not of the same tenor. For instance, Thapa et al. demonstrated that the presence of nanotopographical cues on polymeric materials induced an increase in the proliferation of bladder smooth muscle cells [31]. In contrast, Wan et al. demonstrated that nanoscale (and also microscale) topography did not increase osteoblast-like cell proliferation, although initial cell adhesion was increased compared to smooth control surfaces [34]. As both types of multilayered DNA-coatings used in the current study introduce nanoscale topography and change the chemical properties of the substrate surface, the cause of the increase of RDF cell proliferation cannot be attributed to a single surface property.

Regarding *in vivo* experiments, the results in this study are deduced from tissue specimens, from which the implants were removed, and that were embedded in paraffin. To ensure that implant removal did not affect the interface, the implant surfaces were observed with SEM. Also, intact specimens, containing both implant and surrounding fibrous capsule were processed for MMA-embedding. However, these latter did not always yield satisfactory staining. Nevertheless, based on morphological criteria MMA-embedded specimens demonstrated relatively mature fibrous capsules surrounding all types of implants without inflammatory cells at the interface between implant and surrounding tissue (data not shown). These observations corroborated with those from the specimens from which the implants were excised after implant retrieval. SEM analysis of the excised implants demonstrated only limited coverage with proteinaceous deposits that could not be identified as cellular material. Similarly, based on morphological criteria the paraffin sections of the remaining fibrous capsule showed no infiltration of inflammatory cells.

No data are available currently on the histocompatibility of polyelectrolyte multilayered coatings. However, the use of polyelectrolyte multilayered coatings on tracheal prostheses in rats has been described recently [35]. Tracheal prostheses coated with poly-lysine and poly-glutamic acid did not negatively influence animal survival compared to non-coated prostheses. In the present study, the histocompatibility of multilayered DNA-coatings was assessed using histomorphometrical analyses of capsule quality and thickness (number of fibroblast layers) after subcutaneous implantation in the backs of rats for either 4 or 12 weeks. Additionally, the presence of myofibroblasts in the fibrous capsules was evaluated immunohistochemically.

Histomorphometrically, multilayered DNA-coatings did not affect the quality and thickness of the fibrous capsule. Generally, all capsules consisted of fairly mature tissue without any signs of inflammatory cell infiltration, and both capsule quality and thickness were not significantly different between the two implantation periods (4 and 12 weeks). Similar results were found by Paquay et al., who subcutaneously implanted titanium fibre mesh in the back of goats [36]. The implantation period of the titanium fibre mesh implants ranged from 1 to 6 weeks, after which histological analysis revealed that an inflammatory response was present only during the first 2 weeks. From 2 to 6 weeks, no difference in tissue response was found, either histologically or histomorphometrically.

The presence of α-SMA in connective tissue cells has been proposed to be a marker for myofibroblast identification [37], but does not imply active contraction. Although these myofibroblasts facilitate wound closure, the presence of myofibroblasts in the fibrous capsule surrounding an implant has been related to complications with breast prostheses [38;39]. In the present study, all fibrous capsules revealed similar staining patterns for α-SMA, independent of implant surface and implantation period. The independency of α-SMA staining in fibrous capsules on implantation period and implant surface has already been demonstrated by Parker et al. [40]. These results support our macroscopic observations of the specimens at implant retrieval.

CONCLUSION

In conclusion, the results of the present study confirm our hypothesis that multilayered DNA-coatings are cyto- and histocompatible. *In vitro*, multilayered DNA-coatings increased the proliferation rate of primary rat fibroblasts, and did not cause a decrease in cell viability. Subcutaneous implantation resulted in fibrous capsule formation around all implants, without any signs of severe inflammation or disturbed wound healing. The quality and thickness of capsules around implants containing a multilayered DNA-coating were comparable to those around non-coated control implants. Furthermore, capsule quality and thickness were constant over time, independent of the implant surface and implantation period. The cyto- and histocompatibility of multilayered DNA-coatings demonstrated in this study allows their use and functionalization with appropriate cytokines to modulate cell and tissue responses in dental and medical implantology.

V ACKNOWLEDGEMENTS

We thank Ms. Natasja van Dijk and Ms. Weibo Zhang (Dept. Periodontology & Biomaterials, Radboud University Nijmegen Medical Centre) for their help and assistance with the preparation of histological sections. Dr. Haruchika Sekido (Central Research Laboratory, Nichiro Corporation, Kawasaki-shi, Japan) is acknowledged for providing DNA. Scanning electron microscopy was performed at the Microscopic Imaging Centre (MIC) of the Nijmegen Centre for Molecular Life Sciences (NCMLS), the Netherlands. This study was financially supported by the Dutch Technology Foundation STW, grant # NKG.5758.

VI REFERENCES

1. O'Kane, S. and M. W. Ferguson. 1997. Transforming growth factor beta s and wound healing. *Int J Biochem Cell Biol* 29:63-78.

2. Ashcroft, G. S., S. J. Mills, and J. J. Ashworth. 2002. Ageing and wound healing. *Biogerontology* 3:337-45.

3. Keller, J. C. 1999. Physical and biological characteristics of implant materials. *Adv Dent Res* 13:5-7.

4. Long, M. and H. J. Rack. 1998. Titanium alloys in total joint replacement--a materials science perspective. *Biomaterials* 19:1621-39.

5. Gerritsen, M., Y. G. Paquay, and J. A. Jansen. 1998. Evaluation of the tissue reaction to a percutaneous access device using titanium fibre mesh anchorage in goats. *J Mater Sci Mater Med* 9:523-8.

6. Paquay, Y. C., J. E. de Ruijter, J. P. van der Waerden, and J. A. Jansen. 1994. Titanium fiber mesh anchorage for percutaneous devices applicable for peritoneal dialysis. *J Biomed Mater Res* 28:1321-8.

7. Yamamoto, S., T. Yamamoto, S. Shimada, E. Kuramoto, O. Yano, T. Kataoka, and T. Tokunaga. 1992. DNA from bacteria, but not from vertebrates, induces interferons, activates natural killer cells and inhibits tumor growth. *Microbiol Immunol* 36:983-97.

8. Krieg, A. M., A. K. Yi, S. Matson, T. J. Waldschmidt, G. A. Bishop, R. Teasdale, G. A. Koretzky, and D. M. Klinman. 1995. CpG motifs in bacterial DNA trigger direct B-cell activation. *Nature* 374:546-9.

9. McMichael, A. J. 1992. Antigens and MHC systems. In *Oxford textbook of pathology*. J. O. D. McGee, P. G. Isaacson, and N. A. Wright, eds. Oxford University Press, Oxford, UK.

10. Kamei, S., N. Tomita, S. Tamai, K. Kato, and Y. Ikada. 1997. Histologic and mechanical evaluation for bone bonding of polymer surfaces grafted with a phosphate-containing polymer. *J Biomed Mater Res* 37:384-93.

11. Tretinnikov, O. N., K. Kato, and Y. Ikada. 1994. In vitro hydroxyapatite deposition onto a film surface-grated with organophosphate polymer. *J Biomed Mater Res* 28:1365-73.

12. Bentley, M. D., M. C. Ortiz, E. L. Ritman, and J. C. Romero. 2002. The use of microcomputed tomography to study microvasculature in small rodents. *Am J Physiol Regul Integr Comp Physiol* 282:R1267-79.

13. Decher G. Fuzzy Nanoassemblies: Toward Layered Polymeric Multicomposites. Science 277, 1232-1237. 97.

14. Freshney, R. I. *Culture of animal cells: a manual of basic technique*. Alan R. Liss, Inc, New York, USA.

15. van der Lubbe, H. B., C. P. Klein, and K. de Groot. 1988. A simple method for preparing thin (10 microM) histological sections of undecalcified plastic embedded bone with implants. *Stain Technol* 63:171-6.

16. Jansen J.A. , Dhert W.J.A. , van der Waerden J.P.C.M. , and van Recum A.F. Semiquantitative and qualitative histologic analysis method for the evaluation of implant biocompatibility. J Invest Surg 7, 123-134. 94.

17. Hatefi, Y. The mitochondrial electron transport and oxidative phosphorylation system. Annu Rev Biochem 54, 1015-1069. 85.

18. Boura, C., P. Menu, E. Payan, C. Picart, J. C. Voegel, S. Muller, and J. F. Stoltz. 2003. Endothelial cells grown on thin polyelectrolyte mutlilayered films: an evaluation of a new versatile surface modification. *Biomaterials* 24:3521-30.

19. Ai, H., Y. M. Lvov, D. K. Mills, M. Jennings, J. S. Alexander, and S. A. Jones. 2003. Coating and selective deposition of nanofilm on silicone rubber for cell adhesion and growth. *Cell Biochem Biophys* 38:103-14.

20. Tryoen-Toth, P., D. Vautier, Y. Haikel, J. C. Voegel, P. Schaaf, J. Chluba, and J. Ogier. 2002. Viability, adhesion, and bone phenotype of osteoblast-like cells on polyelectrolyte multilayer films. *J Biomed Mater Res* 60:657-67.

21. Vodouhe, C., M. Schmittbuhl, F. Boulmedais, D. Bagnard, D. Vautier, P. Schaaf, C. Egles, J. C. Voegel, and J. Ogier. 2005. Effect of functionalization of multilayered polyelectrolyte films on motoneuron growth. *Biomaterials* 26:545-54.

22. Ai, H., H. Meng, I. Ichinose, S. A. Jones, D. K. Mills, Y. M. Lvov, and X. Qiao. 2003. Biocompatibility of layer-by-layer self-assembled nanofilm on silicone rubber for neurons. *J Neurosci Methods* 128:1-8.

23. Zhu, H., J. Ji, and J. Shen. 2004. Construction of multilayer coating onto poly-(DL-lactide) to promote cytocompatibility. *Biomaterials* 25:109-17.

24. Vautier, D., V. Karsten, C. Egles, J. Chluba, P. Schaaf, J. C. Voegel, and J. Ogier. 2002. Polyelectrolyte multilayer films modulate cytoskeletal organization in chondrosarcoma cells. *J Biomater Sci Polym Ed* 13:713-32.

25. Jessel, N., Atalar, F., Lavalle, P., Mutterer, J., Decher, G., Schaaf, P., Voegel, J-C., and Ogier, J. Bioactive coatings based on a polyelectrolyte multilayer architecture functionalized by embedded proteins. Adv Mater 15(9), 692-695. 2003.

26. Kim, H., S. You, J. Farris, B. W. Kong, S. A. Christman, L. K. Foster, and D. N. Foster. 2002. Expression profiles of p53-, p16(INK4a)-, and telomere-regulating genes in replicative senescent primary human, mouse, and chicken fibroblast cells. *Exp Cell Res* 272:199-208.

27. Kitamura, H., N. Takemoto, M. Mizuno, Y. Kuboki, N. Sakairi, and N. Nishi. 1997. Suppression for the proliferation of fibroblasts by external DNA. *Int J Biol Macromol* 21:337-40.

28. Kitamura, H. , C. Iwamoto, N. Sakairi, S. Tokura, and N. Nishi. 1997. Marked effect of DNA on collagen fibrillogenesis in vitro. *Int J Biol Macromol* 20:241-4.

29. Diegelmann, R. F., I. K. Cohen, and B. J. McCoy. 1979. Growth kinetics and collagen synthesis of normal skin, normal scar and keloid fibroblasts in vitro. *J Cell Physiol* 98:341-6.

30. Flemming, R. G., C. J. Murphy, G. A. Abrams, S. L. Goodman, and P. F. Nealey. 1999. Effects of synthetic micro- and nano-structured surfaces on cell behavior. *Biomaterials* 20:573-88.

31. Thapa, A., D. C. Miller, T. J. Webster, and K. M. Haberstroh. 2003. Nano-structured polymers enhance bladder smooth muscle cell function. *Biomaterials* 24:2915-26.

32. Zhang, R. and P. X. Ma. 2000. Synthetic nano-fibrillar extracellular matrices with predesigned macroporous architectures. *J Biomed Mater Res* 52:430-8.

33. Teixeira, A. I., G. A. Abrams, P. J. Bertics, C. J. Murphy, and P. F. Nealey. 2003. Epithelial contact guidance on well-defined micro- and nanostructured substrates. *J Cell Sci* 116:1881-92.

34. Wan, Y., Y. Wang, Z. Liu, X. Qu, B. Han, J. Bei, and S. Wang. 2005. Adhesion and proliferation of OCT-1 osteoblast-like cells on micro- and nano-scale topography structured poly(l-lactide). *Biomaterials* 26:4453-9.

35. Schultz, P., D. Vautier, L. Richert, N. Jessel, Y. Haikel, P. Schaaf, J. C. Voegel, J. Ogier, and C. Debry. 2005. Polyelectrolyte multilayers functionalized by a synthetic analogue of an anti-inflammatory peptide, alpha-MSH, for coating a tracheal prosthesis. *Biomaterials* 26:2621-30.

36. Paquay, Y. C., J. E. de Ruijter, J. P. van der Waerden, and J. A. Jansen. 1997. Wound healing phenomena in titanium fibre mesh: the influence of the length of implantation. *Biomaterials* 18:161-6.

37. Gabbiani, G. 1998. Evolution and clinical implications of the myofibroblast concept. *Cardiovasc Res* 38:545-8.

38. Brown, S. L. , B. G. Silverman, and W. A. Berg. 1997. Rupture of silicone-gel breast implants: causes, sequelae, and diagnosis. *Lancet* 350:1531-7.

39. Rubino, C., V. Mazzarello, F. Farace, F. D'Andrea, A. Montella, G. Fenu, and G. V. Campus. 2001. Ultrastructural anatomy of contracted capsules around textured implants in augmented breasts. *Ann Plast Surg* 46:95-102.

40. Parker, J. A., X. F. Walboomers, J. W. Von den Hoff, J. C. Maltha, and J. A. Jansen. 2002. The effect of bone anchoring and micro-grooves on the soft tissue reaction to implants. *Biomaterials* 23:3887-96.

4

MACROPHAGE BEHAVIOR ON MULTILAYERED DNA-COATINGS *IN VITRO*

JJJP van den Beucken, XF Walboomers, MRJ Vos, NAJM Sommerdijk, RJM Nolte, JA Jansen

J Biomed Mater Res A (2006); in press

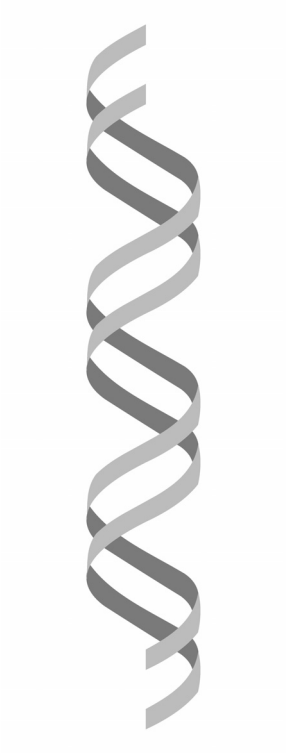

I INTRODUCTION

Due to the ageing of the population in the Western world, biomedical implants are becoming increasingly important tools in the practice of medicine. Examples of such implants include joint replacements, vascular grafts, pacemakers, and catheters. The insertion of implants into bodily tissues evokes a series of responses directed against these foreign objects, which are conjointly known as the 'foreign body response'. Prior to the interaction of cells in these responses, an implant is covered with proteins, which adsorb on the implant surface from bodily fluids and initiate the cell response. In view of this, especially the serum proteins vitronectin and fibronectin have demonstrated to be important for cell attachment [1-3]. Additionally, upon binding specific epitopes in the extracellular matrix, cell surface receptors are known to be involved in the regulation of cell processes including proliferation and differentiation [4]. The subsequent cell responses consist of a series of chronological, though not completely separated, stadia, which are (1) inflammation, (2) tissue repair, and (3) tissue remodeling [5-7].
To study the biocompatibility of biomaterials, assays in which the behavior of macrophages is examined are a useful determinant. In particular biomaterials used in orthopedics and dentistry have been the subject of interest in such assays [8-10]. The use of macrophages for this purpose is based on their role in the foreign body response. By virtue of their capacity to secrete a large array of products, including cytokines and growth factors, macrophages orchestrate the activation of numerous cell types [11], and are considered key regulators of the intensity and duration of inflammatory responses. During the entire foreign body response, macrophages are considered to be the key cell type regulating the duration and intensity of the different stadia of the foreign body response [11;12]. Permanent activation of macrophages during the foreign body response may result in persistent inflammatory reactions, and eventually in the fusion of macrophages into so called 'foreign body giant cells' (FBGCs) [13].
Previous work of Brodbeck et al. was focused at the role of biomaterial surface properties on the expression of cytokines by leucocytes, amongst which macrophages [14;15]. In these studies, cytokines were classified according to their role in the foreign body response (Figure 1).

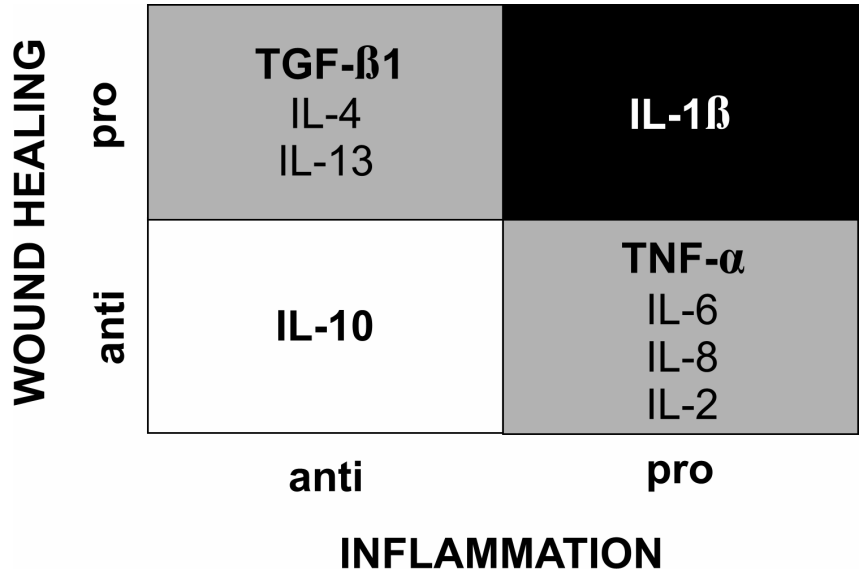

Figure 1: Cytokine classification according to their roles in the foreign body response (adapted with modifications from Brodbeck et al.[15]).

Recently, the fabrication and characterization of a novel biomaterial coating with deoxyribonucleic acid (DNA) as the main constituent was described [16;17]. These coatings were fabricated using the electrostatic self-assembly (ESA) technique [18], using either poly-D-lysine (PDL) or poly(allylamine hydrochloride) (PAH) as the cationic counterpart of anionic DNA. The proposed beneficial effects of these multilayered DNA-coatings on tissue responses upon implantation rely on the homogeneity of the DNA molecule in vertebrate species [19;20], and the capacity of vertebrate DNA to prevent immunological reactions [21;22]. Furthermore, the high phosphate amount in DNA and the capacity of DNA to incorporate other

compounds [23] may favor the deposition of calcium phosphate in a bone environment and allow functionalization of multilayered DNA-coatings with appropriate biologically-active compounds (growth factors, antibiotics, etc.), respectively. Indeed, previous experiments at our department have already demonstrated the histocompatibility of multilayered DNA-coatings [17;24] and the effective functionalization of multilayered DNA-coatings with the osteoinductive factor bone morphogenetic protein 2 (BMP-2) [25]. In view of these properties of DNA, multilayered DNA-coatings could serve as safe coatings for both soft and hard tissue implants that can be functionalized with compounds with desired biological activity.

In view of the proposed beneficial effects of DNA, the aim of the current study was to evaluate the effect of multilayered DNA-coatings on the behavior of macrophages. First, the gross protein adsorption to non-coated controls and the two types of multilayered DNA-coatings was measured. Additionally, two murine macrophage cell lines (J774A.1 and RAW264.7) were cultured on two types of multilayered DNA-coatings ($[PDL/DNA]_5$ and $[PAH/DNA]_5$) for 24 and 48 hours. Non-coated glass substrates served as negative controls, whereas stimulation with lipopolysaccharide (LPS) was used as the positive control. Macrophage behavior was assessed in terms of proliferation, viability, morphology, and cytokine secretion (TNF-α, TGF-β1, IL-10, IL-1β).

II MATERIALS & METHODS

Materials

Polyanionic DNA (300 bp/molecule; sodium salt) was kindly provided by the Central Research Laboratory of Nichiro Corporation (Kawasaki-shi, Kanagawa prefecture, Japan). Potential protein impurities in the DNA were checked using the bicinchoninic acid (BCA) protein assay (Pierce, Rockford, IL, US) and measured to be below 0.20% w/w (data not shown). Polycationic polyelectrolytes poly(allylamine hydrochloride) (PAH; MW ~70000) and poly-D-lysine (PDL; MW 30000 - 70000) were purchased from Sigma (Sigma-Aldrich Chemie B.V., Zwijndrecht, the Netherlands). Lipopolysaccharide (LPS; from *E. coli*) was purchased from Fluka (Fluka Chemie GmbH, Buchs, Germany). All materials were used without further purification.

Substrate preparation and cleaning

Disc-shaped glass substrates (diameter 12 mm; Waldemar Knittel Glasbearbeitungs GmbH, Braunschweig, Germany) were used. Prior to the fabrication of multilayered DNA-coatings, substrates were cleaned in Piranha solution (H_2O_2 / H_2SO_4 – 3:7 v/v) to completely remove all traces of organic materials at the surface, and increase surface hydrophilicity [26]. Subsequently, the substrates were thoroughly rinsed with ultra-pure water from a Millipore system (resistivity > 15 MΩ·cm; Millipore B.V., Amsterdam, the Netherlands) and dried using a pressurized air stream.

Generation of multilayered DNA-coatings

Multilayered DNA-coatings were generated using the ESA-technique, as described previously by Van den Beucken et al. [16]. Briefly, the cleaned substrates were immersed in an aqueous solution of either PDL (0.1 mg/ml) or PAH (1 mg/ml) for 30 minutes, allowing sufficient time for the adsorption of the first cationic polyelectrolyte layer onto the substrates. Subsequently, the substrates were washed in ultra-pure water (5 minutes, continuous water flow) and dried using a pressurized air stream. Thereafter, the substrates were alternately immersed in an anionic aqueous DNA solution (1 mg/ml) and the respective cationic polyelectrolyte solution for 7 minutes each, with intermediate washing in ultra-pure water (5 minutes, continuous water flow) and drying using a pressurized air stream. The build-up of the multilayered DNA-coatings was continued until a total of 5 double-layers were reached, which were designated either $[PDL/DNA]_5$ or $[PAH/DNA]_5$.

All substrates, coated with either type of multilayered DNA-coating or non-coated control substrates, were sterilized using a UV-irradiation treatment (254 nm; 4 hrs).

Protein adsorption

Protein adsorption to the multilayered DNA-coatings and non-coated glass controls was assessed using the BCA protein assay (Pierce Biotechnology, Inc., Rockford, IL, USA), according to the instructions of the manufacturer. Briefly, triplicate substrates (n=3) were immersed in 1 ml culture medium (Minimal Essential Medium (Gibco®, Invitrogen Corporation, Breda, the Netherlands), supplemented with 10% fetal calf serum (FCS; Gibco®) and antibiotics (gentamycin; 50 μg/ml; Gibco®) for incubation periods of 0, ½, 1, 4, and 24 hours. After each incubation period, substrates were washed three times with PBS, transferred into a fresh 24-well plate (Greiner Bio-One). To retrieve adherent proteins, substrates were immersed in 1 ml of a 5% sodium dodecyl sulfate (SDS; Sigma-Aldrich Chemie B.V., Zwijndrecht, the Netherlands) solution in ultra-pure water. The plate was incubated dynamically at room temperature overnight, after which the amount of protein in the SDS-solution was measured as follows: 100 μl of sample or standard was added to 100 μl freshly-prepared working solution in a 96-well plate (Greiner Bio-One) and incubated at 37°C for two hours. After cooling to room temperature, the plate was read in a plate reader at 562 nm. For the standard curve, serial dilutions of bovine serum albumin (BSA) were made (0 – 40 μg/ml) in 5% SDS-solution. Obtained values were corrected by subtracting the values obtained from substrates that were not immersed in culture medium (incubation period = 0 h).

Cell experiments

Macrophage cell lines

The murine macrophage cell lines J774A.1 and RAW264.7 (kindly provided by Dr. F. Wagener, Dept. Pharmacology & Toxicology, NCMLS, Radboud University Nijmegen, Nijmegen, the Netherlands) were cultured in α-MEM medium in tissue culture polystyrene (TCPS) flasks (75 cm^2; Greiner Bio-One B.V., Alphen aan de Rijn, the Netherlands). Cells were routinely detached by mechanical force and subsequently split in a ratio of 1:5.

For every assay, cells were seeded at a density of 1 x 10^5 cells/cm^2 and subsequently cultured for 24 and 48 hours on four types of experimental substrates, which were placed in 24 well plates (Greiner Bio-One B.V.):

1. negative controls (-controls; non-coated glass)
2. positive controls (+controls; non-coated glass + LPS-stimulation)
3. $[PDL/DNA]_5$
4. $[PAH/DNA]_5$

For positive controls, cells were stimulated with LPS (10 μl of 10 μg/ml in PBS; final concentration 100 ng/ml) two hours after cell seeding. Negative controls and both types of multilayered DNA-coatings were comparatively supplemented with 10 μl PBS.

Cell quantification

For the determination of cell amounts (n=3 for each experimental condition at each time point), substrates with adherent cells were washed twice with PBS. Subsequently, adherent cells were lysed through incubation in ultra-pure water, with 3 subsequent repetitive freeze and thaw cycles. Then, the amount of cellular protein in the supernatant was quantified using the BCA protein assay (Pierce Biotechnology, Inc.), according to the instructions of the manufacturer. Briefly, 100 μl of sample or standard was added to 100 μl freshly-prepared working solution in a 96-well plate (Greiner Bio-One B.V.) and incubated at 37°C for two hours. After cooling to room temperature, the plate was read in a plate reader at 562 nm. For the standard curve, serial dilutions of bovine serum albumin (BSA) were made (0.5 – 40 μg/ml) in ultra-pure water.

Cell viability

Cell viability was assessed using a commercially available cytotoxicity assay, according to the instructions of the manufacturer (Promega Corporation, Madison, WI, USA). The test is based on the conversion of a tetrazolium salt ([3-(4,5-dimethylthiazol-2-yl)-2,5-diphenyltetrazoliumbromide], MTT)

into a formazan product. Briefly, at 24 and 48 hours after cell seeding on the experimental substrates (3 substrates per condition; n=3), 150 µl dye solution was added to each well, and cells were incubated at 37°C for 4 hours. Subsequently, 1 ml of solubilization/stop solution was added to each well, and cells were incubated for another hour (at room temperature). Finally, the contents of the wells were mixed thoroughly using a pipette and the absorbance at 570 nm wavelength was read using a spectrophotometer. The results are standardized according to the obtained negative control values (% of negative control).

Cell morphology

To study cell morphology, cells cultured on the experimental substrates for 24 and 48 hours were washed twice with PBS and subsequently fixed for 15 min. in 2% glutaraldehyde in 0.1 M sodium cacodylate buffered solution. Then, samples were rinsed twice with cacodylate buffered solution and dehydrated using a graded series of ethanol. Finally, samples were dried with tetramethylsilane. The samples were sputter coated with gold and examined using a JEOL 6310 scanning electron microscope (SEM) at an acceleration voltage of 10 – 15 kV.

Cytokine secretion

The secretion of four different cytokines was measured in the media from the cultures for cell proliferation and cell morphology, i.e. tumor necrosis factor-alpha (TNF-α), interleukin 1-beta (IL-1β), interleukin 10 (IL-10), and transforming growth factor beta-1 (TGF-β1) using commercially available, enzyme-linked immunosorbent assay (ELISA) based kits (OptEIATM; BD Biosciences, San Diego, CA, US), according to the instructions of the manufacturer. Samples (n=5 for each experimental condition at each time point) were collected during preparation of cell quantification assay and cell morphology, centrifuged to remove potential cellular material, and stored at -80°C. Relative values of cytokine secretion were obtained by dividing the absolute values determined using the ELISA-based kits by the cell quantification values (and expressed as pg/ml/µg cellular protein content).

Statistical analyses

The entire study was performed twice, with independent runs for the cell experiments. Triplicate samples were used for each experimental group at each sampling time to determine protein adhesion, cell quantification, and cell viability; quintuplicate samples were used for each experimental group at each sampling time to determine cytokine secretion. Statistical analyses were performed using GraphPad Instat, version 3.0 (Graphpad Software, San Diego, CA, USA). Experimental results were analyzed using a one-way ANOVA, combined with a post-hoc Tukey-Kramer Multiple Comparisons Test.

III RESULTS

Protein adsorption

Generally, the results (Figure 2) indicated that major protein adsorption occurs within 30 minutes. After this initial adsorption, the additional gross protein adsorption was limited for all experimental substrates. No statistically significant differences in gross protein adsorption were observed between the experimental substrates at each immersion period ($p>0.05$).

Cell experiments

Quantification of the cell amount

The cell amount of both types of macrophages was measured after culture periods of 24 and 48 hours on the experimental substrates. The results showed an increase in cellular protein amount from 24 to 48 hours of culture for both types of macrophage cultures, independent of experimental condition (Figure 3). No statistically significant differences were observed at each culture period of individual cell lines ($p>0.05$).

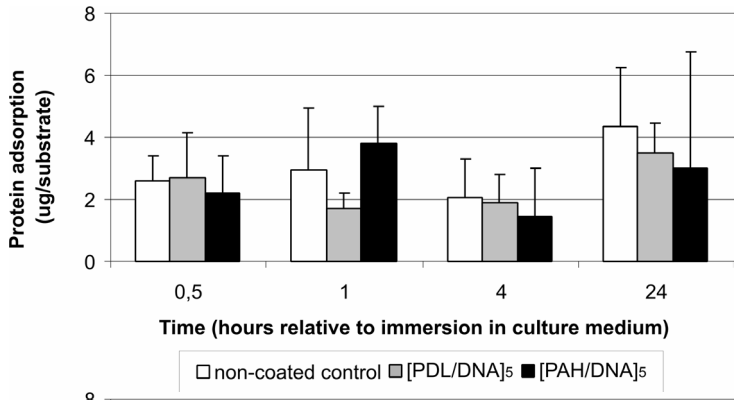

Figure 2 Gross protein adsorption to non-coated controls, $[PDL/DNA]_5$, and $[PAH/DNA]_5$ after indicated immersion periods in cell culture medium. Results represent mean + SD of three experimental substrates per condition (n=3).

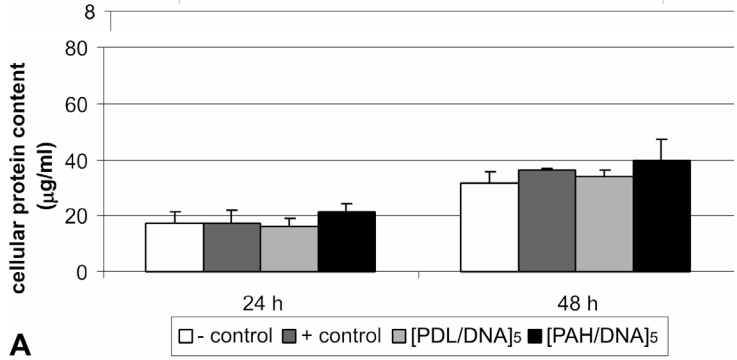

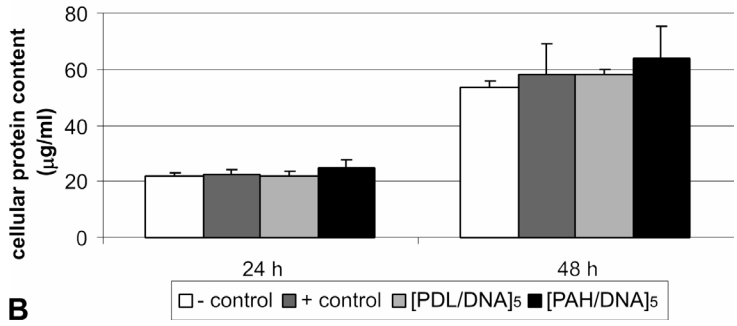

Figure 3 Cellular protein content of macrophages after 24 and 48 hours of culture on experimental substrates. (A) RAW264.7; (B) J774A.1. Results represent mean + SD of three experimental substrates per condition (n=3).

Cell viability

The results of the viability assay are presented in Figure 4. Neither of the two types of multilayered DNA-coatings affected macrophage cell viability ($p>0.05$). On the other hand, LPS-stimulation demonstrated to significantly decrease cell viability of both RAW264.7 ($p<0.05$) and J774A.1 ($p<0.001$) macrophages after 48 hours of cell culture compared to negative controls.

Cell morphology

Both RAW264.7 and J774A.1 macrophages exhibited a typical macrophage-like morphology, indicated by the presence of surface ruffles and numerous extending pseudopodia (Figure 5). Both cultures consisted of cells with a rounded cell morphology and ones with a more spread morphology. Due to the high seeding density, cell-cell contacts were observed in both cultures. No morphological differences were observed between macrophages cultured on either type of DNA-coating or positive controls compared to negative controls (data not shown).

Cytokine secretion

The relative secretion of TNF-α is presented in Figure 6. The secretion of TNF-α, IL-1β, IL-10, and TGF-β1 is summarized in Table 1.

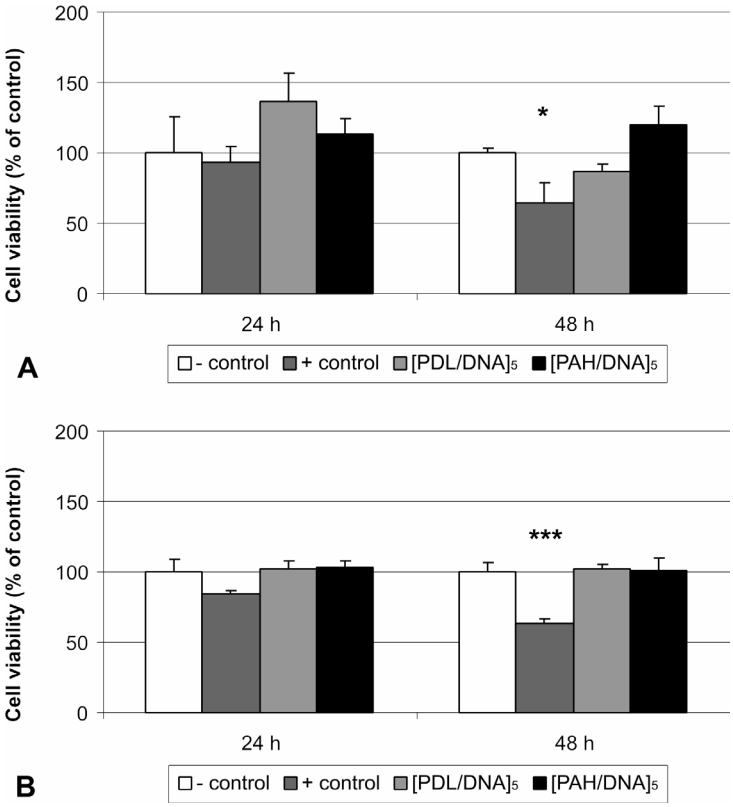

Figure 4: Viability of macrophages after 24 and 48 hours of culture on experimental substrates. (A) RAW264.7; (B) J774A.1. Results represent mean + SD of three experimental substrates per condition (n=3). (, p<0.05; **, p<0.01; ***, p<0.001).*

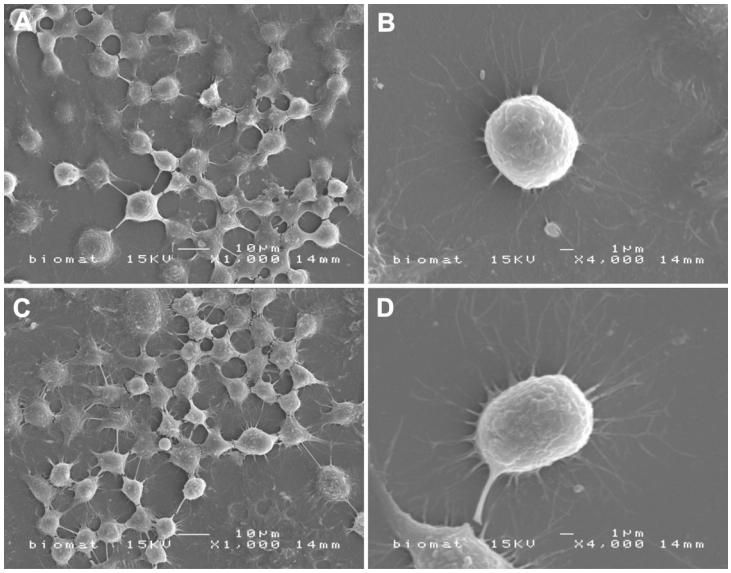

Figure 5: SEM images showing the morphology of RAW264.7 on [PDL/DNA]$_5$ (A-B) and J774A.1 on [PAH/DNA]$_5$ (C-D) after 24 hours of culture.

TNF-α

RAW264.7 macrophages cultured on [PDL/DNA]$_5$ showed TNF-α secretion levels comparable to the negative controls ($p>0.05$). On the other hand, RAW264.7 macrophages cultured on [PAH/DNA]$_5$ showed a significantly decreased TNF-α secretion after both 24 ($p<0.05$) and 48 hours ($p<0.01$) of culture. Positive controls showed significantly increased levels of TNF-α secretion both after 24 and 48 hours ($p<0.001$).

J774A.1 macrophages cultured on either type of multilayered DNA-coating showed TNF-α secretion levels comparable to negative controls after 24 hours of culture. However, after 48 hours of culture, significantly decreased levels of TNF-α secretion were observed on both types of multilayered DNA-

coatings ($p<0.001$). Positive controls showed significantly increased levels of TNF-α secretion both after 24 and 48 hours ($p<0.001$).

TABLE 1: SUMMARY OF MACROPHAGE CYTOKINE SECRETION (PG/ML/µG CELLULAR PROTEIN) ON MULTILAYERED DNA-COATINGS
(MEAN ± SD; * $P<0.05$; ** $P<0.01$; *** $P<0.001$ COMPARED TO NEGATIVE CONTROLS).

condition	RAW264.7 macrophages							
	TNF-α		IL-1β		IL-10		TGF-β1	
	24 h	48 h	24 h	48 h	24 h	48 h	24 h	48 h
negative control	16,5 ± 2,6	19,8 ± 1,6	0,7 ± 1,1	0,4 ± 0,5	3,1 ± 1,6	1,1 ± 0,5	123,8 ± 15,5	41,9 ± 10,9
positive control	53,2 ± 1,6***	26,8 ± 0,2***	1,2 ± 1,5	0,7 ± 0,8	7,4 ± 1,6**	2,2 ± 0,7*	167,3 ± 48,4	59,9 ± 10,8
[PDL/DNA]5	13,2 ± 2,1	19,7 ± 3,2	0,6 ± 0,8	0,3 ± 0,3	5,0 ± 1,3	1,3 ± 0,3	106,3 ± 27,7	52,2 ± 17,2
[PAH/DNA]5	11,9 ± 1,6*	15,5 ± 0,9**	0,5 ± 0,5	0,5 ± 0,7	4,4 ± 2,1	0,5 ± 0,4	122,9 ± 32,8	56,6 ± 22,2
condition	J774A.1 macrophages							
	TNF-α		IL-1β		IL-10		TGF-β1	
	24 h	48 h	24 h	48 h	24 h	48 h	24 h	48 h
negative control	39,7 ± 3,0	42,8 ± 1,7	1,3 ± 1,5	1,3 ± 1,7	0,9 ± 0,5	0,7 ± 0,4	86,1 ± 4,0	41,7 ± 6,3
positive control	77,9 ± 0,9***	58,5 ± 0,9***	2,9 ± 1,6	5,2 ± 3,6*	13,4 ± 2,2***	11,2 ± 1,0***	81,7 ± 3,7	37,4 ± 5,2
[PDL/DNA]5	45,4 ± 4,8	36,9 ± 1,8***	2,5 ± 1,9	1,5 ± 1,0	1,9 ± 1,6	0,9 ± 0,8	72,1 ± 17,9	34,1 ± 5,1
[PAH/DNA]5	34,6 ± 3,5	32,6 ± 2,6***	1,4 ± 1,6	1,0 ± 1,3	2,6 ± 1,5	2,7 ± 2,0	81,0 ± 10,4	34,2 ± 3,7

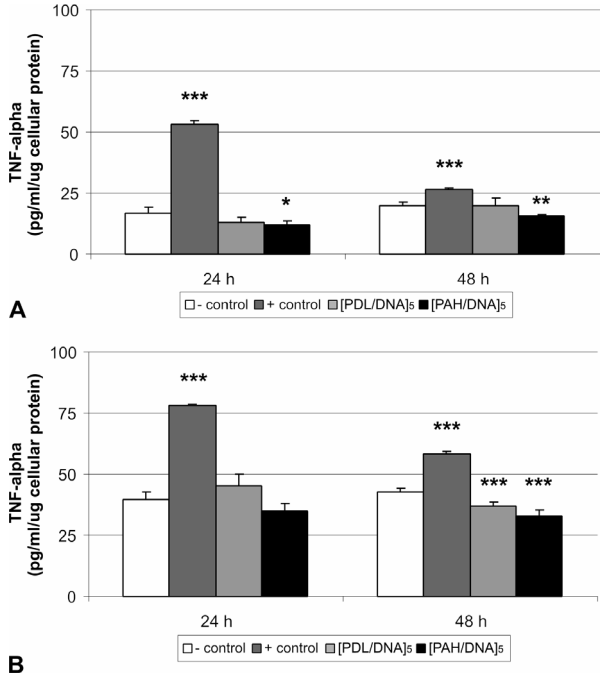

Figure 6: TNF-α secretion of macrophages after 24 and 48 hours of culture on experimental substrates. (A) RAW264.7; (B) J774A.1. Results represent mean + SD of five experimental substrates per condition (n=5). (, $p<0.05$; **, $p<0.01$; ***, $p<0.001$).*

IL-1β

Secretion levels of IL-1β were low for both macrophage cell types under all four experimental conditions. RAW264.7 macrophages showed comparable IL-1β secretion levels for all four conditions after 24 and 48 hours ($p>0.05$).

Similarly, comparable IL-1β secretion levels were observed for J774A.1 macrophages after 24 hours of culture ($p>0.05$). On the other hand, an increased IL-1β secretion was observed for positive controls after 48 hours of culture ($p<0.05$).

IL-10

RAW264.7 macrophages IL-10 secretion levels were comparable for those cultured on both types of multilayered DNA-coatings and negative controls after both 24 and 48 hours ($p>0.05$). The positive controls, however, showed an increased IL-10 secretion both after 24 ($p<0.01$) and 48 hours ($p<0.05$).

Similar IL-10 secretion profiles were observed for J774A.1 macrophages. No significantly different IL-10 secretion levels were observed for J774A.1 macrophages cultured on either type of multilayered DNA-

coating ($p>0.05$), whereas significantly increased levels were observed for positive controls both after 24 ($p<0.001$) and 48 hours ($p<0.001$).

IV DISCUSSION

A pivotal factor to consider in the development of biomaterials and biomaterial coatings is the inflammatory response to these materials. The insertion of implants is followed by protein adsorption and subsequent interactions with cellular components of the biological surroundings, in which macrophages play a dominant role through the production of a myriad of signaling molecules. Previous research aimed at using macrophages (either primary cells or cell lines) as a model system to evaluate biomaterial biocompatibility [8-10;27-31] [32] [33]. Additionally, a classification scheme for cytokines was developed, in which their classification is based on their role in inflammation and wound healing [14;15]. In view of this, the present study evaluated (i) gross protein adsorption to, and (ii) *in vitro* behavior of macrophages on novel biomaterial coatings, consisting of poly-D-lysine (PDL) or poly(allylamine hydrochloride) (PAH) and DNA, and compared it to negative (non-coated glass) and positive controls (non-coated glass + LPS-stimulation). The results demonstrated that protein adsorption was comparable for both types of multilayered DNA-coatings and non-coated negative controls. The behavior of two murine macrophage cell lines, RAW264.7 and J774A.1, was evaluated in terms of proliferation, viability, morphology, and cytokine secretion. Current cell culture experiments demonstrated cell line-dependent differences in cell proliferation and cytokine expression. Both macrophage cell viability and morphology were not affected by the presence of either type of multilayered DNA-coating. Most interesting, a decreased secretion of TNF-α was observed on both types of multilayered DNA-coatings, whereas the secretion of IL-1β, IL-10, and TGF-β1 was not affected by the presence of either type of multilayered DNA-coating.

Cell attachment and proliferation depend on the adsorption of serum proteins, which link cells to the biomaterial. The adsorption of proteins from complex mixtures (e.g. culture medium, blood, etc.) is a dynamic and competitive process. Important proteins promoting cell attachment in this respect are vitronectin and fibronectin [1-3], whose interaction with cells is mainly based on the recognition of RGD-sequences by receptors located on the cell surface [34;35]. In addition to cell binding, these receptors also mediate signaling, and are involved in regulating cell processes including proliferation and differentiation [4]. Consequently, variations in the amount and diversity of adsorbed proteins are likely to affect macrophage attachment and behavior (viability, cytokine secretion, morphology) in the current study. As in the present study cell attachment was enrolled as a parameter, the protein adsorption from cell culture medium containing 10% (v/v) bovine serum was not particularized into adsorption of single cell-attachment promoting proteins (e.g. vitronectin and fibronectin). Protein adsorption demonstrated to be similar for both types of multilayered DNA-coatings and non-coated controls. The combination of the gross protein adsorption results and the cell quantification results after 24 hours of culture indicates that (i) both types of multilayered DNA-coatings allow protein adsorption, and (ii) the protein adsorption to both types of multilayered DNA-coatings does not alter cell attachment compared to non-coated control substrates.

In the present study, cell culture experiments were performed using two different types of murine macrophage cell lines, i.e. RAW264.7 and J774A.1. Both cell lines are derived from BALB/c mice: RAW264.7 macrophages from a virus-induced tumor, J774A.1 macrophages from a reticulum cell sarcoma. In addition to these differences, the former cells have a male genotype, whereas the latter have a female genotype. Both these cell lines have been used extensively to study the effect of materials on macrophage behavior [8;10;27;28;30;31]. Additionally, it is the opinion of the authors that data obtained from experiments that use cell lines rather than primary cells are eligible for comparison. Nevertheless, the authors are aware of the differences between cell lines and primary cells, and the effects these differences can have in *in vitro* cell culture models.

The results for cell viability on multilayered DNA-coatings corroborate our previously reported cell viability data of primary rat dermal fibroblast cultures on multilayered DNA-coatings [17]. A decrease in

macrophage cell viability due to stimulation with LPS, as observed after 48 hours of culture in the present study, has been reported earlier by Li et al. [31]. In their study, RAW264.7 positive controls showed a decreased cell viability as early as 6 hours post-supplementation. Apparently, the concentration of LPS (10 μg/ml vs. 100 ng/ml in the present study) affects cell viability in a temporal fashion.

Local cytokine production by implant-adherent macrophages is an important issue in the intensity and duration of the stages in the foreign body response [11;13]. In the classification presented in Figure 1, the role of single pro-inflammatory or pro-wound healing cytokines is evident. However, a unique position is put aside for IL-10 and IL-1β, as these cytokines have dual roles in the inflammatory and wound healing processes. IL-10 is capable of down-regulating the activity of both inflammatory cells (lymphocytes and monocytes) and wound healing (fibroblasts), and suppresses cytokine production. On the other hand, IL-1β activates those cells and hence is considered to be pro-inflammatory/pro-wound healing.

Previous studies have demonstrated that cytokine expression is affected by biomaterial properties, such as surface topography [10] and surface chemistry [14;15]. Refai et al. used four surface topographies (polished, coarsely blasted, acid etched, and sandblasted + acid etched) of titanium sputter-coated epoxy-resin to study the effect of surface topography on macrophage (RAW264.7) activity and secretion of pro-inflammatory cytokines (TNF-α, IL-1β, and IL-6). Their experiments demonstrated that rough surfaces increased the secretion of TNF-α. Additionally, they observed a synergistic effect of surface roughness and LPS-stimulation by the increased secretion of IL-1β, IL-6, and TNF-α. In our experiments, the increased surface roughness of multilayered DNA-coatings [16] evidently did not increase cytokine secretion. On the contrary, both types of multilayered DNA-coatings had a decreasing effect on TNF-α secretion, whereas the secretion of IL-1β, IL-10, and TGF-β1 was not affected. A reason for this discrepancy could be the scale of roughness, which was limited to the nanometer range in the current study compared to micrometer range differences in the study of Refai et al. [10].

In view of surface chemistry, Brodbeck et al. demonstrated using an *in vitro* human monocyte culture system that of four types of substrates surfaces (i.e. hydrophobic, hydrophilic, anionic, and cationic), those with a hydrophilic or anionic surface promote an anti-inflammatory type of response owing to a decreased IL-8 and an increased IL-10 expression [14]. Additionally, an *in vivo* mouse cage implant system demonstrated that hydrophilic and anionic surfaces decreased leukocyte adhesion, and that hydrophilic surfaces induced a decrease in the expression of both pro-inflammatory (IL-6 and IL-8) and pro-wound healing cytokines (IL-10 and TGF-β) by adherent cells. These results corroborate with our observations of decreased pro-inflammatory responses on both types of multilayered DNA-coatings, albeit that in our experiments TNF-α was used as the cytokine indicative for pro-inflammatory/anti-wound healing responses. It is likely that the decreased TNF-α secretion is caused by the increased hydrophilicity of multilayered DNA-coatings owing to the deposition of anionic DNA as the top layer in the multilayer coatings.

Although the results of the current study indicate that multilayered DNA-coatings reduce the pro-inflammatory response of macrophages as reflected by the decreased secretion of TNF-α, it remains questionable whether the effects observed with the conditions in the model system in the current study (cell density, *in vitro* setting) can be fully extrapolated to *in vivo* situations. The decreased secretion of TNF-α, although significantly lower compared to negative controls, might not suffice to show clinical effects. Additionally, this study only monitored the secretion of a limited number of cytokines by single cell types, whereas in clinical situations the balance between many different cytokines and responsive cells determines the course of biological processes. Appropriate animal models are required to elucidate whether these *in vitro* indications of beneficial immunological effects of multilayered DNA-coatings can have clinical effects on inflammatory and wound healing processes around implants.

CONCLUSION

The results of the present study demonstrate that multilayered DNA-coatings do not affect gross protein adsorption compared to non-coated controls. Cell culture experiments showed that the attachment to,

and viability and morphology of two types of macrophages cultured on multilayered DNA-coatings is comparable to non-coated controls. Macrophages repeatedly showed decreased secretion levels of TNF-α on multilayered DNA-coatings, whereas no differences were observed in the secretion of IL-1β, IL-10, and TGF-β1.

V ACKNOWLEDGEMENTS

This research was supported by the Technology Foundation STW, applied science division of NWO and the technology programme of the Ministry of Economic Affairs, grant # NKG.5758.

VI REFERENCES

1. Howlett, C. R., M. D. Evans, W. R. Walsh, G. Johnson, and J. G. Steele. 1994. Mechanism of initial attachment of cells derived from human bone to commonly used prosthetic materials during cell culture. *Biomaterials* 15:213-22.

2. Steele, J. G., B. A. Dalton, G. Johnson, and P. A. Underwood. 1995. Adsorption of fibronectin and vitronectin onto Primaria and tissue culture polystyrene and relationship to the mechanism of initial attachment of human vein endothelial cells and BHK-21 fibroblasts. *Biomaterials* 16:1057-67.

3. Steele, J. G., G. Johnson, C. McFarland, B. A. Dalton, T. R. Gengenbach, R. C. Chatelier, P. A. Underwood, and H. J. Griesser. 1994. Roles of serum vitronectin and fibronectin in initial attachment of human vein endothelial cells and dermal fibroblasts on oxygen- and nitrogen-containing surfaces made by radiofrequency plasmas. *J Biomater Sci Polym Ed* 6:511-32.

4. Hynes, R. O. 1992. Integrins: versatility, modulation, and signaling in cell adhesion. *Cell* 69:11-25.

5. Harding, K. G., H. L. Morris, and G. K. Patel. 2002. Science, medicine and the future: healing chronic wounds. *BMJ* 324:160-3.

6. Singer, A. J. and R. A. Clark. 1999. Cutaneous wound healing. *N Engl J Med* 341:738-46.

7. Webb, J. C. J. and Tricker, J. Bone biology: A review of fracture healing. Curr Orthop 14, 457-463. 2000.

8. Petit, A., I. Catelas, J. Antoniou, D. J. Zukor, and O. L. Huk. 2002. Differential apoptotic response of J774 macrophages to alumina and ultra-high-molecular-weight polyethylene particles. *J Orthop Res* 20:9-15.

9. Prabhu, A., C. E. Shelburne, and D. F. Gibbons. 1998. Cellular proliferation and cytokine responses of murine macrophage cell line J774A.1 to polymethylmethacrylate and cobalt-chrome alloy particles. *J Biomed Mater Res* 42:655-63.

10. Refai, A. K., M. Textor, D. M. Brunette, and J. D. Waterfield. 2004. Effect of titanium surface topography on macrophage activation and secretion of proinflammatory cytokines and chemokines. *J Biomed Mater Res* 70A:194-205.

11. DiPietro, L. A. 1995. Wound healing: the role of the macrophage and other immune cells. *Shock* 4:233-40.

12. Kao, W. J. 1999. Evaluation of protein-modulated macrophage behavior on biomaterials: designing biomimetic materials for cellular engineering. *Biomaterials* 20:2213-21.

13. Anderson, J. M. Biological responses to materials. Annu Rev Mater Res 31, 81-110. 2001.

14. Brodbeck, W. G., Y. Nakayama, T. Matsuda, E. Colton, N. P. Ziats, and J. M. Anderson. 2002. Biomaterial surface chemistry dictates adherent monocyte/macrophage cytokine expression in vitro. *Cytokine* 18:311-9.

15. Brodbeck, W. G., G. Voskerician, N. P. Ziats, Y. Nakayama, T. Matsuda, and J. M. Anderson. 2003. In vivo leukocyte cytokine mRNA responses to biomaterials are dependent on surface chemistry. *J Biomed Mater Res* 64A:320-9.

16. van den Beucken, J. J., M. R. Vos, P. C. Thune, T. Hayakawa, T. Fukushima, Y. Okahata, X. F. Walboomers, N. A. Sommerdijk, R. J. Nolte, and J. A. Jansen. 2006. Fabrication, characterization, and biological assessment of multilayered DNA-coatings for biomaterial purposes. *Biomaterials* 27:691-701.

17. van den Beucken, J. J., X. F. Walboomers, M. R. Vos, N. A. Sommerdijk, R. J. Nolte, and J. A. Jansen. 2006. Cyto- and histocompatibility of multilayered DNA-coatings on titanium. *J Biomed Mater Res A* 77A:202-211.

18. Decher G. Fuzzy Nanoassemblies: Toward Layered Polymeric Multicomposites. Science 277, 1232-1237. 97.

19. Krieg, A. M. 2000. Immune effects and mechanisms of action of CpG motifs. *Vaccine* 19:618-22.

20. Stryer, L. 1995. *Biochemistry*. Freeman and Company, New York, USA.

21. Yamamoto, S., T. Yamamoto, S. Shimada, E. Kuramoto, O. Yano, T. Kataoka, and T. Tokunaga. 1992. DNA from bacteria, but not from vertebrates, induces interferons, activates natural killer cells and inhibits tumor growth. *Microbiol Immunol* 36:983-97.

22. Krieg, A. M. , A. K. Yi, S. Matson, T. J. Waldschmidt, G. A. Bishop, R. Teasdale, G. A. Koretzky, and D. M. Klinman. 1995. CpG motifs in bacterial DNA trigger direct B-cell activation. *Nature* 374:546-9.

23. Werner, M. H., A. M. Gronenborn, and G. M. Clore. 1996. Intercalation, DNA kinking, and the control of transcription. *Science* 271:778-84.

24. van den Beucken, J. J. J. P., X. F. Walboomers, M. R. J. Vos, N. A. J. M. Sommerdijk, R. J. M. Nolte, and J. A. Jansen. Biological responses to multilayered DNA-coatings. *J Biomed Mater Res B*.

25. van den Beucken, J. J., X. F. Walboomers, O. C. Boerman, M. R. Vos, N. A. Sommerdijk, T. Hayakawa, T. Fukushima, Y. Okahata, R. J. Nolte, and J. A. Jansen. 2006. Functionalization of multilayered DNA-coatings with bone morphogenetic protein 2. *J Control Release*.

26. Luo, L., J. Liu, Z. Wang, X. Yang, S. Dong, and E. Wang. 2001. Fabrication of layer-by-layer deposited multilayer films containing DNA and its interaction with methyl green. *Biophys Chem* 94:11-22.

27. Panilaitis, B., G. H. Altman, J. Chen, H. J. Jin, V. Karageorgiou, and D. L. Kaplan. 2003. Macrophage responses to silk. *Biomaterials* 24:3079-85.

28. Saad, B., S. Matter, G. Ciardelli, G. K. Uhlschmid, M. Welti, P. Neuenschwander, and U. W. Suter. 1996. Interactions of osteoblasts and macrophages with biodegradable and highly porous polyesterurethane foam and its degradation products. *J Biomed Mater Res* 32:355-66.

29. Chomyszyn-Gajewska, M., B. Czajkowska, M. Blazewicz, E. Pamula, and M. Ptak. 2002. In vitro response of macrophages to a new carbon-polylactide composite for the treatment of periodontal diseases. *Biomaterials* 23:463-70.

30. Bailey, L. O., S. Lippiatt, F. S. Biancanello, S. D. Ridder, and N. R. Washburn. 2005. The quantification of cellular viability and inflammatory response to stainless steel alloys. *Biomaterials* 26:5296-302.

31. Li, Y., R. J. Schutte, A. Abu-Shakra, and W. M. Reichert. 2005. Protein array method for assessing in vitro biomaterial-induced cytokine expression. *Biomaterials* 26:1081-5.

32. Bernatchez, S. F., P. J. Parks, and D. F. Gibbons. 1996. Interaction of macrophages with fibrous materials in vitro. *Biomaterials* 17:2077-86.

33. Wimhurst, J. A., R. A. Brooks, and N. Rushton. 2001. Inflammatory responses of human primary macrophages to particulate bone cements in vitro. *J Bone Joint Surg Br* 83:278-82.

34. Giancotti, F. G. and E. Ruoslahti. 1999. Integrin signaling. *Science* 285:1028-32.

35. Pierschbacher, M. D. and E. Ruoslahti. 1984. Cell attachment activity of fibronectin can be duplicated by small synthetic fragments of the molecule. *Nature* 309:30-3.

5

MULTILAYERED DNA-COATINGS: *IN VITRO* BIOACTIVITY STUDIES AND EFFECTS ON OSTEOBLAST-LIKE CELL BEHAVIOR

JJJP van den Beucken, XF Walboomers, SCG Leeuwenburgh, MRJ Vos, NAJM Sommerdijk, RJM Nolte, JA Jansen

Acta Biomaterialia (2006); in press

I INTRODUCTION

The insertion of orthopedic and dental implants to replace malfunctioning articulating joints and lost teeth, is a common surgical procedure. For the construction of orthopedic and dental implants, many types of metals (or metallic alloys), ceramics, and polymers, or combinations thereof, have been used [1;2]. In order to remain functional, the material properties must meet the requirements for a given situation. For instance, functional orthopedic and dental implants require a tight conjunction with the surrounding bone tissue.

Amongst several other materials, calcium phosphate (CaP) ceramics such as hydroxyapatite (HA), have the capacity to form a chemical bond with the bone tissue at the interface and can induce a continuous transition from bone tissue to the implant surface [3]. In view of this, the formation of bone-like apatite on the surface is proposed as the essential requirement for an artificial material to bond to living bone [4]. However, due to their brittleness, the *in vivo* use of these so-called 'bioactive' materials for mechanically loaded applications is limited to coatings on a mechanically stronger implant base material, such as titanium.

The most commonly used methods to provide CaP-coatings on implants, including plasma spraying and sputter techniques, have limitations regarding implant geometry and porosity, and the incorporation of biologicals. Hence, studies have been undertaken to elucidate the mechanism responsible for the apposition of bone tissue to bioactive materials in order to find methods to increase surface bioactivity that do not entail these limitations. In view of this, the role of surface functional groups has been studied using *in vitro* experiments with simulated body fluids (SBF), which are solutions that are compositionally similar to human blood plasma. Such studies, in

which *in vivo* apatite formation can be reproduced [5], indicated that negatively-charged groups, and phosphate-containing groups in particular, are the most potent inducers of the CaP nucleation process [6;7].

A recently proposed implant coating material with high phosphate content is deoxyribonucleic acid (DNA) [8]. In addition to the proposed beneficial effects on CaP nucleation, DNA is an immunologically interesting material [9-11] and has the capacity to incorporate and bind other compounds [12]. In view of this, we recently used electrostatic self-assembly (ESA) to fabricate multilayered DNA-coatings [8], consisting of either poly-D-lysine (PDL) or poly(allylamine hydrochloride) (PAH) as the cationic counterpart of anionic DNA. The buildup of such coatings depends on the adsorption of the first polyelectrolyte to a substrate, after which electrostatic forces between oppositely-charged polyelectrolytes allow the formation of multilayered coatings. Both types of DNA-coatings were shown to contain 15 μg DNA per cm^2, as demonstrated using radiolabeled DNA [8]. Furthermore, these DNA-coatings displayed a polycation-dependent surface roughness, as studied using atomic force microscopy [8]. Finally, both types of DNA-coatings demonstrated (i) to be cyto- and histocompatible [13;14], (ii) to decrease the secretion of the major pro-inflammatory cytokine (tumor necrosis factor alpha; TNF-α) by macrophages [15], and (iii) to be eligible for functionalization with the osteoinductive factor bone morphogenetic protein 2 [16].

In the present study, we aimed at evaluating potential effects of the phosphate groups in both types of DNA-coatings on CaP nucleation and growth in SBF immersion experiments. For this purpose, DNA-coatings were prepared on titanium substrates and immersed in SBF of various compositions. Non-coated titanium substrates served as controls. After immersion in SBF for 1, 2, and 4 weeks, the surfaces of the substrates were evaluated morphologically (scanning electron microscopy, SEM) and chemically (X-ray diffraction, XRD; Fourier transform infrared spectroscopy, FTIR; energy dispersive spectroscopy, EDS). Subsequently, titanium substrates with or without DNA-coatings and subsequent SBF-immersion pretreatment were seeded with primary rat bone marrow-derived osteoblast-like cells to study cell proliferation, differentiation, and morphology.

II MATERIALS & METHODS

Materials

Polyanionic salmon DNA (± 300 bp/molecules; sodium salt) was kindly donated by Nichiro Corporation (Kawasaki-city, Kanagawa prefecture, Japan). Potential protein impurities in the DNA were checked using the bicinchoninic acid (BCA) protein assay (Pierce, Rockford, IL, USA), and were measured to be below 0.20 % w/w (data not shown). Polycationic polyelectrolytes poly-D-lysine (PDL; MW 30000 – 70000) and poly(allylamine hydrochloride) (PAH; MW ~70000) were purchased from Sigma (Sigma-Aldrich Chemie B.V., Zwijndrecht, the Netherlands). All materials were used without further purification.

Substrate preparation and cleaning

Disc-shaped titanium substrates (12 mm diameter; 1.5 mm thickness; commercially-pure titanium (cpTi), as-machined) were cleaned ultrasonically using consecutively nitric acid (10% v/v), acetone, and isopropanol. After the cleaning steps using nitric acid and acetone, the substrates were thoroughly rinsed with ultra-pure water from a Milipore system (Milipore B.V., Amsterdam, the Netherlands). After the isoporopanol step, the substrates were air-dried.

Generation of multilayered DNA-coatings

DNA-coatings were generated using the ESA-technique, as described previously [17]. Briefly, the substrates were immersed in an aqueous solution of either PDL (0.1 mg/ml) or PAH (1 mg/ml) for 30 minutes, allowing sufficient time for the adsorption of the first cationic polyelectrolyte layer onto the substrates. Subsequently, substrates were washed in ultra-pure water (5 minutes; continuous water flow) and dried using a pressurized air stream. Thereafter, substrates were alternately immersed in an anionic aqueous DNA solution (1 mg/ml) and the respective cationic polyelectrolyte solution for 7 minutes each, with intermediate washing in ultra-pure water and subsequent drying using a pressurized air stream to obtain final coating architectures of $[PDL/DNA]_5$ or $[PAH/DNA]_5$ (the number indicates the total number of double-layers).

SBF immersion experiments

Simulated Body Fluid

The recipe for the preparation of SBF was adopted from Kokubo et al. [18;19]. Immersion experiments were performed with SBF containing physiological (SBF_1) and 2-fold increased calcium- and phosphate-ion concentrations (SBF_2) compared to human blood serum (Table 1). The pH-value of both solutions was set at 7.4 after complete preparation. Immersion studies were performed in 15 ml tubes (Greiner Bio-One B.V., Alphen aan de Rijn, the Netherlands), using 1 substrate per tube in 4 ml SBF. Tubes were placed in a water bath at 37°C under continuous shaking. The SBF solution in the tubes was refreshed on a weekly basis. After immersion periods of 1, 2, and 4 weeks, substrates were thoroughly rinsed three times with ultra-pure water, and air-dried.

TABLE 1: CONCENTRATIONS OF IONIC SPECIES (MM) IN SIMULATED BODY FLUID (SBF) OF DIFFERENT Ca^{2+} AND PO_4^{3-} CONCENTRATIONS AND HUMAN BLOOD PLASMA (HBP).

Species	*SBF_1*	*SBF_2*	*HBP*
Na^+	142.0	142.0	142.0
K^+	5.0	7.0	5.0
Ca^{2+}	2.5	5.0	2.5
Mg^{2+}	1.5	1.5	1.5
Cl^-	148.0	147.0	103.0
CO_3^{2-}	4.2	4.2	27.0
PO_4^{3-}	1.0	2.0	1.0
SO_4^{2-}	0.5	0.5	0.5

Evaluation of surface morphology
After the various SBF immersion periods (1, 2, and 4 weeks), the surface morphology of the substrates was examined using scanning electron microscopy (SEM). Therefore, specimens were sputter coated with gold and examined using a Jeol 6310 scanning electron microscope at an acceleration voltage of 10-15 kV.

Surface analysis
The crystallographic structure of depositions on the substrates was characterized using a Philips thin-film X-ray diffractometer with CuKα-radiation (PW3710; 40 mV; 30 mA). For analysis, the substrates were fixed with the angle of incidence at a position of 2.5° (2θ), while scanning from 24° to 36° (2θ) with the solid state detector (step size of 0.02° (2θ); sample time of 25 s/step). Characterization of the molecular structure of depositions on the experimental substrates was performed using Fourier Transform InfraRed spectroscopy (FTIR; Perkin Elmer Instruments, Zoetermeer, the Netherlands). Infrared spectra were recorded in the range from 4000 to 450 cm^{-1}. Energy Dispersive Spectroscopy (EDS) was performed using an energy-dispersive X-ray microanalyzer (Voyager), integrated with the abovementioned SEM. EDS was carried out at a magnification of 500x at an acceleration voltage of 10-15 kV to determine the elemental composition of potential depositions. The calcium amount on the substrates after immersion in SBF for 1, 2, and 4 weeks was measured using the ortho-cresolphtalein (OCPC) method (Sigma) [20]. Briefly, the substrates were placed into a fresh 24 wells plate, 1 ml 0.5 N acetic acid was added per substrate, and the experimental substrates were incubated overnight on a shaking apparatus. For analysis, 300 µl working reagent was added to aliquots of 10 (l sample or standard (in duplo) in a 96-wells plate. A standard curve was prepared using serial dilution of $CaCl_2$ (final concentrations 0 – 100 µg/ml). The plate was incubated at room temperature for 10 minutes and then read in an ELISA reader at 540 nm.

Osteoblast-like cell culture experiments
Three independent experimental runs of cell culture experiments with osteoblast-like cells were performed. For each experimental run, cells were isolated from one individual rat.

Experimental substrates
For cell culture experiments, seven types of experimental substrates were used:

1. Ti-$[PDL/DNA]_5$ (no immersion in SBF_2)
2. Ti-$[PDL/DNA]_5$-1w (1 week immersion in SBF_2)
3. Ti-$[PDL/DNA]_5$-2w (2 weeks immersion SBF_2)
4. Ti-$[PAH/DNA]_5$ (no immersion in SBF_2)
5. Ti-$[PAH/DNA]_5$-1w (1 week immersion in SBF_2)
6. Ti-$[PAH/DNA]_5$-2w (2 weeks immersion in SBF_2)
7. non-coated control (titanium discs)

Prior to use in cell culture experiments, all substrates were sterilized by UV-treatment (254 nm; 4 h.).

Isolation of rat bone marrow cells
Rat bone marrow (RBM) cells were isolated and cultured using a method adapted from Maniatopoulos et al. [21]. Briefly, the femora of male Wistar WU rats were extracted, and epiphyses were cut off. RBM cells were flushed out of the remaining diaphyses using cell culture medium (α-MEM (Gibco) supplemented with 10% fetal calf serum (FCS; Gibco), 50 µg/ml ascorbic acid (Sigma), 10 mM Na-β-glycerophosphate (Sigma), 10^{-8} M dexamethasone (Sigma), and 50 µg/ml gentamycin (Gibco)). RBM cells of two femora were cultured under static conditions in cell culture medium in three 75 cm^2 culture flasks (Greiner Bio-One) in a humidified incubator (37°C; 95% air; 5% CO_2) for one day, after which the medium was refreshed to remove non-adherent cells. Subsequently, the attached cells were pre-cultured for another 6 days. After the total primary culture of 7 days to obtain osteoblast-like cells, cells were detached using

trypsin/EDTA (0.25% w/v trypsin, 0.02% w/v EDTA) and the total cell number was determined using a Coulter® counter (Beckman Coulter Inc., Fullerton, CA, USA). Finally, cells were seeded at a density of 1 x 10^4 cells/cm^2 onto the experimental substrates, which were placed in a 24-wells plate (Greiner Bio-One). The cell culture medium was refreshed 1 day after cell seeding, and thereafter 3 times per week.

Cell proliferation
At 4, 8, 12, and 16 days post-seeding, the medium was removed and the cells were washed with phosphate-buffered saline (PBS; pH 7.4) three times. Subsequently, the experimental substrates (n=3 for each condition at each time point) with attached cells were transferred into fresh 24-well plates, and each experimental substrate was immersed in 1 ml ultra-pure water. These samples were frozen and thawed for 3 repetitive cycles, after which the proliferation of the cells was analyzed by measuring the cellular protein content in the aqueous samples using a micro BCA protein assay (Pierce, Rockford, IL, USA) according to the instructions of the manufacturer.

Alkaline phosphatase activity
The alkaline phosphatase (ALP) activity was measured as a marker for early differentiation of osteoblast-like cells using the same samples (n=3 for each condition at each time point) as for the proliferation assay according to a previously described method [22]. A volume of 80 μl of sample or standard and 20 μl of buffer solution (5 mM $MgCl_2$, 0.5 M 2-amino-2-methyl-1-propanol) was pipetted into a 96-wells plate (Greiner Bio-One) in duplo, and 100 μl of substrate solution (5 mM paranitrophenylphosphate) was added per well. Subsequently, the plate was incubated for one hour at 37°C, after which the reaction was stopped by adding 100 μl 0.3 M NaOH. Serial dilutions of 4-nitrophenol (final concentrations 0 – 25 nM) were used for the standard curve. The plate was read in an ELISA reader at 405 nm.

Osteocalcin assay
To avoid interference of calcium from SBF-pretreated experimental substrates, not calcium deposition but the deposition of osteocalcin in the extracellular matrix was used as a marker of late differentiation of osteoblast-like cells. The amount of deposited osteocalcin after 8, 16, and 24 of cell culture was measured by an enzyme immuno-assay (EIA; Biomedical Technologies, Inc., Stoughton, MA, USA) according to the instructions of the manufacturer. Briefly, samples (n=3 for each condition at each time point) were collected by scraping the surface of the experimental substrates at indicated time points after washing twice with PBS. Samples were stored at -20°C until analyses. For analysis, 100 μl of sample was added to the wells (in duplo) and incubated at 4°C for 24 hours. Wells were washed three times with 300 μl wash buffer, after which 100 μl osteocalcin antiserum was added to each well. After 1 hour incubation at 37°C, wells were washed as before and 100 μl donkey anti-goat IgG-peroxidase was added. After incubation for 1 hour at room temperature and subsequent washing as before, 100 μl substrate solution (1 volume TMB solution + 1 volume hydrogen peroxidase) was added to each well for 30 minutes incubation at room temperature. Subsequently, 100 μl stop solution was added to each well, and the plate was read at 405 nm within 15 minutes. Standards (0 – 40 ng/ml) were enrolled to prepare a standard curve.

Evaluation of cell morphology
Scanning electron microscopy was performed to evaluate the morphological appearance of the cells. At 4 and 16 days post-seeding, substrates with attached cells were washed twice with PBS and fixed using gluteraldehyde (4% in 0.1 M cacodylate buffer) for 20 minutes. Subsequently, the substrates were washed twice with 0.1 M cacodylate buffer and dehydrated in a graded series of ethanol. Finally, the substrates were dried with tetramethylsilane, sputter coated with gold and examined using a JEOL 6310 SEM at an acceleration voltage of 10-15 kV.

Statistical analyses

All data were obtained from triplicate samples and measured in duplo. Measurements were statistically evaluated with Graphpad® Instat 3.05 software (GraphPad Software Inc., San Diego, CA, USA), using a one-way ANOVA combined with a post-hoc Tukey–Kramer Multiple Comparisons test. The significance level was set at $p<0.05$.

III RESULTS

SBF immersion experiments

Surface morphology

During all SBF immersion experiments, no homogeneous precipitates were observed in the SBF solutions, and no precipitation on the test tubes was observed. Immersion of the experimental substrates in SBF_1 did not result in the formation of precipitates on any type of substrate used in this study. In contrast, immersion experiments with SBF_2 resulted in spot-like depositions on all three types of substrates (Ti, Ti-$[PDL/DNA]_5$, and Ti-$[PAH/DNA]_5$) after one week. The spots consisted of compact spheroids, which in SEM observation exhibited diameters of approximately 5 μm. After two weeks immersion in SBF_2, the depositions on Ti-$[PDL/DNA]_5$ and Ti had increased in both size and number, whereas on Ti-$[PAH/DNA]_5$ the complete surface was covered with a continuous thin layer of deposited spheroids (Figure 1). After four weeks of immersion in SBF_2, all of the substrates (Ti, Ti-$[PDL/DNA]_5$, and Ti-$[PAH/DNA]_5$) were covered with a continuous layer of deposited spheroids.

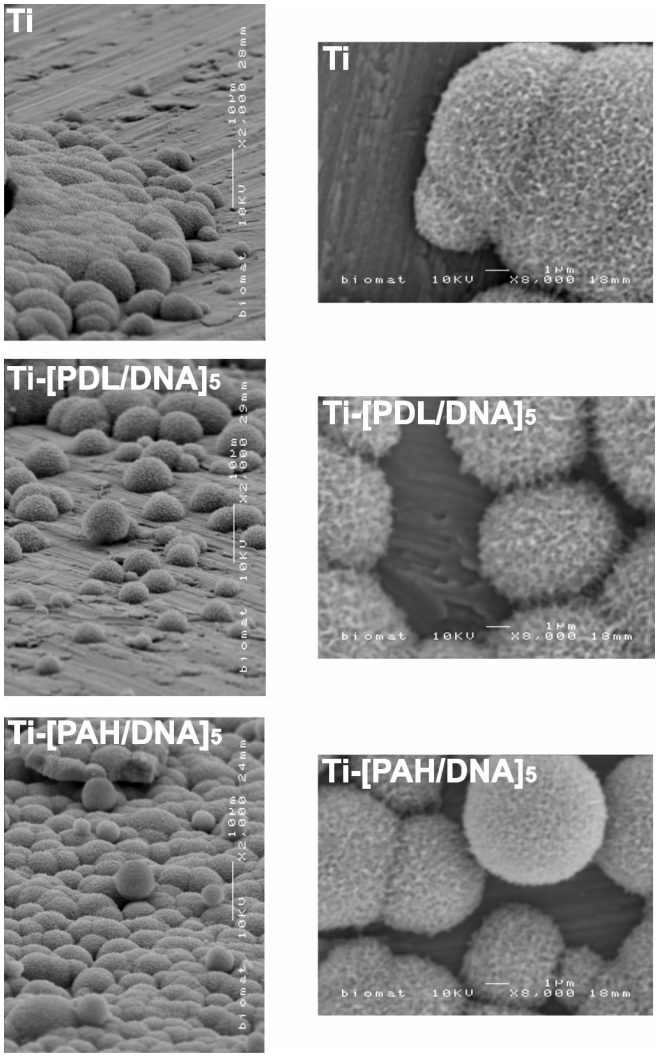

Figure 1: Scanning electron micrographs of Ti, Ti-$[PDL/DNA]_5$, and Ti-$[PAH/DNA]_5$ substrates after immersion in SBF_2 for a period of two weeks. Images on the left were obtained by tilting the samples (approximately 60°). Higher magnifications (of non-tilted samples) are presented in the right panels.

Surface analysis

The XRD analyses revealed that the depositions had a poorly crystalline apatitic nature. Figure 2 presents the XRD-patterns of the substrates after an immersion period of two weeks in SBF_2. Diffraction peaks of apatitic calcium phosphate at $2\theta = 25.7°$ (002) and a broad band around $2\theta = 32°$ [23;24] could be observed on Ti-$[PDL/DNA]_5$ and especially Ti-$[PAH/DNA]_5$. Additionally, only the Ti-$[PAH/DNA]_5$ substrates showed an additional apatitic diffraction peak at $2\theta = 28.0$ (102) [24]. On the other hand, apatitic diffraction peaks were less intense on Ti, and only broad maxima were observed between $2\theta = 28°$ and $2\theta = 32°$. Intensities of apatitic diffraction peaks were higher for Ti-$[PAH/DNA]_5$ as compared to both Ti-$[PDL/DNA]_5$ and Ti. After an immersion period of four weeks, all experimental substrates exhibited XRD-patterns similar to the one of Ti-$[PAH/DNA]_5$ after only two weeks.

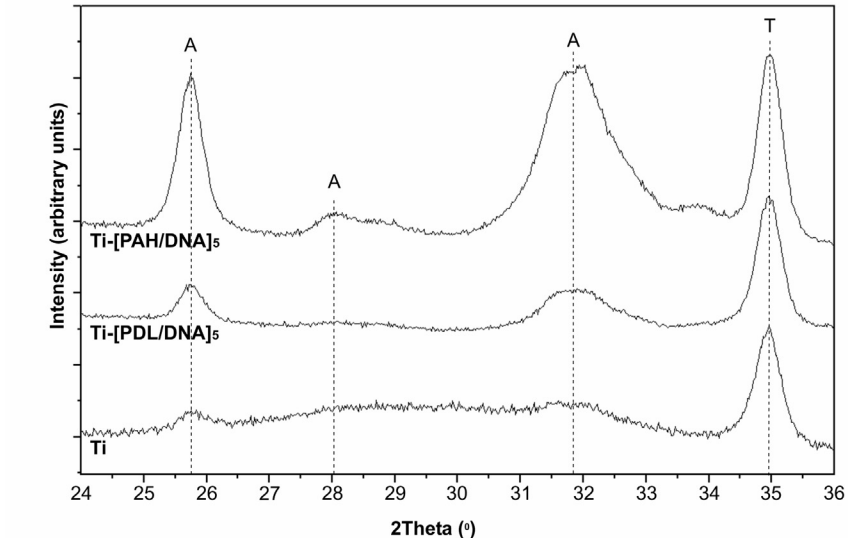

Figure 2: XRD-patterns of Ti, Ti-$[PDL/DNA]_5$, and Ti-$[PAH/DNA]_5$ substrates after immersion in SBF_2 for two weeks. (A: apatite; T: titanium)

FTIR-spectra of all experimental samples after one week of immersion in SBF_2 consisted of weak phosphate absorption bands (data not shown). After two weeks of immersion in SBF_2, FTIR-spectra showed more pronounced absorption bands on all experimental substrates (Figure 3), although substrate-dependent differences in intensity were observed (Ti-$[PAH/DNA]_5$ > Ti-$[PDL/DNA]_5$ > Ti). A broad absorption band at 3400 cm^{-1} (OH-stretching) and a small absorption band at 1646 cm^{-1} (H_2O-bending) were observed on all experimental substrates. Absorption bands characteristic for phosphate were observed at 957 (v_1 PO_4-stretching), 1020 (v_3 PO_4-stretching), and 1113 cm^{-1} (v_3 PO_4-stretching).

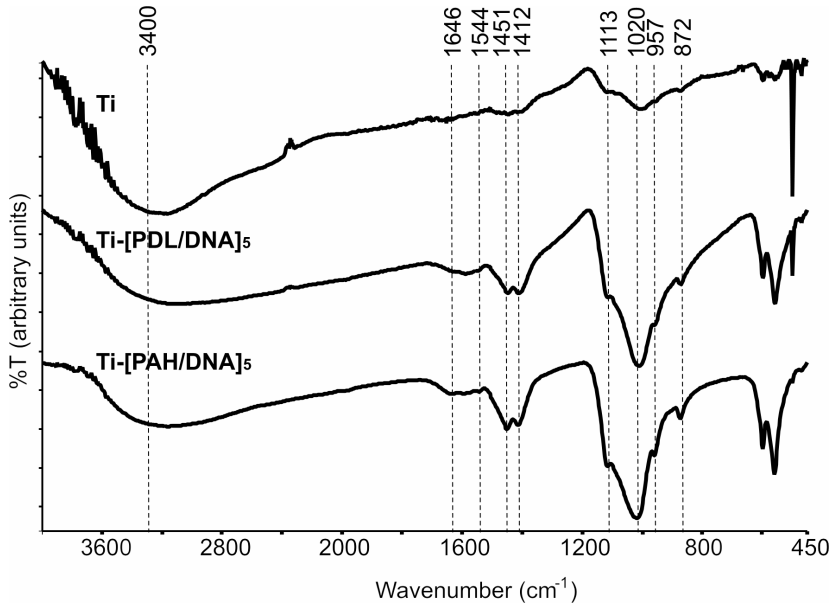

Figure 3: FTIR-spectra of Ti, Ti-$[PDL/DNA]_5$, and Ti-$[PAH/DNA]_5$ substrates after immersion in SBF_2 for two weeks.

The incorporation of CO_3-ions into the apatitic depositions is reflected by absorption bands at 872 (v_2 CO_3), 1412 (v_3 CO_3-stretching B-type), 1451 (v_3 CO_3-stretching B-type), and 1544 (v_3 CO_3-stretching A-type) cm^{-1} [25]. After a four week immersion period in SBF_2, the FTIR-spectra of all experimental substrates were similar with absorption bands at identical positions and similar intensities as those of the spectrum of Ti-$[PAH/DNA]_5$ after two weeks.

Using EDS, it was demonstrated that the deposited spheroids contained calcium- as well as phosphorus-atoms. The calcium/phosphate ratios of the deposited spheroids demonstrated to be in the range of 1.7 – 2.0.

The amount of calcium deposited on the experimental substrates during immersion in SBF_2 was measured using the OCPC-method. The results (Figure 4) showed that a significantly higher amount of calcium ($p<0.05$) was found on Ti-$[PAH/DNA]_5$ after one week compared to Ti. After two weeks, both Ti-$[PDL/DNA]_5$ and Ti-$[PAH/DNA]_5$ showed significantly higher amounts of calcium ($p<0.05$) compared to Ti. No statistically significant ($p>0.05$) differences in the amount of deposited calcium were measured after an immersion period of 4 weeks.

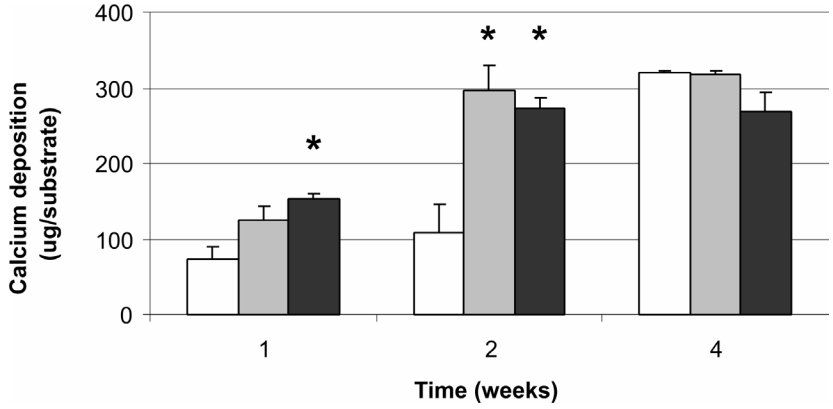

Figure 4: Calcium deposition on Ti (controls; white bars), Ti-$[PDL/DNA]_5$ (grey bars), and Ti-$[PAH/DNA]_5$ (black bars) after immersion in SBF_2. ($p<0.05$ compared to controls [Ti])*

Osteoblast-like cell culture experiments

Three independent runs of cell culture experiments showed similar results. Non-SBF-immersed DNA-coatings were found to have no effects on osteoblast-like cell proliferation, differentiation, and morphology compared to controls. Therefore, only the results of SBF-pretreated DNA-coatings and non-coated/non-SBF-pretreated controls are described in the following section.

In Figure 5, the results for osteoblast-like cell proliferation are depicted. All experimental groups showed an increase in the cellular protein content between day 4 and 8 after cell seeding. Around day 12, a maximum was reached in all experimental groups, after which cellular protein content in all experimental groups decreased from day 12 to day 16. Compared to controls, significantly decreased values were observed for Ti-$[PDL/DNA]_5$-2w ($p<0.05$) at day 4, and for Ti-$[PDL/DNA]_5$-1w ($p<0.05$) and Ti-$[PAH/DNA]_5$-1w ($p<0.05$) at day 8.

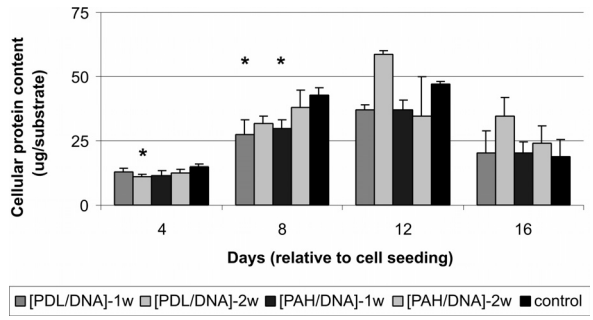

Figure 5: Cellular protein content of osteoblast-like cells after culture on Ti-$[PDL/DNA]_5$-1w, Ti-$[PDL/DNA]_5$-2w, Ti-$[PAH/DNA]_5$-1w, Ti-$[PAH/DNA]_5$-2w, and controls for 4, 8, 12, and 16 days. Bars represent mean ± SD of one representative experiment out of 3. ($p<0.05$ compared to controls [Ti])*

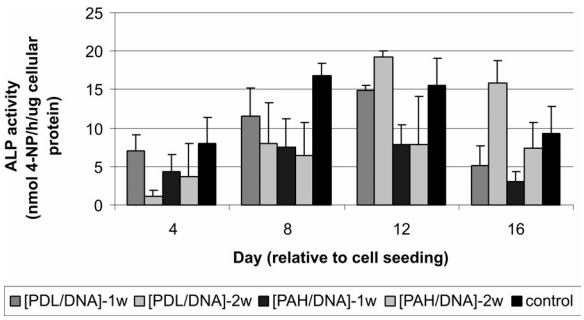

Figure 6: Alkaline phosphatase (ALP) activity of osteoblast-like cells after culture on Ti-$[PDL/DNA]_5$-1w, Ti-$[PDL/DNA]_5$-2w, Ti-$[PAH/DNA]_5$-1w, Ti-$[PAH/DNA]_5$-2w, and controls for 4, 8, 12, and 16 days. Bars represent mean ± SD of one representative experiment out of 3.

The results of the ALP activity measurements are depicted in Figure 6, and are indicative for the early differentiation of osteoblast-like cells. Similar to the results of cell proliferation, an increase in ALP activity was observed for all experimental groups from day 4 to day 8 after cell seeding. All experimental groups reached maximal ALP activity around day 12, after which in all groups ALP activity decreased. No statistically significant differences were observed compared to controls ($p>0.05$).

The deposition of osteocalcin, as a marker of matrix mineralization, was measured on days 8, 16, and 24 after cell seeding (Figure 7). The deposition of osteocalcin showed an increase in all experimental groups from day 8 to day 24 after cells seeding. Compared to controls, significantly increased levels were observed for Ti-$[PDL/DNA]_5$-2w at day 16 ($p<0.01$) and day 24 ($p<0.05$), and for Ti-$[PAH/DNA]_5$-2w at day 24 ($p<0.05$).

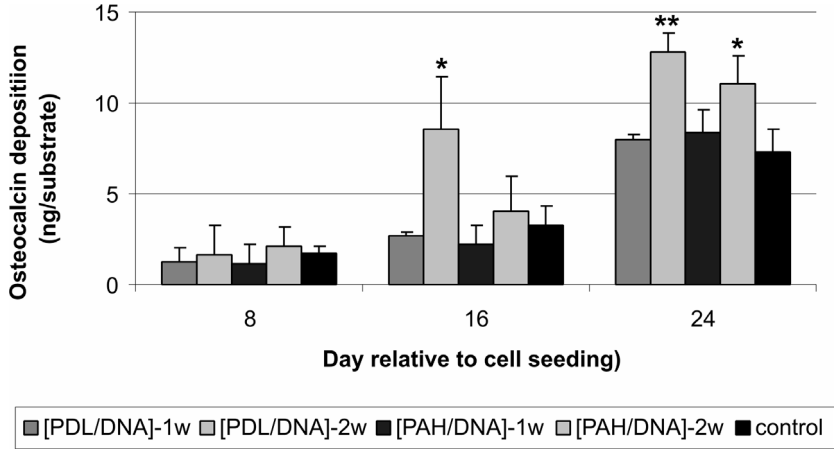

Figure 7: Osteocalcin deposition in extracellular matrix by osteoblast-like cells cultured on Ti-$[PDL/DNA]_5$-1w, Ti-$[PDL/DNA]_5$-2w, Ti-$[PAH/DNA]_5$-1w, Ti-$[PAH/DNA]_5$-2w, and controls after 8, 16, and 24 days. Bars represent mean ± SD of one representative experiment out of 3. ($p<0.05$; ** $p<0.01$ compared to controls [Ti])*

Examination of the osteoblast-like cell cultures on the experimental substrates using electron microscopy indicated that in all experimental groups cells proliferated (Figure 8). No apparent microscopic differences were observed after 4 days osteoblast-like cell culture between the experimental groups. Generally, after 4 days of culture none of the surfaces of the experimental substrates was covered completely with a confluent layer of osteoblast-like cells. Instead, relatively large areas of the uncovered substrate surfaces were visible. On SBF-pretreated DNA-coatings, cells were positioned on the deposited CaP spheroids and cellular extensions were observed to bridge gaps between relatively high CaP spheroids (Figure 8A,D). On control substrates, osteoblast-like cells had a flat appearance and were spread out over the surface (Figure 8G). After 16 days of osteoblast-like cell culture, cells had formed a cellular multilayer on all experimental substrates. Furthermore, abundant formation of extracellular matrix, consisting of collagen fibers and mineralized globules, was observed on all experimental substrates. However, on Ti-$[PDL/DNA]_5$-2w, on basis of visual inspection, the formation of mineralized globules appeared to be more pronounced than on any of the other experimental substrates (Figure 8B,C), which corroborates the results of the osteocalcin deposition.

IV DISCUSSION

The objective of this study was to detect potential effects of abundant phosphate groups in two types of multilayered DNA-coatings on (i) CaP nucleation and growth in SBF immersion experiments, and (ii) the behavior of osteoblast-like cells *in vitro* with or without pretreatment in SBF. It was demonstrated that DNA-coatings increase the deposition of CaP spheroids from SBF with doubled concentrations of calcium and phosphate ions compared to non-coated titanium controls. Deposited CaP spheroids were found to be composed of a poorly crystalline carbonated apatitic nature. Furthermore, cell culture experiments with osteoblast-like cells demonstrated that non-SBF-pretreated DNA-coatings did not affect cell proliferation, differentiation, and morphology compared to non-coated controls. However, two weeks pretreatment of DNA-coatings in SBF appeared to increase osteoblast-like cell differentiation, as observed by a decreased proliferation and an increased deposition of osteocalcin in the extracellular matrix. The formation of CaP depositions on biomaterials after immersion in SBF is a

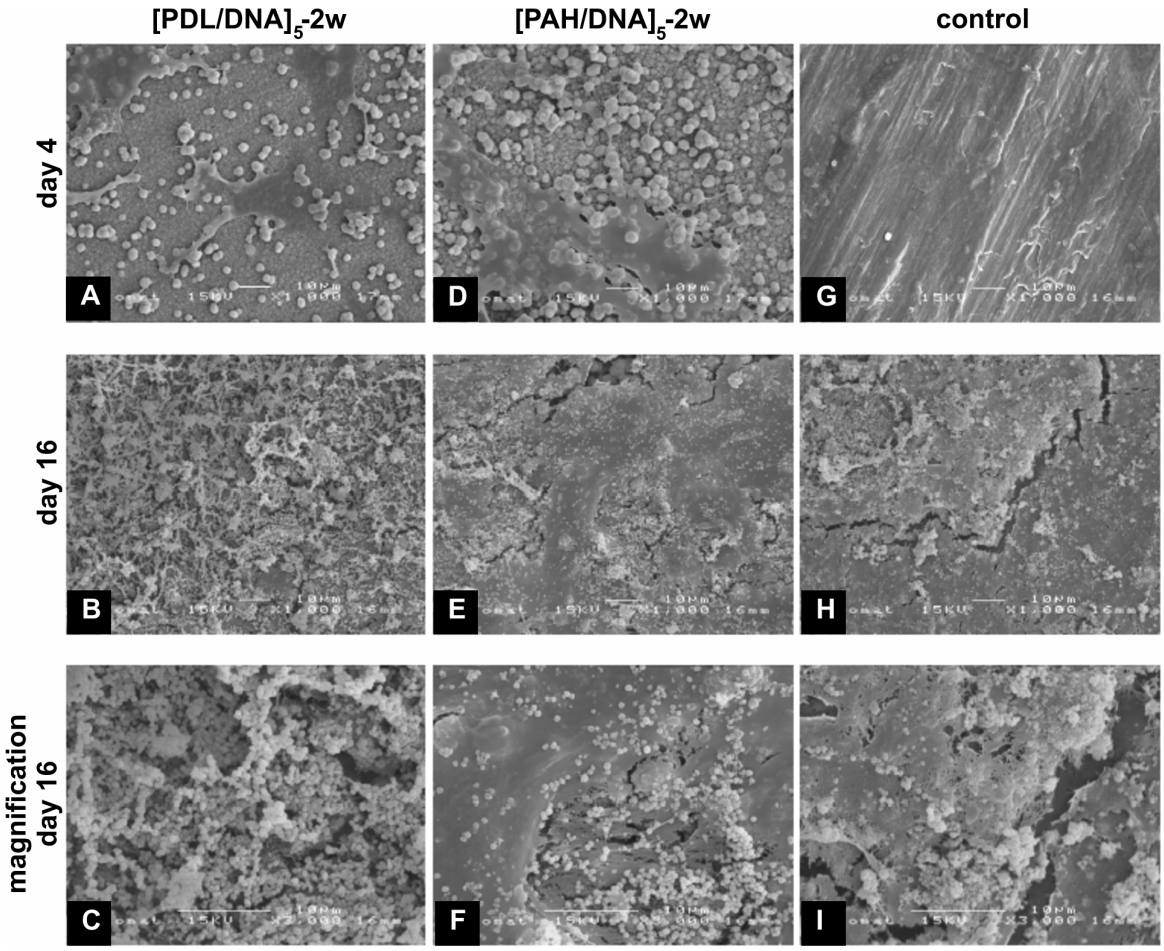

Figure 8: Scanning electron microscopy images of osteoblast-like cell cultures on Ti-[PDL/DNA]$_5$-2w (A,B,C), Ti-[PAH/DNA]$_5$-2w (D,E,F), and controls (G,H,I) after 4 (A,D,G) and 16 (B,C,E,F,H,I) days post-seeding.

well defined method to obtain first indications about potential bone bonding properties of biomaterials *in vivo*. Recently, Van der Wal et al. demonstrated that several types of ceramics remained inert in SBF_x, with *x* below 1.4 [26]. Therefore, SBF with two different compositions (SBF_1 and SBF_2) were used in our immersion experiments. Immersion of Ti, Ti-[PDL/DNA]$_5$, and Ti-[PAH/DNA]$_5$ in SBF_1 did not result in the formation of depositions on any of the substrates, which corroborates with the results of Van der Wal [26]. However, immersion of the substrates in SBF_2 resulted in substrate-dependent deposition of apatitic spheroids. At two weeks after immersion, the complete surface of Ti-[PAH/DNA]$_5$ was covered with a thin layer of spheroids. In contrast, the deposition of spheroids on Ti and Ti-[PDL/DNA]$_5$ was found to be directed away from the substrate surface, resulting in higher deposition spots (islands) rather than a complete surface coverage. The amount of calcium deposited on the experimental surfaces appeared to be significantly higher on both types of DNA-coatings. Together, these results indicate a predisposition of DNA-coatings for the deposition of apatitic spheroids and corroborate the results of experiments that demonstrated that phosphate groups at the substrate surface are potent inducers of heterogeneous CaP nucleation and growth in SBF [6;7]. Differences in the amount and morphological appearance of the depositions are probably related to (i) differences in surface roughness of both types of DNA-coatings prior to SBF immersion [8], (ii) the conformation of DNA-molecules in the coating (Z-conformation in [PDL/DNA]$_5$; B-conformation in [PAH/DNA]$_5$ [17]), and/or the interference of the cationic polyelectrolyte. The influence of surface roughness remains speculative as the data on this subject are contradictory. Leitao et al. demonstrated that rougher surfaces induce scattered crystal-like depositions, whereas smoother surfaces exhibit a more plate-like deposition morphology [27]. On the other hand, Barrere et al. [28] demonstrated that heterogeneous nucleation of CaP on titanium from a supersaturated SBF (SBF_5)

was independent of surface roughness, but that rough topography was beneficial for further growth and mechanical attachment of the final CaP-coating. In view of DNA-conformation in the DNA-coatings, the difference in screw sense between the Z- and the B-form of DNA is accompanied by differences in helix diameter and hence the number of base pairs per turn of the helix, which is increased in Z-form DNA [29]. This results in specific spatial distributions of the phosphate groups in the DNA-molecules. Interference of the cationic electrolyte used during the build up of the coatings, either PDL or PAH, in terms of blocking phosphate groups in the electrostatically bonded DNA molecules with calcium ions in the SBFs is more likely for PDL, as this polymer is capable of diffusing throughout polyelectrolyte multilayers [30]. However, this property of PDL, which is also the critical factor for exponential growth of polyelectrolyte multilayers after the deposition of multiple double-layers, is expected to be of limited relevance in the present study, which used linearly-growing DNA-coating consisting of only 5 double-layers [8].

The results of the XRD and FTIR measurements corroborate the findings of SEM and calcium deposition. The intensities of the absorbance bands were high on Ti-$[PAH/DNA]_5$, intermediate on Ti-$[PDL/DNA]_5$, and low on Ti after a two week immersion period in SBF_2. The apatitic spheroids deposited on all types of substrates contained carbonate ions, which became apparent after two weeks of immersion in SBF_2. The carbonate ions were incorporated at PO_4-sites (B-type substitution), and via hydroxyl substitution (A-type substitution). The presence of a mixed-type AB carbonate apatite might further explain the increased calcium-to-phosphate ratios compared to those in biological HA (Ca/P = 1.67), measured by EDS, as the substitution of phosphate by carbonate results in increased calcium-to-phosphate ratios.

For cell culture experiments, the choice of experimental groups was based on (i) the effects DNA-configuration and roughness of non-SBF-immersed DNA-coatings, and (ii) the CaP-coverage and roughness of SBF pretreated DNA-coatings. Since an immersion period of 4 weeks resulted in the complete coverage of the non-coated control substrates and both types of DNA-coatings, these substrates were not enrolled in the cell culture experiments with osteoblast-like cells.

Cell culture experiments with osteoblast-like cells revealed that non-SBF-immersed DNA-coatings do not change osteoblast-like cell behavior. In contrast, previous experiments in our group have demonstrated that the proliferation of primary rat dermal fibroblast was increased on both types of DNA-coatings compared to non-coated controls [13;14]. Apparently, the increased proliferation on DNA-coatings is cell type-dependent.

Pretreatment of DNA-coatings in SBF was found to affect osteoblast-like cell differentiation, as evidenced by the increased deposition of osteocalcin in the extracellular matrix. It may be argued that for proper comparison of osteocalcin deposition levels these data should be corrected for cell amount. Unfortunately, prolonged culture of osteoblast-like cells and concomitant differentiation of these cells are related to difficulties in retrieving samples for the determination of cell amount [31]. On the other hand, the data on osteocalcin deposition are supported by the SEM observations, which show more pronounced extracellular matrix formation, especially for Ti-$[PDL/DNA]_5$-2w substrates. Furthermore, the increase in osteocalcin deposition corroborates with other studies that demonstrated the cytoactive nature of CaP [32;33].

Unambiguously, the 2-week pretreatment of DNA-coatings in SBF resulted in a complete change in surface characteristics from those described in our previous work [8] to a CaP surface as characterized in this work. The differences in CaP-coverage and final substrate roughness can explain the observed differences in osteocalcin deposition by osteoblast-like cells on the two experimental groups that received a 2-week pretreatment and are in line with previously reported effects of surface roughness on osteoblast-like cell behavior [34-36]. Pretreatment of DNA-coatings in SBF for 1 week resulted in surfaces with properties that are a mixture of those of these DNA-coatings [8] and those of coatings with partial CaP-coverage. This could be an explanation for the similarities in osteoblast-like cell behavior on 1-week pretreated DNA-coatings and that on non-coated controls.

Although the results of this study can be interpreted as being promising for the *in vivo* bioactivity of DNA-coatings, future animal experiments are necessary to classify DNA-coatings as bioactive. In such *in*

vivo experiments, many important biological processes that affect direct bone-bonding are combined in an overlapping sequential fashion, including both non-cellular and cellular interactions. Furthermore, as the formation of CaP-depositions was observed to be dependent on the cationic polyelectrolyte used for the built up of the DNA-coatings, other cationic counterparts may further enhance the deposition process.

CONCLUSION

This study demonstrates that surface treatment of titanium with DNA-coatings increases its potential to nucleate CaP-deposition from SBF. The surface coverage was dependent on the cationic counterpart of DNA in the DNA-coating. While $[PDL/DNA]_5$ coatings and non-coated titanium controls showed spot-like depositions after two weeks of immersion in SBF_2, $[PAH/DNA]_5$ coatings were completely covered by a continuous layer of carbonated apatitic spheroids. Non-SBF-pretreated DNA-coatings were found to have no effects on osteoblast-like cell behavior. On the other hand, SBF-pretreatment of DNA-coatings affected the differentiation of osteoblast-like cells through an increased deposition of osteocalcin. The results of this study are indicative for bone-bonding capacities of DNA-coatings. Nevertheless, future animal experiments are required to provide conclusive evidence for the bioactivity of DNA-coatings.

V ACKNOWLEDGEMENTS

The authors would like to acknowledge Nichiro Corporation (Kawasaki-city, Kanagawa prefecture, Japan) for providing DNA. Scanning electron microscopy was performed in collaboration with the Microscopical Imaging Center of the Nijmegen Center for Molecular Life Sciences (NCMLS). This research was financially supported by the Technology Foundation STW, applied science division of NWO and the technology programme of the Ministry of Economic Affairs, grant # NKG.5758.

VI REFERENCES

1. Galante, J. O., J. Lemons, M. Spector, P. D. Wilson Jr, and T. M. Wright. 1991. The biologic effects of implant materials. *J Orthop Res* 9:760-75.

2. Santavirta, S., M. Takagi, E. Gomez-Barrena, J. Nevalainen, J. Lassus, J. Salo, and Y. T. Konttinen . 1999. Studies of host response to orthopedic implants and biomaterials. *J Long Term Eff Med Implants* 9:67-76.

3. Ducheyne, P., Bianco, P., Radin, S., and Scherpers, E. Bioactive Materials: Mechanisms and Bioengineering Considerations. 92. Leiderdorp, the Netherlands, Reed Healthcare Communications. Bone-bonding biomaterials. Ducheyne, P., Kokubo, T., and van Blitterswijk, C. A.

4. Kokubo, T., S. Ito, Z. T. Huang, T. Hayashi, S. Sakka, T. Kitsugi, and T. Yamamuro. 1990. Ca,P-rich layer formed on high-strength bioactive glass-ceramic A-W. *J Biomed Mater Res* 24:331-43.

5. Kokubo, T. and H. Takadama. 2006. How useful is SBF in predicting in vivo bone bioactivity? *Biomaterials* 27:2907-15.

6. Liu, Q., J. Ding, F. K. Mante, S. L. Wunder, and G. R. Baran. 2002. The role of surface functional groups in calcium phosphate nucleation on titanium foil: a self-assembled monolayer technique. *Biomaterials* 23:3103-11.

7. Tanahashi, M. and T. Matsuda. 1997. Surface functional group dependence on apatite formation on self-assembled monolayers in a simulated body fluid. *J Biomed Mater Res* 34:305-15.

8. van den Beucken, J. J., M. R. Vos, P. C. Thune, T. Hayakawa, T. Fukushima, Y. Okahata, X. F. Walboomers, N. A. Sommerdijk, R. J. Nolte, and J. A. Jansen. 2006. Fabrication, characterization, and biological assessment of multilayered DNA-coatings for biomaterial purposes. *Biomaterials* 27:691-701.

9. McMichael, A. J. 1992. Antigens and MHC systems. In *Oxford textbook of pathology*. J. O. D. McGee, P. G. Isaacson, and N. A. Wright, eds. Oxford University Press, Oxford, UK.

10. Yamamoto, S., T. Yamamoto, S. Shimada, E. Kuramoto, O. Yano, T. Kataoka, and T. Tokunaga. 1992. DNA from bacteria, but not from vertebrates, induces interferons, activates natural killer cells and inhibits tumor growth. *Microbiol Immunol* 36:983-97.

11. Krieg, A. M. , A. K. Yi, S. Matson, T. J. Waldschmidt, G. A. Bishop, R. Teasdale, G. A. Koretzky, and D. M. Klinman. 1995. CpG motifs in bacterial DNA trigger direct B-cell activation. *Nature* 374:546-9.

12. Werner, M. H., A. M. Gronenborn, and G. M. Clore. 1996. Intercalation, DNA kinking, and the control of transcription. *Science* 271:778-84.

13. van den Beucken, J. J. J. P., X. F. Walboomers, M. R. J. Vos, N. A. J. M. Sommerdijk, R. J. M. Nolte, and J. A. Jansen. Biological responses to multilayered DNA-coatings. *J Biomed Mater Res B*.

14. van den Beucken, J. J., X. F. Walboomers, M. R. Vos, N. A. Sommerdijk, R. J. Nolte, and J. A. Jansen. 2006. Cyto- and histocompatibility of multilayered DNA-coatings on titanium. *J Biomed Mater Res A* 77A:202-211.

15. van den Beucken, J. J. J. P., X. F. Walboomers, M. R. J. Vos, N. J. A. M. Sommerdijk, R. J. M. Nolte, and J. A. Jansen. Macrophage behavior on multilayered DNA-coatings *in vitro*. *J Biomed Mater Res A*.

16. van den Beucken, J. J., X. F. Walboomers, O. C. Boerman, M. R. Vos, N. A. Sommerdijk, T. Hayakawa, T. Fukushima, Y. Okahata, R. J. Nolte, and J. A. Jansen. 2006. Functionalization of multilayered DNA-coatings with bone morphogenetic protein 2. *J Control Release* 113:63-72.

17. van den Beucken, J. J., M. R. Vos, P. C. Thune, T. Hayakawa, T. Fukushima, Y. Okahata, X. F. Walboomers, N. A. Sommerdijk, R. J. Nolte, and J. A. Jansen. 2006. Fabrication, characterization, and biological assessment of multilayered DNA-coatings for biomaterial purposes. *Biomaterials* 27:691-701.

18. Kokubo, T., H. Kushitani, S. Sakka, T. Kitsugi, and T. Yamamuro. 1990. Solutions able to reproduce in vivo surface-structure changes in bioactive glass-ceramic A-W. *J Biomed Mater Res* 24:721-34.

19. Kokubo, T., S. Ito, Z. T. Huang, T. Hayashi, S. Sakka, T. Kitsugi, and T. Yamamuro. 1990. Ca,P-rich layer formed on high-strength bioactive glass-ceramic A-W. *J Biomed Mater Res* 24:331-43.

20. van den Dolder, J., G. N. Bancroft, V. I. Sikavitsas, P. H. Spauwen, J. A. Jansen, and A. G. Mikos. 2003. Flow perfusion

culture of marrow stromal osteoblasts in titanium fiber mesh. *J Biomed Mater Res A* 64:235-41.

21. Maniatopoulos C. , Sodek J. , and Melcher A.H. Bone formation in vitro by stromal cells obtained from bone marrow of young adult rats. Cell Tissue Res 63, 171-176. 88.

22. de Ruijter, J. E., P. J. ter Brugge, S. C. Dieudonne, S. J. van Vliet, R. Torensma, and J. A. Jansen. 2001. Analysis of integrin expression in U2OS cells cultured on various calcium phosphate ceramic substrates. *Tissue Eng* 7:279-89.

23. Takeuchi, A., C. Ohtsuki, T. Miyazaki, H. Tanaka, M. Yamazaki, and M. Tanihara. 2003. Deposition of bone-like apatite on silk fiber in a solution that mimics extracellular fluid. *J Biomed Mater Res A* 65:283-9.

24. LeGeros, R. Z. *Calcium Phosphates in Oral Biology and Medicine*, Vol. S. Karger, Basel, Switzerland.

25. Leeuwenburgh, S., J. Wolke, J. Schoonman, and J. Jansen. 2003. Electrostatic spray deposition (ESD) of calcium phosphate coatings. *J Biomed Mater Res* 66A:330-4.

26. Van der Wal, E. *Bioactivity and Surface Reactivity of RF-sputtered Calcium Phosphate Thin Films*, Vol. PrintPartners Ipskamp, Enschede, the Netherlands.

27. Leitao, E., M. A. Barbosa, and K. de Groot. 1997. Influence of substrate material and surface finishing on the morphology of the calcium-phosphate coating. *J Biomed Mater Res* 36:85-90.

28. Barrere, F., M. M. Snel, C. A. van Blitterswijk, K. de Groot, and P. Layrolle. 2004. Nano-scale study of the nucleation and growth of calcium phosphate coating on titanium implants. *Biomaterials* 25:2901-10.

29. Stryer, L. *Biochemistry*..

30. Picart, C., J. Mutterer, L. Richert, Y. Luo, G. D. Prestwich, P. Schaaf, J. C. Voegel, and P. Lavalle. 2002. Molecular basis for the explanation of the exponential growth of polyelectrolyte multilayers. *Proc Natl Acad Sci U S A* 99:12531-5.

31. Van Den Dolder, J., P. H. Spauwen, and J. A. Jansen. 2003. Evaluation of various seeding techniques for culturing osteogenic cells on titanium fiber mesh. *Tissue Eng* 9:315-25.

32. van der Wal, E., A. M. Vredenberg, P. J. ter Brugg, J. G. C. Wolke, and J. A. Jansen. 2005. The in vitro behavior of as-prepared and pre-immersed RF-sputtered calcium phosphate thin films in a rat bone marrow cell model. *Biomaterials* 27:1333-1340.

33. Shu, R., R. McMullen, M. J. Baumann, and L. R. McCabe. 2003. Hydroxyapatite accelerates differentiation and suppresses growth of MC3T3-E1 osteoblasts. *J Biomed Mater Res A* 67:1196-204.

34. Siebers, M. C., X. F. Walboomers, S. C. Leeuwenburgh, J. G. Wolke, and J. A. Jansen. 2004. Electrostatic spray deposition (ESD) of calcium phosphate coatings, an in vitro study with osteoblast-like cells. *Biomaterials* 25:2019-27.

35. ter Brugge, P. J., J. G. Wolke, and J. A. Jansen. 2002. Effect of calcium phosphate coating crystallinity and implant surface roughness on differentiation of rat bone marrow cells. *J Biomed Mater Res* 60:70-8.

36. Wang, J., P. Layrolle, M. Stigter, and K. de Groot. 2004. Biomimetic and electrolytic calcium phosphate coatings on titanium alloy: physicochemical characteristics and cell attachment. *Biomaterials* 25:583-92.

6

FUNCTIONALIZATION OF MULTILAYERED DNA-COATINGS WITH BONE MORPHOGENETIC PROTEIN 2

JJJP van den Beucken, XF Walboomers, OC Boerman, MRJ Vos, NAJM Sommerdijk, T Hayakawa, T Fukushima, Y Okahata, RJM Nolte, JA Jansen

Journal of Controlled Release 113 (2006); 63-72

I INTRODUCTION

In the field of implantology, control over tissue responses after the insertion of a biomaterial remains a challenge. Several approaches to modulate tissue responses have been investigated in the past decades, including topographical and/or chemical modulations at the biomaterial surface. Additionally, biomaterials have been combined with biologically active factors to induce desired tissue responses in the direct vicinity of the implant.

In the early 90's, a versatile coating technique has been developed [1], known as layer by layer (LbL) assembly or electrostatic self-assembly (ESA). This technique is based on the sequential adsorption of oppositely-charged polyelectrolytes into multilayered structures (polyelectrolyte multilayers; PEMs) [2]. Due to the wide choice of polyelectrolytes, this technique allows the generation of coatings with numerous different properties.

Previously, the application of ESA to fabricate multilayered coatings consisting of DNA and a polycationic counterpart has been described [3-8]. In our previous work, we fabricated multilayered DNA-coatings onto glass and titanium substrates consisting of deoxyribonucleic acid (DNA) as the anionic polyelectrolyte and either poly-D-lysine (PDL) or poly(allylamine hydrochloride) (PAH) as its cationic counterpart [9]. In these studies, in particular DNA was chosen not for its genetic information, but for its beneficial biomaterial properties, which include non- or low-immunogenicity [10-12], capability to incorporate other compounds [13;14], and high phosphate content. In view of these properties, multilayered DNA-coatings are known to be cyto- and histocompatible [15], and proposed to be eligible for drug-delivery and favorable for the deposition of calciumphosphates in a bony environment. Additionally, the complexation of DNA with cationic polyelectrolytes has demonstrated to prevent DNA from nucleolytic degradation [16], which is indicative for the stability of multilayered DNA-coatings.

For drug-delivery purposes, the use of multilayered coatings can be based on functional components of the (biodegradable) multilayered structure itself [17-20]. On the other hand, functionalization of multilayered coatings can be based on the incorporation of biologically active factors within the basic multilayer structure. Several reports have already demonstrated this approach for the regulation of biological responses, using both *in vitro* [21-27] and *in vivo* [28] experiments. In these latter studies, a variety of biologically active factors were used, which were embedded through covalent bonding [21;25;27;28], adsorption [22], or complexation (with or without chaperone molecules) [23;24;26;29]. However, the focus of these studies was to evaluate the potential of functionalized multilayered coatings, in which the biologically active factor was incorporated at a single location in a multilayer architecture. On the contrary, the present study is aimed at the functionalization of multilayered DNA-coatings with the osteoinductive factor bone morphogenetic protein 2 (BMP-2) using different loading modalities. Clinically, BMP-2 could be used to accelerate the process of osseo-integration of orthopedic and dental implants. It is hypothesized that the location of the factor in a multilayered coating influences its release profile and affects the behavior of osteoblast-like cells in *in vitro* experiments.

The current study focused on three types of functionalization of multilayered DNA-coatings built up from either poly-D-lysine (PDL) or poly(allylamine hydrochloride) (PAH) as the cationic component and DNA as the anionic component. The amounts of BMP-2 loaded into the multilayered DNA-coatings and its subsequent release characteristics were determined using radiolabeled BMP-2. Subsequently, the effect of BMP-2 functionalized multilayered DNA-coatings on the *in vitro* behavior of bone marrow-derived osteoblast-like cells was evaluated in terms of proliferation, differentiation, mineralization, and cell morphology.

II MATERIALS & METHODS

Materials

Polyanionic DNA (300 bp/molecule; sodium salt) was kindly provided by the Central Research Laboratory of Nichiro Corporation (Kawasaki-shi, Kanagawa prefecture, Japan). Potential protein impurities in the DNA were checked using the BCA protein assay (Pierce, Rockford, IL, US) and measured to be below 0.20% w/w (data not shown). Polycationic polyelectrolytes poly(allylamine hydrochloride)

(PAH; MW ~70000) and poly-D-lysine (PDL; MW 30,000 – 70,000) were purchased from Sigma (Sigma-Aldrich Chemie B.V., Zwijndrecht, the Netherlands). Recombinant human bone morphogenetic protein 2 (rhBMP-2; MW 32,000; in MFR buffer [containing 0.5% sucrose, 2.5% glycine, 30 mM L-glutamic acid, 0.01% polysorbate 80, pH 4.5]) was generously supplied by Yamanouchi Europe B.V. (Leiderdorp, the Netherlands). All materials were used without further purification.

Substrate preparation and cleaning
Disc-shaped titanium substrates (diameter 12 mm; as machined) were used. Prior to the fabrication of multilayered DNA-coatings, substrates were cleaned ultrasonically in nitric acid (10% v/v), acetone, and isopropanol, respectively. Subsequently, the substrates were air-dried.

Generation of multilayered DNA-coatings
Multilayered DNA-coatings were generated using the ESA-technique, as described previously [9]. Briefly, the cleaned substrates were immersed in an aqueous solution of either PDL (0.1 mg/ml) or PAH (1 mg/ml) for 30 minutes, allowing sufficient time for the adsorption of the first cationic polyelectrolyte layer onto the substrates. Subsequently, the substrates were washed in ultra-pure water (5 minutes, continuous water flow) and dried using a pressurized air stream. Thereafter, the substrates were alternately immersed in an anionic aqueous DNA solution (1 mg/ml) and the respective cationic polyelectrolyte solution for 7 minutes each, with intermediate washing in ultra-pure water (5 minutes, continuous water flow) and drying using a pressurized air stream. The build-up of the multilayered DNA-coatings was continued until a total of 5 double-layers were reached. These coatings were designated either $[PDL/DNA]_5$ or $[PAH/DNA]_5$.

Functionalization of multilayered DNA-coatings
Multilayered DNA-coatings were functionalized with rhBMP-2 according to three different loading modalities (Figure 1). The loading modalities are designated superficial (s), deep (d), and double-layer (dl), depending on the location of the BMP-2. During the build-up of the multilayered DNA-coatings, rhBMP-2 was loaded at the appropriate location from a rhBMP-2 solution without precipitates (10 μl of a 10 μg/ml rhBMP-2 solution in 0.5% (w/v) BSA/PBS) and allowed to adsorb for 7 minutes. Unless the rhBMP-2 was applied on top of the multilayered DNA-coatings, substrates were washed in ultra-pure water, after which the build up of the coatings was continued as described above. rhBMP-2 applied on top of the coatings (in case of s-loading and the final loading step in dl-loading) was allowed to dry at room temperature.

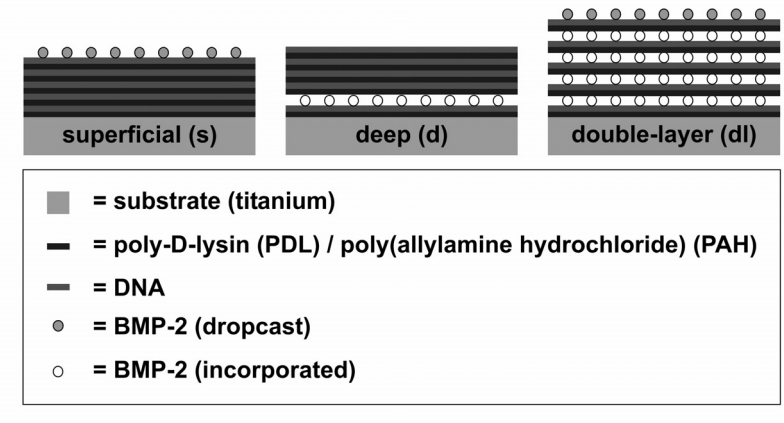

Figure 1: Schematic representation of the different loading modalities of multilayered DNA-coatings with BMP-2. Note the difference in BMP-2 (green spheres indicate dropcast BMP-2 without subsequent wash steps; white spheres indicate incorporated BMP-2 with subsequent wash steps during build-up of the coatings).

Radioiodination of rhBMP-2

rhBMP-2 was labeled with ^{125}I according to the iodogen method, as described previously [30]. Briefly, to a 500 μl eppendorf vial containing 100 μg iodogen, 10 μl 0.5 M phosphate buffer (pH 7.4), 80 μl 50 mM phosphate buffer (pH 7.4), 10 μg rhBMP-2 (in 2.6 μl PBS), and 3 μl ^{125}I (0.3 mCi) were added. The vial was incubated at room temperature for 10 minutes. Subsequently, the quench reaction was initiated by adding 100 μl of a saturated Tyrosine solution in PBS. Finally, the reaction mixture was eluted with 0.5% BSA/PBS on a pre-rinsed disposable Sephadex G25M column (PD-10; Pharmacia, Uppsala, Sweden) to separate labeled rhBMP-2 from free ^{125}I. To prevent sticking of the rhBMP-2, pipette tips and vials used during the radioiodination procedure were silanized with SigmaCoat® (Sigma).

The radiochemical purity of the ^{125}I-labeled rhBMP-2 was determined by instant thin-layer chromatography (ITLC) on Gelman ITLC-SG strips (Gelman Laboratories, Ann Arbor, MI, USA) with 0.1 M citrate, pH 5.0 as the mobile phase. The radiochemical purity of the ^{125}I-labeled rhBMP-2 preparation was 97.3%, which indicates that 97.3% of the ^{125}I-label was covalently linked to rhBMP-2. The specific activity of the labeled rhBMP-2 was 14.1 μCi/μg.

Determination of rhBMP-2-loading and in vitro rhBMP-2 release

The amount of rhBMP-2 loaded in the functionalized multilayered DNA-coatings was determined using radiolabeled rhBMP-2. Functionalization was performed as described in the section 'Functionalization of multilayered DNA-coatings', with the exception that radiolabeled rhBMP-2 was used. For each type of coating, three substrates (n=3) were coated with a functionalized multilayered DNA-coating.

The loaded amount of rhBMP-2 was determined by measuring activity of the experimental substrates in a shielded well-type gamma counter (Wizard, Pharmacia-LKB, Sweden). The amount of gamma radiation from the deep (d-functionalization) and double-layer (dl-functionalization) loaded multilayered DNA-coatings was calculated using that of superficially loaded (s-functionalization) multilayered DNA-coatings, which was artificially set at 100 ng.

To study the *in vitro* release characteristics of rhBMP-2, the substrates modified with a type of functionalized multilayered DNA-coating (n=3) were placed separately in 10 ml glass vials containing 4 ml PBS, and incubated statically at 37°C for up to 8 weeks. At selected time points (4 hours, 1, 7, 14, 22, 28, 42, and 56 days) the samples were carefully transferred into new vials containing fresh PBS. Subsequently, the activity on the substrates was measured in a gamma counter. Standards were counted simultaneously to correct for radioactive decay.

In vitro experiments

Experimental groups

For cell culture experiments, 7 experimental groups were used, based on coating composition and loading modality:

1. $[PDL/DNA]_5$-s (superficial)
2. $[PDL/DNA]_5$-d (deep)
3. $[PDL/DNA]_5$-dl (double-layer)
4. $[PAH/DNA]_5$-s (superficial)
5. $[PAH/DNA]_5$-d (deep)
6. $[PAH/DNA]_5$-dl (double-layer)
7. control (non-coated titanium)

The use of a control consisting of non-coated titanium is justified as previous *in vitro* experiments have demonstrated that osteoblast-like cells behave similar on non-coated titanium compared to both $[PDL/DNA]_5$ and $[PAH/DNA]_5$ multilayered coatings with respect to cell proliferation, differentiation, mineralization, and morphology (unpublished data).

All substrates, coated with either type of multilayered DNA-coating or non-coated

control substrates, were sterilized using a UV-irradiation treatment (254 nm; 4 hrs). The entire cell culture experiment was performed in two independent runs, using rat bone marrow cells from one rat per experimental run.

Isolation and pre-culture of rat bone marrow cells

Rat bone marrow (RBM) cells were isolated an cultured according to the method adapted from Maniatopoulos et al. [31]. Briefly, the femora of male Wistar WU rats were retrieved, cleaned, and epiphyses were cut off. The marrow was flushed out of the remaining diaphyses using cell culture medium (α-MEM (Gibco) supplemented with 10% fetal calf serum (FCS; Gibco), 50 µg/ml ascorbic acid (Sigma), 10 mM Na-β-glycerophosphate (Sigma), 10^{-8} M dexamethasone (Sigma), and 50 µg/ml gentamycin (Gibco)). RBM cells of two femora were cultured under static conditions in cell culture medium in three 75 cm^2 culture flasks (Greiner Bio-One) for one day, after which the medium was refreshed to remove non-adherent cells. Subsequently, the attached cells were pre-cultured for another 6 days. After the primary culture of 7 days to obtain osteoblast-like cells, cells were detached using trypsin/EDTA (0.25% (w/v) trypsin, 0.02% (w/v) EDTA) and the total cell number was determined using a Coulter® counter (Beckman Coulter Inc., Fullerton, CA, USA). Finally, cells were seeded at a density of 1 x 10^4 cells/cm^2 onto the experimental substrates, which were placed in a 24-wells plate (Greiner Bio-One). Cell culture medium was refreshed 1 day after cell seeding, and thereafter 3 times per week.

Cell proliferation

Cell proliferation curves were made based on a total cellular protein measurement. At 4, 8, 12, and 16 days post-seeding, the medium was removed and the cells were washed with PBS three times. Subsequently, the experimental substrates with attached cells were transferred into fresh 24-wells plates, and each experimental substrate was immersed in 1 ml ultra-pure water. These samples were frozen and thawed for 3 repetitive cycles, after which the cellular protein content in the aqueous samples was analyzed using a micro BCA protein assay (Pierce, Rockford, IL, USA) according to the instructions of the manufacturer. In each experimental run, three samples per time point for each experimental condition (n=3) were used to ensure reproducibility.

Alkaline phosphatase activity

The alkaline phosphatase (ALP) activity of the osteoblast-like cells was measured as a marker for early differentiation of osteoblast-like cells using the aqueous samples of the proliferation assay according to a previously described method [32]. A volume of 80 µl of sample or standard and 20 µl of buffer solution (5 mM $MgCl_2$, 0.5 M 2-amino-2-methyl-1-propanol) was pipetted into a 96-wells plate (Greiner Bio-One) in duplo, and 100 µl of substrate solution (5 mM p-nitro-phenyl-phosphate) was added per well. Subsequently, the plate was incubated for one hour at 37°C, after which the reaction was stopped by adding 100 µl 0.3 M NaOH. Serial dilution of 4-nitrophenol (final concentrations 0 – 25 nM) were used for the standard curve. The plate was read in an ELISA reader at 405 nm. In each experimental run, three samples per time point for each experimental condition (n=3) were used.

Calcium deposition

The deposition of calcium was used as a marker of late differentiation of osteoblast-like cells. The amount of calcium deposited after 4, 8, 12, 16, and 24 days of cell culture was measured by the orthocresolphtalein complexone (OCPC) method (Sigma), as described previously [33]. Briefly, the experimental substrates were washed twice using PBS, after which 1 ml 0.5 N acetic acid was added. After overnight incubation on a shaking apparatus, 300 µl working solution was added to 10 µl sample in a 96-wells plate (Greiner Bio-One). Working solution consisted of (a) OCPC solution (80 mg OCPC in 75 ml milliQ + 0.5 ml 1 M KOH + 0.5 ml 0.5 N acetic acid), (b) 14.8 M ethanolamine/boric acid buffer (pH=11), (c) 8-hydroxyquinoline (1 g in 20 ml 95% ethanol), and (d) milliQ, in a ratio of 5:5:2:88 (a:b:c:d). A standard curve was generated by preparing serial dilutions of $CaCl_2$ (0 – 100 µg/ml). For each

experimental run, the calcium assay was performed using 3 substrates per experimental condition at each time point (n=3).

Cell morphology

Scanning electron microscopy (SEM) was performed to evaluate the morphological appearance of the cells. At 4 and 16 days post-seeding, substrates with attached cells were washed twice with PBS and fixed using gluteraldehyde (4% in 0.1 M cacodylate buffer) for 20 minutes. Subsequently, the substrates were washed twice with 0.1 M cacodylate buffer and dehydrated in a graded series of ethanol. Finally, the substrates were dried with tetramethylsilane, sputter coated with gold and examined using a JEOL 6310 SEM at an acceleration voltage of 10 kV.

Statistical analysis

Measurements were statistically evaluated with Graphpad® Instat 3.05 software (GraphPad Software Inc., San Diego, CA, USA). Data of the *in vitro* release experiment and the cell culture experiments were analyzed using a one-way ANOVA, combined with a post-hoc Tukey-Kramer Multiple Comparisons test. The significance level was set at $p<0.05$.

III RESULTS

Loading of multilayered DNA-coatings with rhBMP-2

The amounts of rhBMP-2 loaded into the multilayered DNA-coatings are presented in Figure 2. The results demonstrate that the amount of rhBMP-2 incorporated into the differently-loaded multilayered DNA-coatings was highest with dl-loading (± 160 ng ≈ 140 ng/cm^2), intermediate with s-loading (100 ng ≈ 88 ng/cm^2), and lowest with d-loading (± 15 ng ≈ 13 ng/cm^2). No statistically significant differences were observed between [PDL/DNA]-based coatings and [PAH/DNA]-based coatings. The loading efficiency was 100% for s-loading, 15% for d-loading, and 32% for dl-loading.

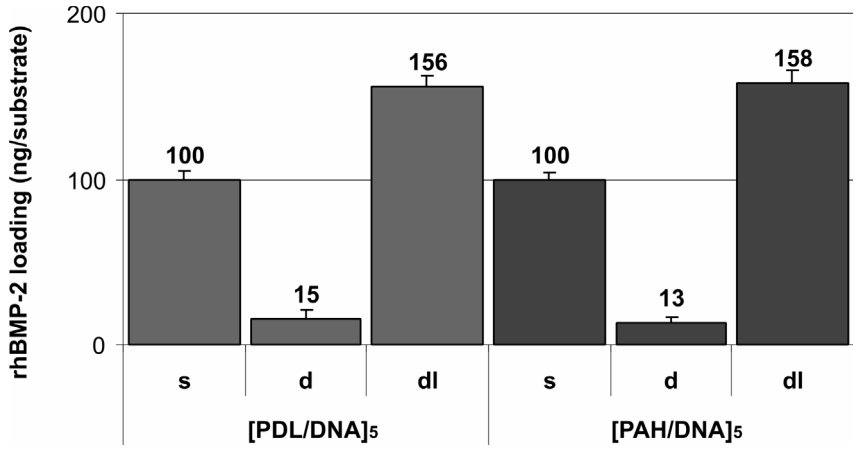

Figure 2: Incorporation of rhBMP-2 into multilayered DNA-coatings. The amount of gamma radiation of s-loaded coatings was artificially set at 100 ng, after which d- and dl-loading were calculated accordingly. Results are presented as mean + SD (n=3). (Loading efficiencies are 100, 15, and 32% for s-, d-, and dl-loading, respectively)

In vitro release of rhBMP-2 from multilayered DNA-coatings

The *in vitro* release characteristics of rhBMP-2 from multilayered DNA-coatings were determined using radiolabeled rhBMP-2. In Figures 3A and 3B, the cumulative release of rhBMP-2 out of the differently-loaded multilayered DNA-coatings is depicted. All differently-loaded multilayered DNA-coatings revealed an initial burst release within the first 24 hours of incubation in PBS, ranging from 35 to 75% of the initially loaded amount rhBMP-2. Proportionally, the burst release was low for d-loaded (47.6% for [PDL/DNA]-based and 34.8% for [PAH/DNA]-based multilayered DNA-coatings) and high for both s- and dl-loaded multilayered DNA-coatings (>60%). After the burst release, all differently-loaded multilayered DNA-coatings showed an incremental sustained release, in which a continuous fraction of approximately 6 - 8% of the remaining rhBMP-2 was released in each week (Table 1). After an incubation period of 8 weeks, the cumulative rhBMP-2 release of the d-loaded multilayered DNA-coatings approximated 70%, whereas both the s-loaded and the dl-loaded DNA-coatings released

approximately 85%, cumulatively. Statistical analysis revealed that actual cumulative amounts of released rhBMP-2 were highest for dl-loading, intermediate for s-loading, and lowest for d-loading. No statistically significant differences were observed between equivalently functionalized coatings based on either [PDL/DNA] or [PAH/DNA] regarding release characteristics in percentage terms ($p>0.05$).

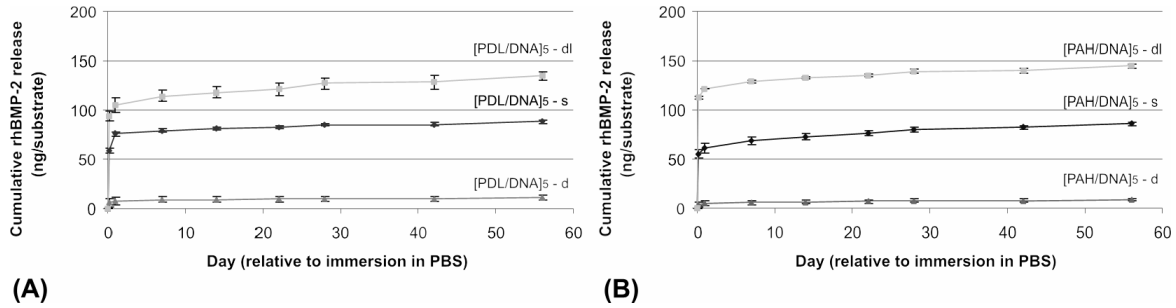

Figure 3: In vitro release of rhBMP-2 from differently-loaded multilayered DNA-coatings after immersion in PBS. (A) Release characteristics of [PDL/DNA]-based multilayered DNA-coatings; (B) Release characteristics of [PAH/DNA]-based multilayered DNA-coatings (s = superficial, d = deep, dl = double-layer). Results are presented as mean± SD (n=3).

Osteoblast-like cell behavior on rhBMP-2-loaded multilayered DNA-coatings

The behavior of osteoblast-like cells on the differently-loaded multilayered DNA-coatings was evaluated to detect biological activity of the incorporated rhBMP-2.

Cell proliferation

The proliferation of osteoblast-like cells, based on total cellular protein content measurements, is depicted in Figure 4. Osteoblast-like cells showed a similar proliferation pattern on all types of differently-loaded multilayered DNA-coatings and non-coated control substrates. After cell seeding, osteoblast-like cells started proliferating, reaching a maximum around day 12, after which a decrease was observed. Somewhat lower, but significantly different levels of cellular protein content were observed in both types of d-loaded multilayered DNA-coatings on day 12 ($[PDL/DNA]_5$-d vs. control, $p<0.01$; $[PAH/DNA]_5$-d vs. control, $p<0.05$). After 16 days of osteoblast-like cell culture, no significant different levels were observed between both types of d-loaded multilayered DNA-coatings and controls ($p>0.05$).

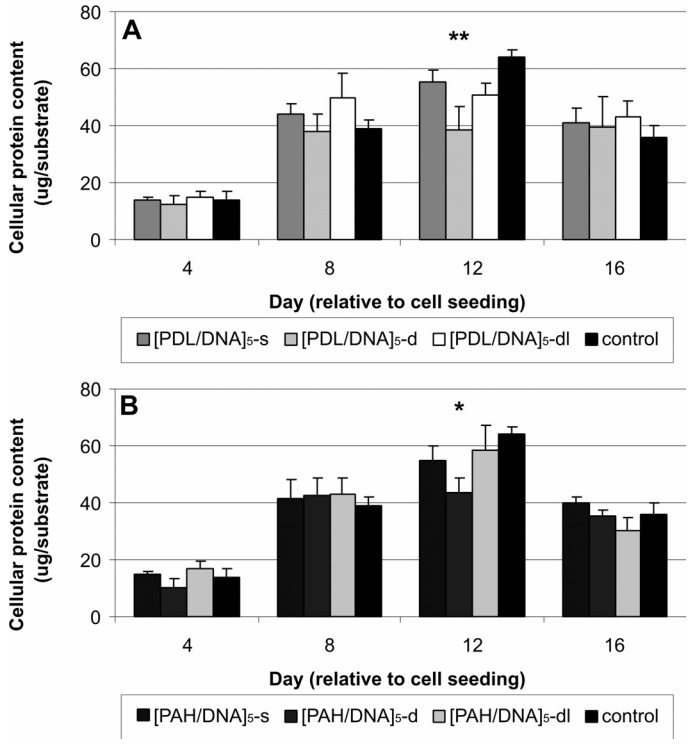

Figure 4:Proliferation of bone marrow-derived osteoblast-like cells on differently-loaded multilayered (A) [PDL/DNA]- and (B) [PAH/DNA]-coatings. (p<0.05; ** p<0.01 compared to controls)*

Alkaline phosphatase activity

Osteoblast-like cells showed a normal ALP-activity expression on all experimental substrates. The ALP-activity increased on all experimental substrates during the first 12 days of culture, after which a rapid decrease in ALP-activity was observed (Figure 5). Significant differences compared to controls ($p<0.05$) were observed on day 12 for both types of d-loaded multilayered DNA-coatings.

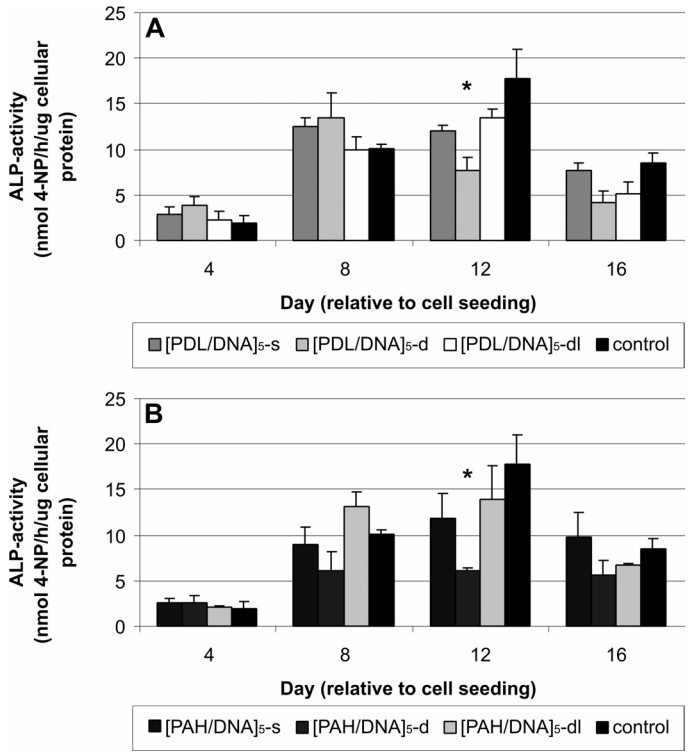

*Figure 5: Alkaline phosphatase (ALP) activity of bone marrow-derived osteoblast-like cells on differently-loaded multilayered (A) [PDL/DNA]- and (B) [PAH/DNA]-coatings. (*p<0.05 compared to controls)*

Calcium deposition

The deposition of a mineralized extracellular matrix by osteoblast-like cells was determined by measuring the amounts of calcium deposited on the experimental substrates during cell culture (Figure

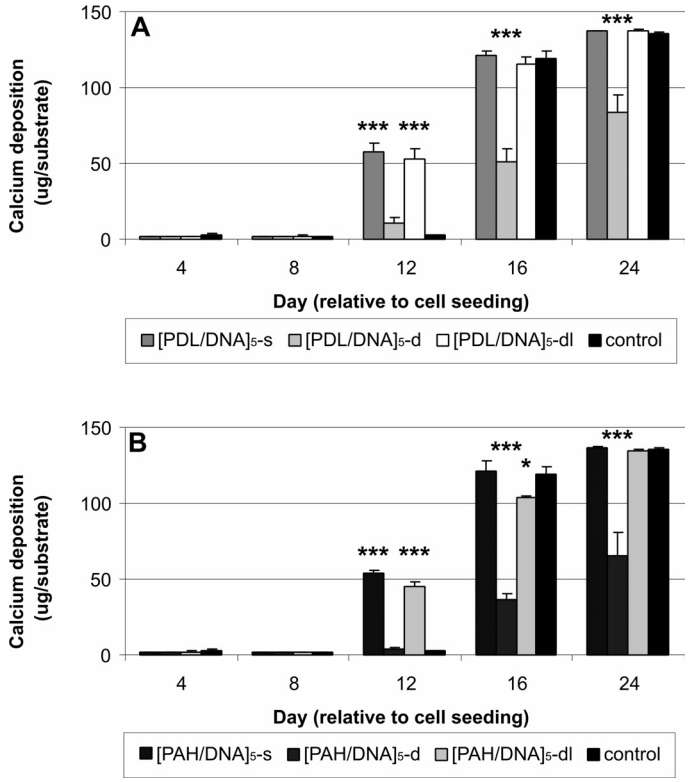

Figure 6: Mineralization (calcium deposition) by bone marrow-derived osteoblast-like cells on differently-loaded multilayered (A) [PDL/DNA]- and (B) [PAH/DNA]-coatings. (p<0.05; *** p<0.001 compared to controls)*

6). An accelerated calcium deposition by osteoblast-like was observed on s- and dl-loaded multilayered DNA-coatings compared to non-coated controls. On day 12, osteoblast-like cells on s- and dl-loaded multilayered DNA-coatings had deposited significantly increased amounts of calcium compared to non-coated controls ($p<0.001$). On the other hand, d-loaded multilayered DNA-coatings demonstrated to decrease calcium deposition by osteoblast-like cells. Significantly decreased amounts of deposited calcium were observed on these types of functionalized multilayered DNA-coatings on days 16 and 24 ($p<0.001$).

Cell morphology

The morphological appearance of the osteoblast-like cells cultured on the differently-loaded multilayered DNA-coatings was evaluated using scanning electron microscopy. At day 4, all differently-loaded multilayered DNA-coatings and non-coated controls were covered with a layer of osteoblast-like cells. No apparent differences in cell morphology were observed. In contrast, at day 16 d-loaded multilayered DNA-coatings showed an aberrant morphological appearance of osteoblast-like cells compared to all other experimental groups (Figure 7). Many calcified globular accretions associated with collagen bundles were present on s-, and dl-loaded multilayered DNA-coatings, and non-coated controls. Less characteristics of mineralization were observed on d-loaded multilayered DNA-coatings.

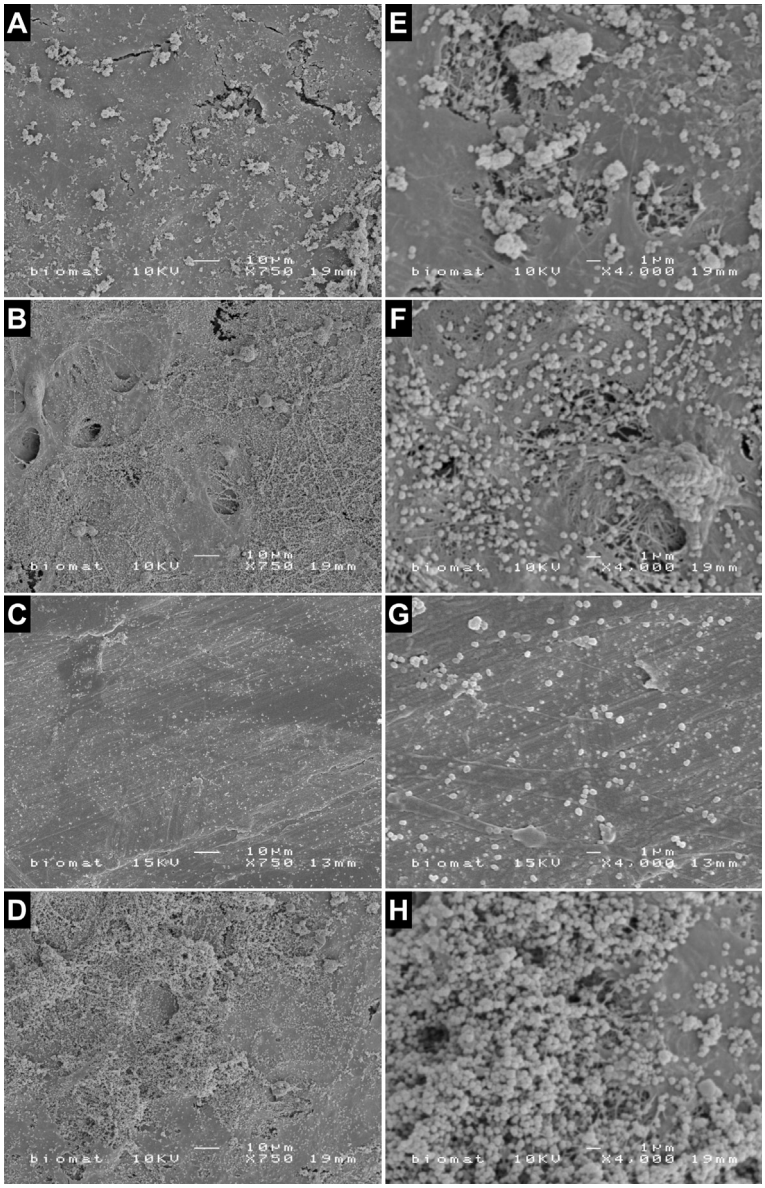

Figure 7: Scanning electron microscopy images of bone marrow-derived osteoblast-like cells after 16 days of culture on differently-loaded multilayered DNA-coatings. (A) non-coated control, (B) $[PAH/DNA]_5$-s, (C) $[PAH/DNA]_5$-d, and (D) $[PAH/DNA]_5$-dl. Note the difference in globular accretions at the high magnification images (E-H).

IV DISCUSSION

The functionalization of biomaterial coatings with biologically-active factors is of interest, as localized drug delivery reduces systemic side effects and increases drug efficiency. In view of this, the functionalization of polyelectrolyte multilayers offers increased application due to the possibility of generating ESA-based coatings onto many different materials used for both soft and hard tissue implants without restrictions regarding geometry. The aim of the current study was to explore the potential of multilayered DNA-coatings, based on [PDL/DNA] and [PAH/DNA] double-layers, for functionalization with the osteoinductive factor BMP-2. To that end, three different modalities of BMP-loading were chosen, based on the location of BMP-2 in the multilayered DNA-coating (i.e. superficial, deep, and double-layer). The incorporation and release of BMP-2 were quantitatively assessed using radiolabeled BMP-2. Additionally, functionalized multilayered DNA-coatings were used in cell culture experiments to assess their biological effects on rat bone marrow-derived osteoblast-like cells. The results demonstrated the feasibility of multilayered DNA-coatings to be functionalized with BMP-2 according to all three loading modalities, and that the loading and release characteristics are independent of the cationic counterpart of DNA in the multilayered coating (i.e. PDL or PAH). All types of functionalized multilayered DNA-coatings showed an initial bulk release within 24 hours followed by an incremental sustained release. The *in vitro* experiments with osteoblast-like cells revealed that the loaded BMP-2 remained biologically active. Superficial and double-layer loading resulted in accelerated calcium deposition, whereas deep loading decreased the deposition of calcium by osteoblast-like cells.

The use of multilayered coatings to modulate cell/tissue responses has been described previously and was based on the functionality of basic multilayered structure components (i.e. polyelectrolytes) [17-20] or additional biologically-active components [21-26;28]. In the present study, BMP-2 was incorporated as an additional component in multilayered coatings, which consisted of either PDL or PAH as the cationic counterpart of anionic DNA. These coatings demonstrated to contain approximately 3 μg DNA per double-layer per square centimeter, irrespective of the cationic polyelectrolyte used [9]. Recombinant human BMP-2 was incorporated after the adsorption of a negatively-charged DNA-layer, as the iso-electric point of BMP-2 is 8.5, which indicates a positive charge of BMP-2 under physiological conditions [34]. However, due to the presence of (negatively-charged) BSA in the BMP-2 solution, interference of electrostatic interactions between the BMP-2 and DNA is likely. Additionally, the interaction of BSA with BMP-2 potentially results in the incorporation of BSA-BMP-2 complexes rather than pure BMP-2, which could also affect its release.

Functionalization of multilayered DNA-coatings according to the chosen loading modalities (Figure 1) demonstrated that the differently-loaded multilayered DNA-coatings bear the following proportion to one another: $s + (4 * d) = dl$. From this proportion it becomes evident that constant amounts of BMP-2 of approximately 15 ng can be incorporated into the coatings after a DNA-layer in case of subsequent wash steps. Additionally, this proportion indicates that the build-up of the multilayered DNA-coatings is not affected by the incorporation of factor. In view of this, the continuous build-up of multilayered coatings with adsorbed factors has already been demonstrated previously using Optical Waveguide Lightmode Spectrometry [22]. Calculations on the loading of multilayered DNA-coatings correspond to a BMP-2 incorporation of ~13 ng/cm^2 (1 μg DNA immobilizes ~4.5 ng BMP-2), which are well in line with incorporation efficiencies of other factors into other types of multilayers. For instance, brain-derived neurotrophic factor (BDNF) could be incorporated through adsorption to an amount of 96.4 ng/cm^2 into [PSS/PAH]-based multilayers [22]. Similarly, the chemorepulsive protein Semaphorin 3A could be incorporated to an amount of 25.4 ng/cm^2 into identical multilayer structures [22]. Both BDNF and Semophorin 3A were adsorbed after polystyrene sulphonate in [PSS/PAH]-based multilayers. Although these studies as well as the present study show loading efficiencies of tens of nanograms per square centimeter, it has to be emphasized that due to differences in properties of the multilayer components, the factors used for functionalization, and the conditions during multilayer build-up (e.g. salt concentration, pH, etc.), the actual loading efficiency through adsorption is likely to be influenced. Additionally, an increase in the amount of functionalization factor can be achieved using several

approaches. The most feasible one is to increase the number of double-layers in a multilayer structure, which will increase the total amount of biologically-active factor and has been demonstrated to be effective [35]. Another approach is the complexation of the biologically-active factor with chaperone molecules. This method has demonstrated to be applicable for anti-inflammatory agents, including piroxicam [23] and a lipid A-antagonist [24], and increases the loading efficiency without affecting the biological activity of the factor. Other approaches include covalent bonding of factors to polyelectrolytes [21;25;28] prior to the generation of multilayered structures. Although this last method seems preferable in terms of controlling the loaded amount of factor, the biological activity of the factor might be affected by covalent bonding. For instance, covalent bonding might change the native structure of the factor, which impairs the availability of functional epitopes for cell surface receptors. Additionally, covalent bonding only allows release of the factor in case of degradation of the multilayered coating, which might limit its availability in the peri-implant surroundings. This has been demonstrated previously by Jessel et al. [21], who showed a reduced biological activity of a covalently-bound factor underneath poly-D-lysine-containing compared to biodegradable poly-L-lysine-containing double-layers. Consequently, covalent bonding of factors in an effort to introduce biological activity into multilayered coatings is only functional if (i) the polyelectrolytes are biodegradable, (ii) the factor is located such, that it is available for cells via cellular membrane extension, or (iii) a combination of both.

For bone tissue engineering approaches, in which BMP-2 is the most powerful osteoinductive factor to be used [36], it is important to tailor the availability of the osteoinductive factor in such a way that the behavior of mesenchymal stem cells is controlled in terms of migration, differentiation, and secretion of extracellular matrix. The current study showed that the BMP-2 release pattern of the differently-loaded multilayered DNA-coatings consisted of two phases: (i) a bulk release of 35 – 75% within 24 hours, and (ii) an incremental sustained release of approximately 6 – 8% of the remaining BMP-2 weekly for (at least) 8 weeks. The bulk release might be due to differences in the composition of the solutions used during multilayer build-up and the release medium, which contained ionic species that are likely to affect electrostatic interactions. Bulk release was lowest for both types of d-loaded multilayered DNA-coatings. This is most likely due to the absence of dropcast BMP-2 on top of these multilayered DNA-coatings and increased interactions of BMP-2 with the polyelectrolytes in the coating. Different BMP-2 release profiles have been reported by others using different carriers. For instance, ceramics have demonstrated to bind BMP-2 with high affinity, resulting in a limited release [37;38]. On the other hand, biodegradable scaffolds consisting of either polycaprolactone (PCL) or a composite of PCL with calcium phosphate showed BMP-2 release profiles in which 100% release was established within 3 weeks [39]. The specific requirements for BMP-2 to be effective *in vivo*, however, remain unclear, since both release profiles induced osteogenic differentiation *in vivo* and *in vitro*, respectively.

The bioactivity of the BMP-2 loaded into the multilayered DNA-coatings was assessed using an *in vitro* cell culture model with rat bone marrow-derived osteoblasts. The results indicate the presence of a threshold for the osteoinductive capacity of BMP-2, as only functionalized multilayered DNA-coatings containing relatively high amounts of BMP-2 (s- and dl-loaded coatings) accelerated the deposition of calcium by osteoblast-like cells. Although the actual comparative fraction of biologically-active BMP-2 under the different loading modalities is unknown, these results corroborate those obtained by Van den Dolder et al. [40] and Vehof et al. [41]. In their studies, in which rat bone marrow-derived osteoblast-like cells were cultured in medium to which 0, 10, 100, or 1000 ng/ml BMP-2 was supplemented, effects of the supplemented BMP-2 became apparent from 100 ng/ml. A remarkable difference, however, is the altered behavior of osteoblast-like cells at low BMP-2 concentrations. Whereas the supplementation of 10 ng/ml BMP-2 to the culture medium did not affect osteoblast-like cell behavior in terms of proliferation and ALP expression [40;41], in our study osteoblast-like cells on d-loaded multilayered DNA-coatings proliferated and differentiated to a lesser extent compared to the control substrates. Additionally, the deposition of calcium was significantly decreased compared to controls. Although no elusive explanation is available currently for this observation in osteoblast-like cell cultures with sub-

treshold BMP-2 concentrations, it can be speculated that the amount and the temporal and spatial availability of factor are causal issues in the ultimate effect of factors.

CONCLUSION

This study demonstrates the feasibility of multilayered DNA-coatings to be functionalized by embedding BMP-2 according to three different loading modalities: superficial (s), deep (d), and double-layer (dl). BMP-2 was incorporated proportionally into the multilayered DNA-coatings as: $s + (4 * d) = dl$. The release profiles of all differently-loaded multilayered DNA-coatings showed an initial burst release, followed by a sustained release of the remaining BMP-2 for (at least) 8 weeks. *In vitro* culture experiments with rat bone marrow-derived osteoblast-like cells demonstrated that the loaded factor remained biologically active, as an accelerated calcium deposition was observed on s- and dl-loaded multilayered DNA-coatings, without affecting cell proliferation. In contrast, d-loaded multilayered DNA-coatings influenced the behavior of osteoblast-like cells by decreasing the deposition of calcium.

V ACKNOWLEDGEMENTS

The authors would like to thank dr. Haruchika Sekido (Nichoro Corporation, Japan) for providing DNA. Scanning electron microscopy was performed in collaboration with the Microscopical Imaging Center of the Nijmegen Center for Molecular Life Sciences (NCMLS). This research was supported by the Technology Foundation STW, applied science division of NWO and the technology programme of the Ministry of Economic Affairs, grant # NKG.5758.

VI REFERENCES

1. Decher, G., Hong, J. D., and Schmitt, J. Buildup of ultrathin multilayer films by a self-assembly process: III. Consecutively alternating adsorption of anionic an cationic polyelectrolytes on charged surfaces. Thin Solid Films 210-211, 831-835. 92.

2. Decher G. Fuzzy Nanoassemblies: Toward Layered Polymeric Multicomposites. Science 277, 1232-1237. 97.

3. Gong, H., J. Garcia-Turiel, K. Vasilev, and O. I. Vinogradova. 2005. Interaction and adhesion properties of polyelectrolyte multilayers. *Langmuir* 21:7545-50.

4. Chen, X., J. Lang, and M. Liu. 2002. Layer-by-layer assembly of DNA-dye complex films. *Thin Solid Films* 409:227-232.

5. Luo, L., J. Liu, Z. Wang, X. Yang, S. Dong, and E. Wang. 2001. Fabrication of layer-by-layer deposited multilayer films containing DNA and its interaction with methyl green. *Biophys Chem* 94:11-22.

6. Sukhorukov G.B. , Mohwald H. , Decher G. , and Lvov Y.M. Assembly of polyelectrolyte multilayer films by consecutively alternating adsorption of polynucleotides and polycations. Thin Solid Films 284-285, 220-223. 96.

7. Lvov Y. , Decher G. , and Sukhorukov G. Assembly of thin films by means of successive deposition of alternate layers of DNA and Poly(allylamine). Macromolecules 26, 5396-5399. 93.

8. Shi, X., Sanedrin, R. J., and Zhou, F. Structural characterization of multilayered DNA and polylysine composite films: influence of ionic strength of DNA solutions on the extent of DNA incorporation. J Phys Chem B 106, 1173-1180. 2002.

9. van den Beucken, J. J., M. R. Vos, P. C. Thune, T. Hayakawa, T. Fukushima, Y. Okahata, X. F. Walboomers, N. A. Sommerdijk, R. J. Nolte, and J. A. Jansen. 2006. Fabrication, characterization, and biological assessment of multilayered DNA-coatings for biomaterial purposes. *Biomaterials* 27:691-701.

10. Yamamoto, S., T. Yamamoto, S. Shimada, E. Kuramoto, O. Yano, T. Kataoka, and T. Tokunaga. 1992. DNA from bacteria, but not from vertebrates, induces interferons, activates natural killer cells and inhibits tumor growth. *Microbiol Immunol* 36:983-97.

11. Krieg, A. M. , A. K. Yi, S. Matson, T. J. Waldschmidt, G. A. Bishop, R. Teasdale, G. A. Koretzky, and D. M. Klinman. 1995. CpG motifs in bacterial DNA trigger direct B-cell activation. *Nature* 374:546-9.

12. McMichael, A. J. 1992. Antigens and MHC systems. In *Oxford textbook of pathology*. J. O. D. McGee, P. G. Isaacson, and N. A. Wright, eds. Oxford University Press, Oxford, UK.

13. Wilson, W. D. 1996. Reversible interactions of nucleic acids with small molecules. In *Nucleic acids in chemistry and biology*. G. M. Blackburn and M. J. Gait, eds. Oxford University Press, Oxford, UK.

14. Werner, S. and R. Grose. 2003. Regulation of wound healing by growth factors and cytokines. *Physiol Rev* 83:835-70.

15. Hsieh, C. Y., S. P. Tsai, D. M. Wang, Y. N. Chang, and H. J. Hsieh. 2005. Preparation of gamma-PGA/chitosan composite tissue engineering matrices. *Biomaterials* 26:5617-23.

16. Hill, I. R., M. C. Garnett, F. Bignotti, and S. S. Davis. 2001. Determination of protection from serum nuclease activity by DNA-polyelectrolyte complexes using an electrophoretic method. *Anal Biochem* 291:62-8.

17. Jewell, C. M., J. Zhang, N. J. Fredin, and D. M. Lynn. 2005. Multilayered polyelectrolyte films promote the direct and localized delivery of DNA to cells. *J Control Release* 106:214-23.

18. Wood, K. C., J. Q. Boedicker, D. M. Lynn, and P. T. Hammond. 2005. Tunable drug release from hydrolytically degradable layer-by-layer thin films. *Langmuir* 21:1603-9.

19. Zhang, J., L. S. Chua, and D. M. Lynn. 2004. Multilayered thin films that sustain the release of functional DNA under physiological conditions. *Langmuir* 20:8015-21.

20. Vazquez, E., D. M. Dewitt, P. T. Hammond, and D. M. Lynn. 2002. Construction of hydrolytically-degradable thin films via layer-by-layer deposition of degradable polyelectrolytes. *J Am Chem Soc* 124:13992-3.

21. Jessel, N., Atalar, F., Lavalle, P., Mutterer, J., Decher, G., Schaaf, P., Voegel, J-C., and Ogier, J. Bioactive coatings based on a polyelectrolyte multilayer architecture functionalized by embedded proteins. Adv Mater 15(9), 692-695. 2003.

22. Vodouhe, C., M. Schmittbuhl, F. Boulmedais, D. Bagnard, D. Vautier, P. Schaaf, C. Egles, J. C. Voegel, and J. Ogier. 2005. Effect of functionalization of multilayered polyelectrolyte films on motoneuron growth. *Biomaterials* 26:545-54.

23. Benkirane-Jessel, N., P. Schwinte, P. Falvey, R. Darcy , Y. Haikel, P. Schaaf, J.-C. Voegel, and J. Ogier. 2004. Build-up of Polypeptide Multilayer Coatings with Anti-Inflammatory Properties Based on the Embedding of Piroxicam-Cyclodextrin Complexes. *Adv Funct Mater* 14:174-182.

24. Gangloff, S. C., G. Ladam, V. Dupray, K. Fukase, K. Brandenburg, M. Guenounou, P. Schaaf, J. C. Voegel, and N. Jessel. 2005. Biologically active lipid A antagonist embedded in a multilayered polyelectrolyte architecture. *Biomaterials*.

25. Chluba, J., J. C. Voegel, G. Decher, P. Erbacher, P. Schaaf, and J. Ogier. 2001. Peptide hormone covalently bound to polyelectrolytes and embedded into multilayer architectures conserving full biological activity. *Biomacromolecules* 2:800-5.

26. Benkirane-Jessel, N., P. Schwinte, R. Donohue, P. Lavalle, F. Boulmedais, R. Darcy, B. Szalontai, J.-C. Voegel, and J. Ogier. 2004. Pyridylamino-β-cyclodextrin as a molecular chaperone for lipololysaccharide embedded in a multilayered polyelectrolyte architecture. *Adv Funct Mater* 14:963-969.

27. Picart, C., R. Elkaim, L. Richert, F. Audoin, Y. Arntz, M. Da Silva Cardoso, P. Schaaf, J.-C. Voegel, and B. Frisch. 2005. Primary cell adhesion on RGD-functionalized and covalently crosslinked thin polyelectrolyte multilayer films. *Adv. Funct. Mater.* 15:83-94.

28. Schultz, P., D. Vautier, L. Richert, N. Jessel, Y. Haikel, P. Schaaf, J. C. Voegel, J. Ogier, and C. Debry. 2005. Polyelectrolyte multilayers functionalized by a synthetic analogue of an anti-inflammatory peptide, alpha-MSH, for coating a tracheal prosthesis. *Biomaterials* 26:2621-30.

29. Thierry, B., F. M. Winnik, Y. Merhi, J. Silver, and M. Tabrizian. 2003. Bioactive coatings of endovascular stents based on polyelectrolyte multilayers. *Biomacromolecules* 4:1564-71.

30. Fraker, P. J. and J. C. Speck Jr. 1978. Protein and cell membrane iodinations with a sparingly soluble chloroamide, 1,3,4,6-tetrachloro-3a,6a-diphrenylglycoluril. *Biochem Biophys Res Commun* 80:849-57.

31. Maniatopoulos C. , Sodek J. , and Melcher A.H. Bone formation in vitro by stromal cells obtained from bone marrow of young adult rats. Cell Tissue Res 63, 171-176. 88.

32. de Ruijter, J. E., P. J. ter Brugge, S. C. Dieudonne, S. J. van Vliet, R. Torensma, and J. A. Jansen. 2001. Analysis of integrin expression in U2OS cells cultured on various calcium phosphate ceramic substrates. *Tissue Eng* 7:279-89.

33. van den Dolder, J., G. N. Bancroft, V. I. Sikavitsas, P. H. Spauwen, J. A. Jansen, and A. G. Mikos. 2003. Flow perfusion culture of marrow stromal osteoblasts in titanium fiber mesh. *J Biomed Mater Res A* 64:235-41.

34. Yamamoto, M., Y. Ikada, and Y. Tabata. 2001. Controlled release of growth factors based on biodegradation of gelatin hydrogel. *J Biomater Sci Polym Ed* 12:77-88.

35. Etienne, O., C. Picart, C. Taddei, Y. Haikel, J. L. Dimarcq, P. Schaaf, J. C. Voegel, J. A. Ogier, and C. Egles. 2004. Multilayer polyelectrolyte films functionalized by insertion of defensin: a new approach to protection of implants from bacterial colonization. *Antimicrob Agents Chemother* 48:3662-9.

36. Kofron, M. D., X. Li, and C. T. Laurencin. 2004. Protein- and gene-based tissue engineering in bone repair. *Curr Opin Biotechnol* 15:399-405.

37. Ruhe, P. Q., H. C. Kroese-Deutman, J. G. Wolke, P. H. Spauwen, and J. A. Jansen. 2004. Bone inductive properties of rhBMP-2 loaded porous calcium phosphate cement implants in cranial defects in rabbits. *Biomaterials* 25:2123-32.

38. Jansen, J. A., J. W. Vehof, P. Q. Ruhe, H. Kroeze-Deutman, Y. Kuboki, H. Takita, E. L. Hedberg, and A. G. Mikos. 2005. Growth factor-loaded scaffolds for bone engineering. *J Control Release* 101:127-36.

39. Rai, B., S. H. Teoh, D. W. Hutmacher, T. Cao, and K. H. Ho. 2005. Novel PCL-based honeycomb scaffolds as drug delivery systems for rhBMP-2. *Biomaterials* 26:3739-48.

40. van den Dolder, J., A. J. de Ruijter, P. H. Spauwen, and J. A. Jansen. 2003. Observations on the effect of BMP-2 on rat bone marrow cells cultured on titanium substrates of different roughness. *Biomaterials* 24:1853-60.

41. Vehof, J. W., A. E. de Ruijter, P. H. Spauwen, and J. A. Jansen. 2001. Influence of rhBMP-2 on rat bone marrow stromal cells cultured on titanium fiber mesh. *Tissue Eng* 7:373-83.

7

IN VITRO AND *IN VIVO* EFFECTS OF DNA-BASED COATINGS FUNCTIONALIZED WITH VASCULAR ENDOTHELIAL GROWTH FACTOR

JJJP van den Beucken, XF Walboomers, STM Nillesen, MRJ Vos, NAJM Sommerdijk, TH van Kuppevelt RJM Nolte, JA Jansen

Tissue Eng (2006); in press

I INTRODUCTION

An important physiological aspect in the healing around biomaterials is vascular development. For tissue engineering matrices, particularly those that are pre-seeded with cells, fast development of a vascular network is required for tissue ingrowth and cell survival, respectively. Also for solid devices, such as subcutaneously implantable biosensors, the development of a contiguous vascular network is important for their functionality [1;2]. For instance, previous studies have demonstrated that the responsiveness of implanted biosensors to fluctuations of analytes in the interstitial fluid is diminished by the formation of a largely avascular fibrous tissue capsule and the resulting increased diffusion distance between sensor and blood supply to the sensor surrounding tissue [1;2]. Furthermore, Gerritsen et al. showed that inflammatory cells as well as low molecular weight serum components influence the performance of amperometric glucose sensors [3]. The basis for these findings was the secretion of enzymes by stimulated granulocytes, which consumed the hydrogen peroxide formed by the oxidation of glucose, and both the formation of a diffusional barrier for glucose and the inhibition of glucose oxidase activity by serum components. Consequently, the authors of these publications suggested that biosensor functionality is likely to improve if (i) the vascularity in the direct vicinity of the device is increased, and (ii) inflammatory responses to the device are minimal.

The development of the vasculature depends on two processes, e.g. vasculogenesis and angiogenesis, which are responsible for de novo vessel formation and sprouting from already existing vessels, respectively [4]. Therapeutical modulation of vascular supply, however, is limited to angiogenesis, since vasculogenesis is believed to occur only during early embryogenesis. Angiogenesis is a complex process, which involves subtle interactions of cells, extracellular matrix components, and regulatory molecules. Decisive steps in this process are the localized proteolytic degradation of the subendothelial basement membrane, migration of endothelial cells, the formation of sprouts, extracellular matrix remodeling, and the formation of anastomoses, which all together precede the establishment of blood flow [5]. Potentially, the delivery of growth factors with pro-angiogenic action is a powerful tool in the control over vascular development. A widely used pro-angiogenic growth factor in tissue engineering is vascular endothelial growth factor (VEGF) [6]. VEGF affects endothelial cells through positive effects on proliferation, migration, tubule formation, survival, and integrin expression [7].

In order to increase vascularity around subcutaneously implanted biosensors, we hypothesized that VEGF-functionalization of DNA-based coatings could be beneficial. These coatings, whose generation is based on the layer-by-layer (LbL) deposition of either cationic poly-D-lysine (PDL) or poly(allylamine hydrochloride) (PAH) with anionic DNA [8], were demonstrated to be fully histocompatible upon subcutaneous implantation showing no adverse reactions in terms of inflammation and wound healing [9;10]. Furthermore, it was shown that these DNA-based are eligible for functionalization with the osteo-inductive factor bone morphogenetic protein 2 (BMP-2) using different loading modalities, and that this factor retained its biological activity [11]. Another important feature of the fabrication method of these DNA-based coatings is its simplicity, which allows a wide variability of substrate materials (e.g. ceramics, metals, and polymers) with almost unrestricted substrate geometry [12].

In view of the described disadvantageous effects of lack of vascularity on biosensor functionality, we hypothesized that VEGF-functionalization of DNA-based coatings would be beneficial for the vascularization of the peri-implant tissue. Consequently, the aim of this study was to evaluate the effect of VEGF-functionalized DNA-based coatings on (i) endothelial cell behavior *in vitro,* and (ii) vascular development *in vivo*. Therefore, $[PDL/DNA]_5$-coatings on glass substrates were functionalized with a low (25 ng) or a high (250 ng) amount of VEGF to study dosage-dependent effects. These VEGF-functionalized DNA-based coatings, as well as non-functionalized coatings and non-coated controls, were enrolled in an *in vitro* experiment to study the proliferation, migration, and morphology of endothelial cells. Additionally, these four types of substrates were implanted in the backs of rats in an *in vivo* animal model to study vascular development in the direct vicinity of the implants.

II MATERIALS & METHODS

Materials

Polyanionic salmon DNA (± 300 bp/molecules; sodium salt) was kindly provided by Nichiro Corporation (Kawasaki-city, Kanagawa prefecture, Japan). Potential protein impurities in the DNA were checked using the bicinchoninic acid (BCA) protein assay (Pierce, Rockford, IL, USA), and were measured to be below 0.20 % w/w (data not shown). Polycationic polyelectrolyte poly-D-lysine (PDL; MW 30000 – 70000) was purchased from Sigma (Sigma-Aldrich Chemie B.V., Zwijndrecht, the Netherlands). All materials were used without further purification.

Substrate preparation and cleaning

Disc-shaped glass substrates (12 mm diameter; 1.5 mm thickness; Waldemar-Knittel Glasbearbeitung GmbH, Braunschweig, Germany) were cleaned in Piranha solution (H_2O_2 (30% aqueous solution) / H_2SO_4 – 3:7 v/v) to completely remove all traces of organic materials at the surface, and to increase the wettability of the surface. Subsequently, the substrates were thoroughly rinsed with ultra-pure water from a Millipore system (resistivity ≥ 18.2 MW×cm; Millipore B.V., Amsterdam, the Netherlands) and dried using a pressurized air stream.

Generation of multilayered DNA-coatings

DNA-coatings were generated using the layer-by-layer (LbL) deposition, as described previously [8]. Briefly, the substrates were immersed in an aqueous solution of PDL (0.1 mg/ml) for 30 minutes, allowing sufficient time for the adsorption of the first cationic polyelectrolyte layer onto the substrates. Subsequently, substrates were washed in ultra-pure water (5 minutes; continuous water flow) and dried using a pressurized air stream. Thereafter, substrates were alternately immersed in an anionic aqueous DNA solution (1 mg/ml) and the PDL solution for 7 minutes each, with intermediate washing in ultra-pure water and subsequent drying using a pressurized air stream to obtain final coating architecture of $[PDL/DNA]_5$ (the number indicates the total number of double-layers).

Experimental groups:

Non-coated substrates and $[PDL/DNA]_5$-coated substrates were sterilized using a UV-treatment (254 nm; 4h). Subsequent, VEGF-functionalization of $[PDL/DNA]_5$-coated substrates was carried out as described below. The experimental groups used in this study were:

1. controls (non-coated glass substrates)
2. $[PDL/DNA]_5$ (glass substrates with a $[PDL/DNA]_5$-coating)
3. $[PDL/DNA]_5$-VEGF25 ($[PDL/DNA]_5$-coated glass substrates with 25 ng VEGF)
4. $[PDL/DNA]_5$-VEGF250 ($[PDL/DNA]_5$-coated glass substrates with 250 ng VEGF)

Functionalization with VEGF:

Recombinant rat VEGF ($rrVEGF_{164}$; 164 amino acids; Dept. Biochemistry, Radboud University Nijmegen Medical Center, Nijmegen, the Netherlands) was serially diluted in phosphate-buffered saline (PBS), after which amounts of either 25 or 250 ng VEGF were administered in 10 μl aliquots on the sterilized $[PDL/DNA]_5$-coated substrates. Due to the iso-electric point of VEGF (pI 8.5)[13], this factor will be positively-charged at neutral pH and show similar interaction with the negatively-charged DNA top-layer in the multilayered structure as observed previously for BMP-2[11]. The solvent was evaporated during incubation at 37°C.

In vitro experiments

Cell culture and seeding

Human umbilical vein endothelial cells (HUVEC; PromoCell GmbH, Heidelberg, Germany) were expanded in growth medium, containing basic fibroblast growth factor (1 ng/ml), endothelial cell growth supplement/heparin (0.4% v/v), epidermal growth factor (0.1 ng/ml), hydrocortisone (1 μg/ml),

phenol red (0,62 ng/ml), and fetal calf serum (2% v/v) (GM; PromoCell GmbH, Heidelberg, Germany). To increase cell attachment, prior to cell seeding, the experimental substrates were incubated for 1 hour at 37°C in assay medium (AM; alpha-Minimal Essential Medium (α-MEM; Gibco), supplemented with 10% v/v fetal calf serum (FCS) and gentamycin (50 μg/ml)). For each experimental run, cells were seeded at a density of 20 x 10^3 cells/cm^2 and maintained in AM to exclude potential effects of factors supplemented in GM. Medium was refreshed at 1 day after cell seeding, and thereafter 3 times per week.

Proliferation of endothelial cells
At selective time points after cell seeding (1, 4, 7, and 10 days post-seeding), cells were trypsinized and counted using a Coulter® counter. Data were obtained from two independent experimental runs, with in each run triplicate samples for each condition (n=3) at each time point.

Morphology of endothelial cells
Parallel to the proliferation assays, two independent runs to study endothelial cell morphology were carried out. In each of these runs, two experimental samples for each condition at each time point (n=2) were seeded with HUVECs at a density of 20 x 10^3 cells/cm^2 and incubated for 3 and 10 days. After these culture periods, cell layers were washed twice with PBS, fixed with 2% gluteraldehyde, and dehydrated in a graded series of ethanol. Finally, cell layers were dried using tetramethylsilane (TMS), sputter-coated with gold, and morphologically examined using a scanning electron microscope (JEOL 6310 SEM).

Migration of endothelial cells
The migrational behavior of endothelial cells (HUVEC) was assessed in one experimental run using a commercially available *in vitro* endothelial cell migration assay platform (BD BioCoat™ Angiogenesis System: Endothelial Cell Migration; BD Biosciences, Bedford MA, US), according to the instructions of the manufacturer. The assay measures the migration of cells (located in an insert) through a microporous membrane towards medium (with or without supplement) in the well. Briefly, $[PDL/DNA]_5$-VEGF25 and $[PDL/DNA]_5$-VEGF250 experimental substrates (n=3) were placed in a 24-well plate, and incubated with 1 ml AM for 1, 4, 7, 10, and 14 days. At each time point, the medium was collected, after which fresh medium was added to each experimental substrate for subsequent VEGF release. Collected medium was stored at -80°C until use in the migration kit. For the assay, 225 μl collected medium was added in duplicate in a 96-well plate. Subsequently, HUVECs were added to each insert (25 x 10^3 cells in 75 μl α-MEM 2% BSA), whose content is separated from the well volume by a fluorescence blocking microporous (3 μm) PET membrane. The migration of HUVECs was quantified using post-labeling of the cells with Calcein-AM, and subsequent fluorescence-measurements (excitation 485 nm, emission 530 nm) of the PET membrane after 22 hours of incubation. For comparison, the migration of endothelial cells towards medium with known amounts of VEGF (standards; range 0 – 250 ng/ml) was measured. Data were corrected for fluorescence-values of blanks (inserts without endothelial cells) and expressed as fold migration, which is set at 1 for the lowest VEGF-concentration of the standard.

In vivo experiment
Animals and implantation procedure
For implantation, male Wistar rats of 200-250 g were used. The animals were housed in the central animal facility at the Radboud University Nijmegen Medical Center (Nijmegen, the Netherlands), observing all national guidelines for care and use of laboratory animals. The animals received chow and water *ad libitum*. Prior to the implantation procedure, approval was acquired from the Ethical Committee for animal experiments at the Radboud University Nijmegen (KUNDEC #2003-14).
Surgery was performed under general inhalation anesthesia with nitrous oxide, oxygen, and isoflurane. The animals were immobilized and placed in a ventral position. Subsequently, the dorsal skin of the animals was shaved, washed and disinfected with povidone-iodine. On each side of the vertebral

column, 2 paravertebral incisions were made (~ 10 mm), after which a subcutaneous pocket was created using blunt dissection with scissors lateral to each incision. The insertion of substrates was performed such, that the VEGF-functionalized side faced the dorsal skin. After insertion of an implant, the skin was closed using skin staples (Agraves®; InstruVet C.V., Cuijk, the Netherlands). A total of 64 implants (16 implants of each group) were distributed over 16 rats (4 implants per rat) according to a Latin square randomization scheme.

Implant retrieval and histological preparations

At the end of each implantation period (either 1 or 3 weeks), 8 rats were sacrificed using CO_2-suffication. Subsequently, tissue-covered specimens (n=8 for each implant type and implantation period) were collected, the implants excised from the tissue capsule and checked for potential tissue remains using SEM as described previously [9;10], and the implant-surrounding tissue processed for embedding in paraffin. Paraffin sections were analyzed histologically (haematoxylin/eosin-staining) to obtain complete descriptions of the observed thin sections.

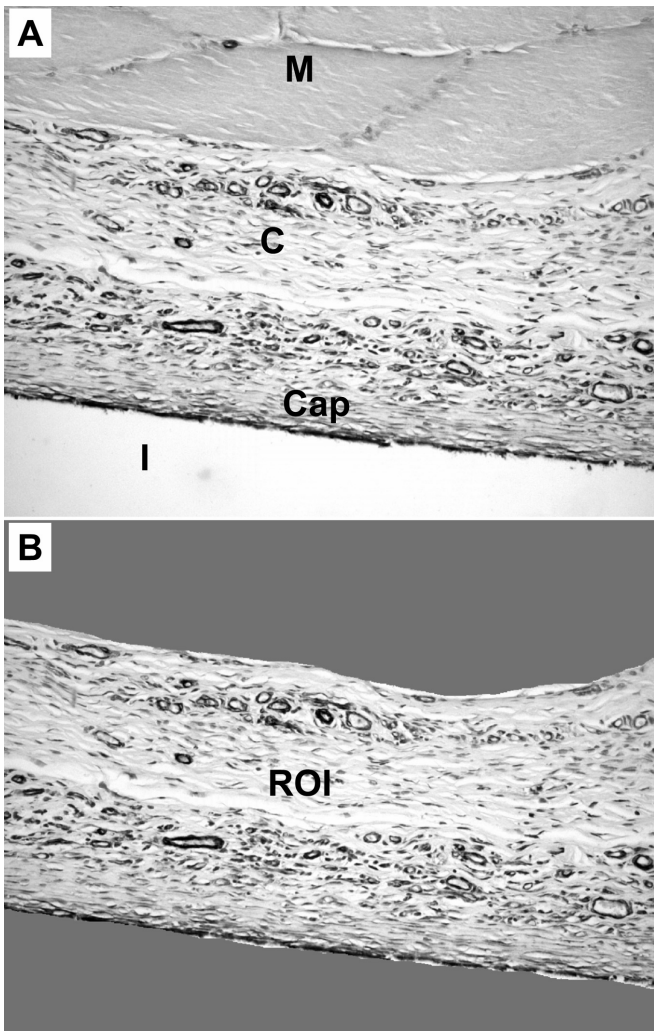

Figure 1: Schematic overview of histomorphometric parameters in immunohistochemically (anti-αSMA) stained sections. (A) Representative image showing the original location of the implant (I), the surrounding fibrous capsule (Cap), the connective tissue (C), and muscle tissue (M). (B) Qwin Pro-image analysis software was used to indicate the region of interest (ROI), after which the number of positively-stained vascular structures within the ROI was counted.

Immunohistochemistry

Parallel to haematoxylin/eosin-staining, paraffin sections were used for immunohistochemical staining using an anti-alpha smooth muscle actin (anti-αSMA) antibody. Amongst other tissues, α-SMA is present in blood vessel walls [14] and myofibroblasts [15], and its expression was used to determine the total number of blood vessels in the peri-implant area. Deparaffinated sections were treated with 3% H_2O_2 in phosphate-buffered saline solution (PBS) for 20 min to block endogenous peroxidase, fixed with

4% formalin and blocked with 5% BSA (Sigma), incubated with monoclonal IgG2a mouse anti-αSMA (1:1600; Sigma), thereafter incubated with biotinylated donkey anti-mouse secondary antibody (1:500; Jackson Laboratories, West Grove, PA, USA). Staining was performed with a biotin-streptavidin detection system (Vectra Elite kit; Vector Laboratories, Burlingame, CA, USA) for 45 min. Positive controls (rat brain tissue sections with positive staining in previous immunohistochemical procedures) and negative controls (1% BSA in PBS) were included.

Histological and histomorphometrical evaluation

A light microscope (Leica Microsystems AG, Wetzlar, Germany) was used for histological evaluation of the haematoxylin/eosin-stained sections. Immunohistochemically (anti-αSMA) stained sections were used for histomorphometrical evaluation of the number of blood vessels per area. Computer-based image analysis techniques (Leica Qwin Pro-image analysis software; Leica, Wetzlar, Germany) were used to determine the following parameters in digital images of immunohistochemically stained sections:

- region of interest (ROI): the connective tissue area at the dorsal site of the implant (i.e. excluding muscle and fat tissue) in a digital image of approximately 700 x 560 μm (original magnification 20x; see Figure 1).
- number of blood vessels (BV): number of positively-stained vascular structures (blood vessels) within the ROI

The values obtained with these parameters were used to determine the vascularization (vessel density, VD):

$$VD = BV/ROI \quad (1)$$

For each implant surrounding tissue section, VD was determined by averaging the numbers of counted vascular structures per ROI of three digital images (at 20x magnification) per tissue section. A total of eight averages VDs (n=8) were obtained for each group at each time period.

Statistical analysis

All measurements were statistically evaluated using GraphPad Instat software (version 3.05; GraphPad Instat, San Diego, CA, USA). Statistical analysis was performed using a one-way ANOVA with a post-hoc Tukey-Kramer Multiple Comparisons test for cell proliferation, migration, and vascularization at individual implantation periods. Vascularization for individual groups and pooled groups at different implantation periods was assessed using an unpaired t-test. A probability (p) value smaller than 0.05 was considered statistically significant.

III RESULTS

In vitro experiments

Proliferation of endothelial cells

The two independent runs of endothelial cell proliferation showed comparable results. The results of one of these runs are presented in Figure 2. Initial cell numbers (on day 1) showed that comparable numbers of endothelial cells attached to the experimental substrates after cell seeding. From day 4, 7, and 10, however, endothelial cells on both $[PDL/DNA]_5$-VEGF25 and $[PDL/DNA]_5$-VEGF250 showed statistically significant increased cell numbers compared to controls and $[PDL/DNA]_5$ ($p<0.05$, $p<0.01$, and $p<0.001$ for days 4, 7, and 10, respectively). Whereas cell numbers on $[PDL/DNA]_5$-VEGF25 and $[PDL/DNA]_5$-VEGF250 increased in time, those on controls and $[PDL/DNA]_5$ were constant in time and did not differ statistically from each other ($p>0.05$). Furthermore, no statistically significant differences were found between $[PDL/DNA]_5$-VEGF25 and $[PDL/DNA]_5$-VEGF250 at individual time points ($p>0.05$).

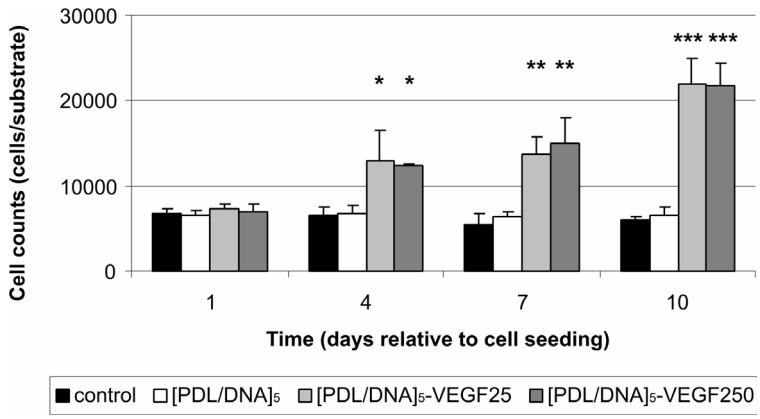

Figure 2: Proliferation of endothelial cells (HUVECs) on experimental substrates. Results are shown as means ± SD of triplicate samples for one representative experiment out of two. (*) $p<0.05$ compared to controls, (**) $p<0.01$ compared to controls, (***) $p<0.001$ compared to controls.

Morphology of endothelial cells

The morphological appearance of the endothelial cells (HUVECs) on the experimental substrates was evaluated using scanning electron microscopy. In Figure 3, representative images of endothelial cells cultured for 4 days on control and $[PDL/DNA]_5$-VEGF250 substrates are depicted. Endothelial cells showed a similar morphology on all types of experimental substrates. The cells exhibited a flat appearance and had several cellular extensions. After both 4 and 10 days of cell culture, an optically increased number of cells were observed on $[PDL/DNA]_5$-VEGF25 and $[PDL/DNA]_5$-VEGF250 compared to controls and $[PDL/DNA]_5$.

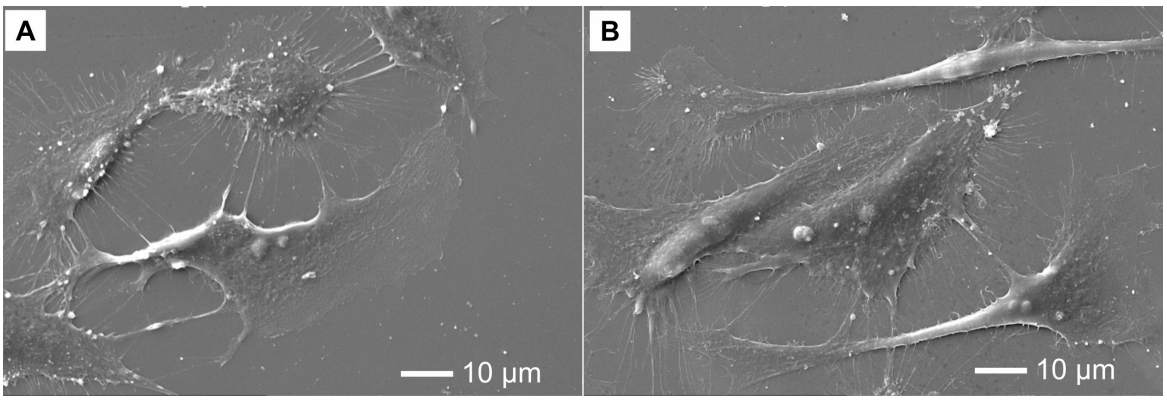

Figure 3: Morphology of endothelial cells (HUVECs) after culture on experimental substrates after 4 days. Representative SEM images of endothelial cells (HUVECs) on (A) control and (B) $[PDL/DNA]_5$-VEGF250 substrates, showing a flat morphology of endothelial cells with several cellular extensions.

Migration of endothelial cells

An *in vitro* migration assay was used to study the effect of VEGF-release from VEGF-functionalized DNA-based coatings on endothelial cell migration. The migration of endothelial cells towards a concentration gradient of VEGF-standards ($rrVEGF_{164}$ in AM; range 0 – 250 ng/ml) is depicted in Figure 4 (inset), and was used to obtain information on the VEGF-release from VEGF-functionalized DNA-based coatings. The results show that VEGF significantly increased endothelial cell migration at concentrations ranging from 1.25 – 100 ng/ml ($p<0.05$). In contrast, a VEGF-concentration of 250 ng/ml demonstrated to have no effect on endothelial cell migration.

Collected medium from the incubation of $[PDL/DNA]_5$-VEGF25 and $[PDL/DNA]_5$-VEGF250 experimental substrates showed that these media also increased endothelial cell migration (Figure 4). The increased effect on endothelial cell migration was observed in medium that had been collected from 1 to at least 14 days after initiation of incubation. No statistically significant differences were observed between media collected from $[PDL/DNA]_5$-VEGF25 and $[PDL/DNA]_5$-VEGF250 experimental substrates ($p>0.05$).

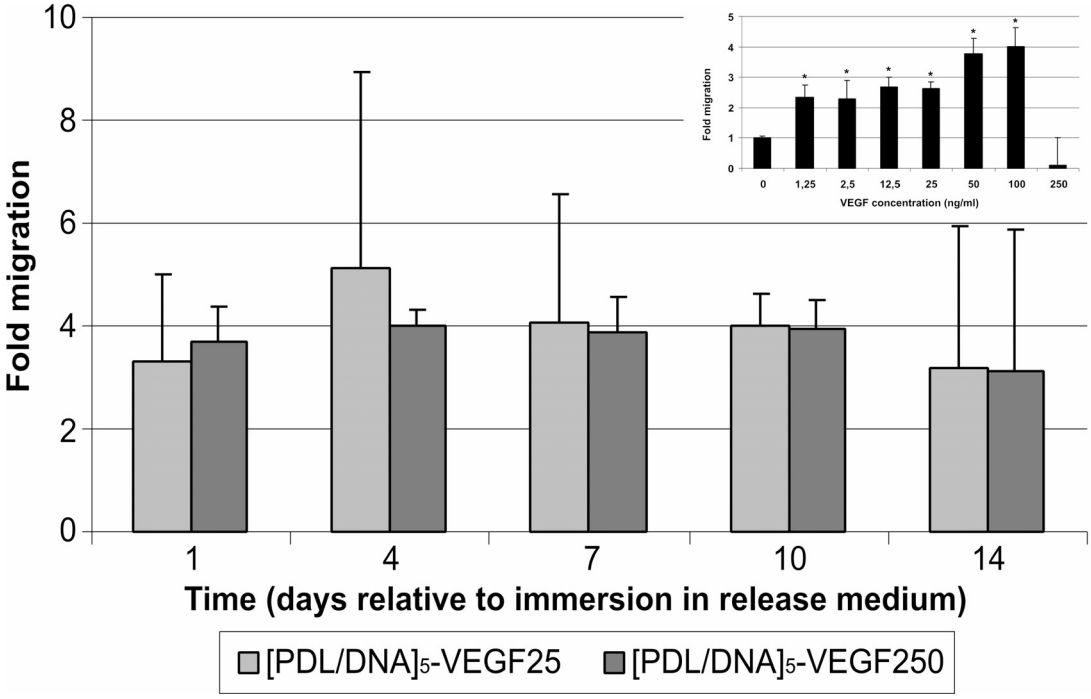

*Figure 4: Migration of endothelial cells (HUVECs) in response to rrVEGF$_{164}$ release from VEGF-functionalized experimental substrates ([PDL/DNA]$_5$-VEGF25 and [PDL/DNA]$_5$-VEGF250). Inset shows migration effects of different concentrations of VEGF (rrVEGF$_{164}$; range 0 – 250 ng/ml; *p<0.05 compared to 0 ng/ml).*

In vivo experiment

General observations

All 16 rats in the animal experiment remained in good health during the implantation periods and did not show any wound complications after surgery. At 1 week after implantation, a total of 32 implants were retrieved. At retrieval, all subcutaneous implants were surrounded by a thin fibrous capsule. None of the implant sites showed macroscopic signs of inflammation or adverse tissue reaction. Similarly, at 3 weeks after implantation, another 32 implants were retrieved, which were all surrounded by a thin fibrous capsule and devoid of any macroscopic signs of inflammation or adverse tissue reactions.

Descriptive histological evaluation

Scanning electron microscopic examination of the excised implants showed that implants were scarcely covered with proteinaceous-like deposits, which were not identifiable as cellular material (data not shown). Gross evaluation of the haematoxylin/eosin-stained sections of the implant surrounding tissue capsules after 1 week of subcutaneous implantation revealed a relatively uniform tissue response to all implants (Figure 5). Tissue at the dorsal side of the implants consisted of a fibrous capsule, connective tissue, muscle tissue, and the dermis. Occasionally, fat tissue was observed in the vicinity of the implants. The fibrous capsule was immature, reflected by the absence of flat fibrocytes at the implant side of the capsule. Little or no inflammatory cells could be observed at the interface implant/capsule or in the direct vicinity of the implants.

After 3 weeks of subcutaneous implantation, a tissue response similar to that after 1 week was observed for all implants. However, the fibrous tissue capsules had matured, as indicated by the presence of fibrocytes with a flat appearance within the tissue capsules (Figure 5 A&B). The thickness of the fibrous capsules was within the range of 5 – 30 fibroblasts, independent of implant type. No gross differences in tissue response were observed depending on implant type.

Histomorphometrical evaluation of vascularization at the dorsal site of the implant

For the evaluation of the vascularization of the connective tissue at the dorsal site of the implants, paraffin sections were subjected to immunohistochemical techniques using a monoclonal antibody

against αSMA. Representative images of the stained sections are presented in Figure 6 C&D. Positive staining was observed for vascular structures and fibrous capsules. A difference was observed in immunohistochemical staining of fibrous capsules after 1 and 3 weeks of implantation, with increased staining in the more mature fibrous capsules at 3 weeks after implantation.

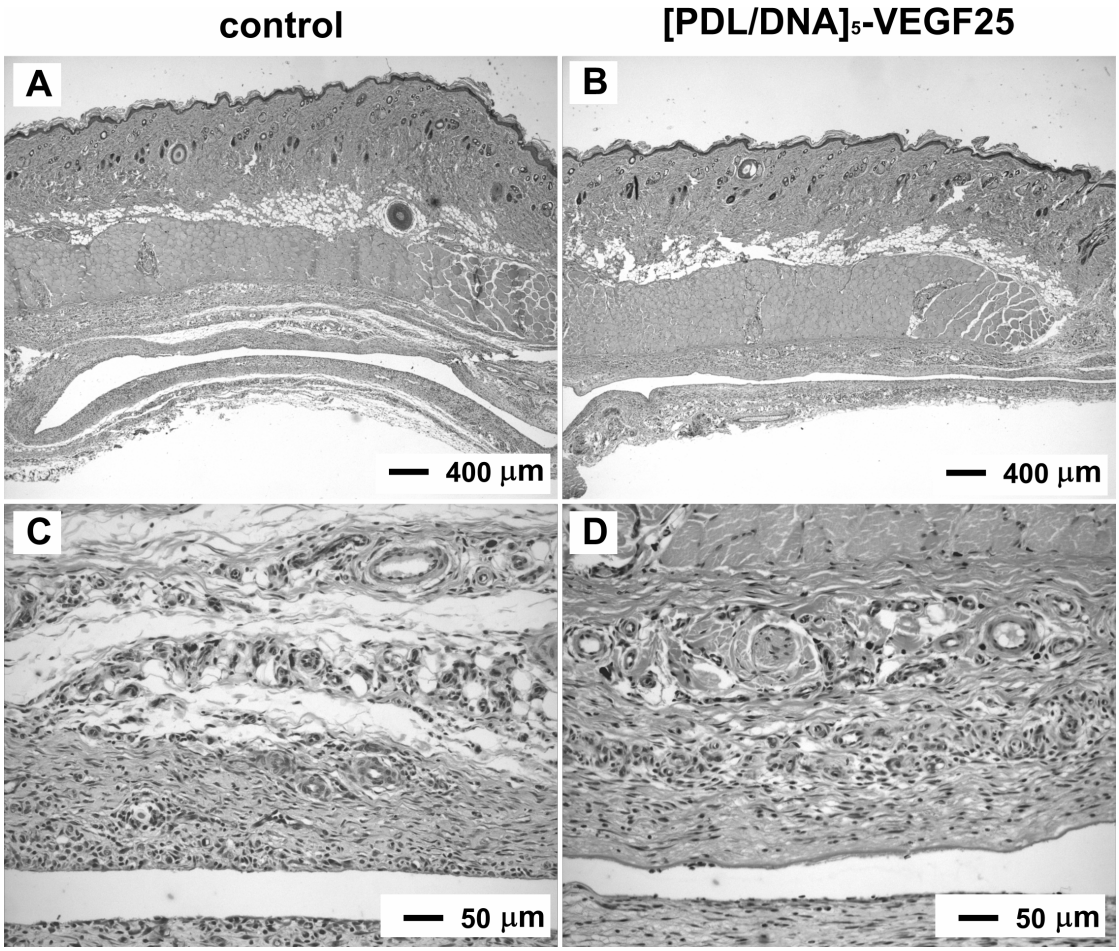

Figure 5: Representative histological sections (haematoxylin/eosin-staining) of implant-surrounding tissue at 1 week after subcutaneous implantation in the back of rats. (A&B) Overview showing the fibrous tissue capsule with connective tissue, a muscle layer, and dermis at the dorsal side of the implant. (C&D) Magnification of A&B showing the thin fibrous capsule and connective tissue at the dorsal side of the implant.

Histomorphometrically, the vascularity in the tissue at the dorsal site of the implant was calculated by determining the region of interest (ROI) and the number of positively-stained vascular structures (blood vessels) within this ROI. The histomorphometrical results are presented in Table 1. The average ROI of the digitally imaged area in all experimental groups ranged from 0.25 – 0.28 mm^2. Vascularization (vessel density VD; # vascular structures/ mm^2 ROI) of the analyzed areas showed a tendency to increase in both groups of VEGF-functionalized DNA-based coatings. However, no statistically significant differences between the individual experimental groups at individual implantation periods were found ($p>0.05$). On the other hand, pooled data of VEGF-functionalized experimental implants ($[PDL/DNA]_5$-VEGF25 + $[PDL/DNA]_5$-VEGF250) and non-functionalized implants (controls + $[PDL/DNA]_5$) showed a significantly increased vascularization in the peri-implant tissue of VEGF-functionalized implants ($p<0.05$). Vascularization in the peri-implant tissue was in the range of 102 – 155 and 66 – 142 vascular structures per mm^2 at 1 and 3 weeks after subcutaneous implantation, respectively. No statistically significant differences were found for individual experimental groups at different implantation periods, except for $[PDL/DNA]_5$, which showed decreased vascularization after 3 weeks compared to after 1 week.

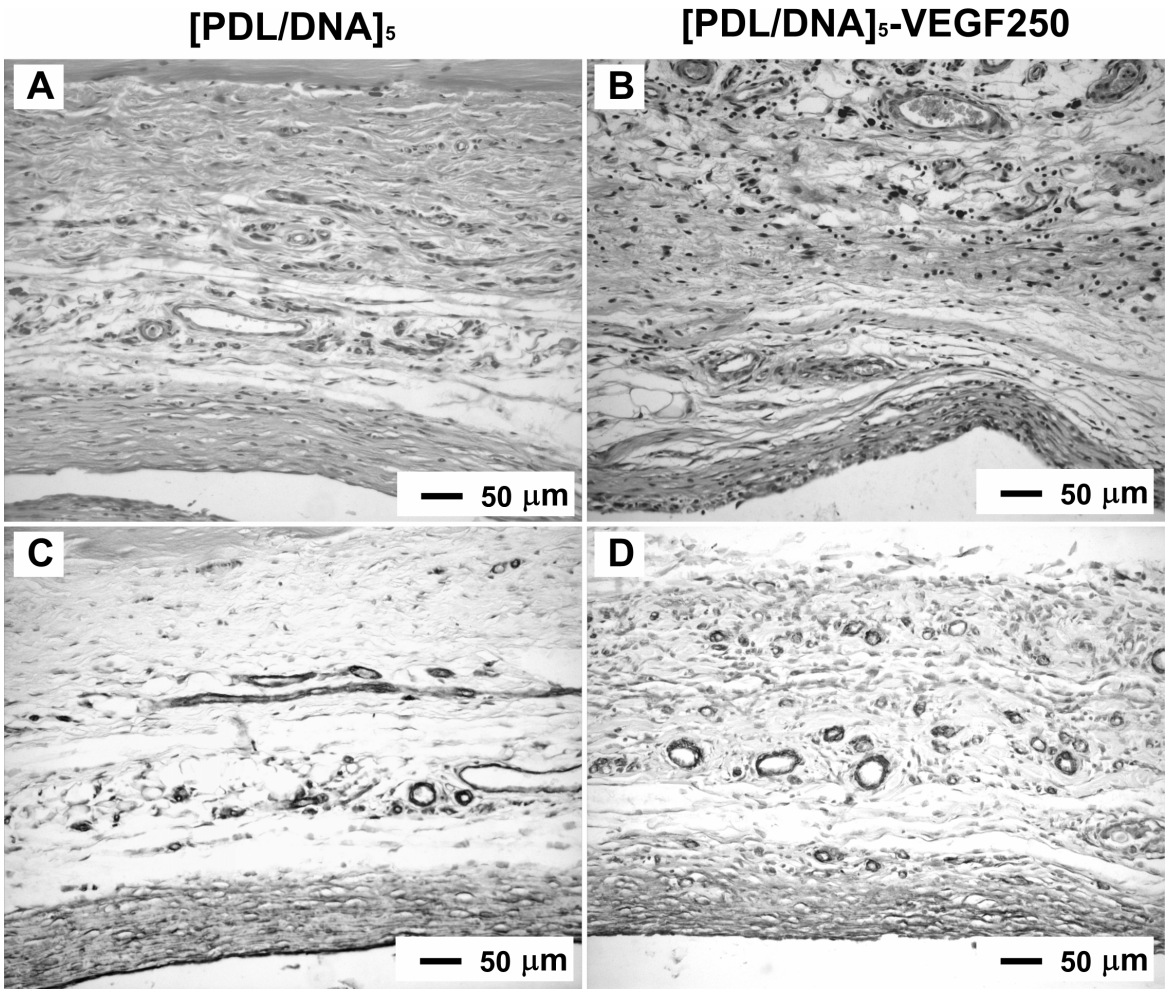

Figure 6: Representative histological sections of implant-surrounding tissue at 3 weeks after subcutaneous implantation in the back of rats. (A&B) Haematoxylin/eosin staining showing the fibrous tissue capsule with connective tissue at the dorsal side of the implant. (C&D) Immunohistochemical staining (anti-αSMA) showing the blood vessels in the connective tissue at the dorsal side of the implant.

IV DISCUSSION

This study was initiated to study the effect of functionalization of a DNA-based coating with the pro-angiogenic factor VEGF on (i) endothelial cell behavior *in vitro*, and (ii) vascularization of the peri-implant tissue *in vivo*. *In vitro*, the effects of DNA-based coatings with low (25 ng) and high (250 ng) amounts of VEGF on endothelial cell proliferation, morphology, and migration were evaluated and compared to non-coated controls and non-functionalized DNA-based coatings. *In vivo*, these four types of substrates were implanted subcutaneously in the back of rats. After implantation periods of 1 and 3 weeks, the vascularization in the direct vicinity of the implants was determined. The results of the *in vitro* experiments indicate that the pro-angiogenic factor VEGF remains biologically active within the functionalized DNA-based coatings, as reflected by an increasing effect of functionalized DNA-based coatings on endothelial cell proliferation and migration compared to non-coated controls and non-functionalized DNA-base coatings. Furthermore, an increased vascularization of the peri-implant tissue surrounding VEGF-functionalized DNA-based coatings was observed *in vivo*.

In an attempt to optimize the functionality of biosensors, this study was a first exploration for the use of DNA-based coatings for this purpose in view of their feasibility to be functionalized with desired factors [11]. Consequently, this study focused on functionalization of DNA-based coatings with the pro-angiogenic factor VEGF, and experiments were aimed at elucidating *in vitro* effects on endothelial cells and *in vivo* effects on implant site vascularization. The type of DNA-based coating was limited to only $[PDL/DNA]_5$, although the fabrication and characterization of different types of DNA-based coatings

have been described previously [8]. The choice for one single type of DNA-based coatings is justified as previous experiments have demonstrated that cellular and histological responses to different types of DNA-based coatings were found to be similar [8-10;16]. The amount of VEGF needed for biological activity *in vitro* and *in vivo* appears to be unclear. Amounts as low as 10 ng have shown biological effects *in vitro* [17], whereas others used micrograms to induce biological effects of VEGF. [18;19]. It is likely that the amount needed for biological effects on vascular development are dependent on issues including type of VEGF, release profile, and animal model. For our experiments, as a first approach, two amounts (i.e. 25 and 250 ng) were chosen with a 10-fold difference.

TABLE 1: HISTOMORPHOMETRICAL ANALYSIS OF VASCULARIZATION AT THE DORSAL SITE OF SUBCUTANEOUSLY-INSERTED IMPLANTS (MEANS ± SD FOR N=8; *P<0.05).

	Implantation time (weeks)	Vascularization (# vascular structures/mm^2)	
control	1	111 ± 55	
[PDL/DNA]$_5$		111 ± 39	
[PDL/DNA]$_5$-VEGF25		155 ± 46	
[PDL/DNA]$_5$-VEGF250		102 ± 40	*
control	3	102 ± 30	
[PDL/DNA]$_5$		66 ± 40	*
[PDL/DNA]$_5$-VEGF25		142 ± 54	
[PDL/DNA]$_5$-VEGF250		136 ± 65	

The increased proliferation of endothelial cells on VEGF-functionalized DNA-based coatings in the *in vitro* experiments demonstrates that the pro-angiogenic factor VEGF remains biologically active. Similar results were recently found for the osteo-inductive factor bone morphogenetic protein 2, which was superficially loaded onto DNA-based coatings and accelerated the differentiation of osteoblast-like cells [11]. Furthermore, our proliferation experiments demonstrated that the presence of VEGF is a prerequisite for endothelial cells (HUVECs) to proliferate, since cells cultured on controls and DNA-based coatings did not proliferate. Additionally, no negative effects of DNA-based coatings on endothelial cells were observed, which corroborates observations of others using polyelectrolyte multilayers as a substrate for endothelial cells [20;21].

The efficacy of biomaterial devices in combination with growth factors depends partly on the availability of the growth factors for sensible cells. For instance, a minimal release of BMP-2 from a porous calcium phosphate scaffold appeared to be sufficient for enhanced bone formation [22]. However, for our purpose an increasing effect of VEGF on the vascularity in the peri-implant area in our *in vivo* experiment is likely to be dependent on release of the factor from the DNA-based coating. Additionally, the increased effect on the proliferation of endothelial cells observed on VEGF-functionalized DNA-based coatings does not necessitate factor release, as also bound factor might be available for adherent cells. In view of this, the results of the migration assay indicate a continuous release of VEGF from VEGF-functionalized DNA-based coatings. Although this assay does not provide detailed information on exact amounts of VEGF released at each incubation period, it shows that released amounts are sufficient for the chemotaxis of endothelial cells. On the basis of the release profiles of BMP-2 from [PDL/DNA]$_5$ coatings and the comparable iso-electric point and molecular weight of BMP-2 and VEGF [13], it can be speculated that VEGF release profiles also show an initial burst release followed by a sustained release for several weeks. This would indicate that the initial VEGF burst release would approximate 17 and 170 ng for DNA-based coatings functionalized with 25 and 250 ng VEGF, respectively. The subsequent sustained VEGF release would then approximate 0,5 and 5 ng per week, respectively. Although the exact released amounts are not clear, the amounts released in the collected release media apparently are sufficient for an effect on endothelial cell migration.

Several animal models to study angiogenesis have been described in detail, including dorsal skinfold chambers [23] and ear pinnae [24]. However, these models have limitations regarding implant size [25], which impedes their use for our implants. Additionally, since the focus of our study was monitor vascularity

effects of the peri-implant tissue of subcutaneous implants, we used a simplistic subcutaneous implantation model in rats. Inevitably, also this simplistic approach for the detection of effects on vascularization has several drawbacks. For instance, the confinement of the area for evaluation of the effects of VEGF on vascularization was difficult to standardize. In contrast to previous studies, in which vascularization was determined in porous implants [26;27], the use of solid implants is associated with concessions in peri-implant area. Standardization of the peri-implant area was further hampered by the excision of the implants, allowing deformations of the fibrous capsule and surrounding tissue during subsequent histological processing. Nevertheless, the approach used in this study allows the comparison of vessel density in the peri-implant area, in which the maximum distance of vessels to the implant surface approximates 600 μm (image height of αSMA-stained sections ≈ 650 μm). The results show no significant effects of individual VEGF-functionalized DNA-based coatings on peri-implant vessel density. However, in comparison to controls and non-functionalized DNA-base coatings, a significant increase in peri-implant vascularity was observed in VEGF-functionalized DNA-based coatings. Further, a significant decrease in vascularity from 1 to 3 weeks after implantation was observed in tissue surrounding non-functionalized DNA-based coatings. This observation might be related to effect of DNA-based coatings on fibroblasts [9;10], which form the fibrous capsule, and subsequent intercellular signaling between fibroblasts and cells in their surroundings. However, the actual cause for this observation remains unclear and should be addressed in future experiments.

Although the functionalization of DNA-based coatings in this study was restricted to one single angiogenic factor, considerable debate is ongoing on the necessity for combined growth factor delivery for angiogenesis and vessel maturation. Indeed, synergistic effects of combined administration of VEGF and basic fibroblast growth factor (bFGF) have been demonstrated on collateral circulation in a hind limb ischemia model [28]. Additionally, Peattie et al. demonstrated enhancement of angiogenic responses in a murine ear pinnea model by dual delivery of VEGF and keratinocyte growth factor (KGF) [29]. Such combined delivery vehicles could also be fabricated using DNA-based coatings, since the mechanism of fabrication has been demonstrated to be applicable for compartmentalization of such polyelectrolyte multilayers [30], which would allow temporal control over growth factor release.

CONCLUSION

This study demonstrates that the functionalization of DNA-based coatings with the pro-angiogenic factor VEGF results in an increased proliferation and migration of endothelial cells *in vitro*, indicating that the VEGF retained its biological activity. In an *in vivo* implantation experiment in rats, increased vascularization of the peri-implant tissue surrounding VEGF-functionalized DNA-based coatings was observed.

V ACKNOWLEDGEMENTS

The authors would like to acknowledge Nichiro Corporation (Kawasaki-city, Kanagawa prefecture, Japan) for providing DNA. Scanning electron microscopy was performed in collaboration with the Microscopical Imaging Center of the Nijmegen Center for Molecular Life Sciences (NCMLS). Ms. Natasja van Dijk, dr. Weibo Zhang (both Dept. of Periodontology & Biomaterials), and mr. René van Rheden (Dept. of Orthodontics & Oral Biology) are acknowledged for their help with histological preparations and immunohistochemical staining. Mr. Vincent Cuijpers (Dept. of Periodontology & Biomaterials) is acknowledged for assistance with histomorphometrical analyses. This research was financially supported by the Technology Foundation STW, applied science division of NWO and the technology programme of the Ministry of Economic Affairs, grant # NKG.5758.

VI REFERENCES

1. Sharkawy, A. A., B. Klitzman, G. A. Truskey, and W. M. Reichert. 1997. Engineering the tissue which encapsulates subcutaneous implants. I. Diffusion properties. *J Biomed Mater Res* 37:401-12.

2. Woodward, S. C. 1982. How fibroblasts and giant cells encapsulate implants: considerations in design of glucose sensors. *Diabetes Care* 5:278-81.

3. Gerritsen, M., J. A. Jansen, A. Kros, D. M. Vriezema, N. A. Sommerdijk, R. J. Nolte, J. A. Lutterman, S. W. Van Hovell, and A. Van der Gaag. 2001. Influence of inflammatory cells and serum on the performance of implantable glucose sensors. *J Biomed Mater Res* 54:69-75.

4. Pepper, M. S. 1997. Manipulating angiogenesis. From basic science to the bedside. *Arterioscler Thromb Vasc Biol* 17:605-19.

5. Klagsbrun, M. and M. A. Moses. 1999. Molecular angiogenesis. *Chem Biol* 6:R217-24.

6. Nomi, M., A. Atala, P. D. Coppi, and S. Soker. 2002. Principals of neovascularization for tissue engineering. *Mol Aspects Med* 23:463-83.

7. Li, J., Y. P. Zhang, and R. S. Kirsner. 2003. Angiogenesis in wound repair: angiogenic growth factors and the extracellular matrix. *Microsc Res Tech* 60:107-14.

8. van den Beucken, J. J., M. R. Vos, P. C. Thune, T. Hayakawa, T. Fukushima, Y. Okahata, X. F. Walboomers, N. A. Sommerdijk, R. J. Nolte, and J. A. Jansen. 2006. Fabrication, characterization, and biological assessment of multilayered DNA-coatings for biomaterial purposes. *Biomaterials* 27:691-701.

9. van den Beucken, J. J., X. F. Walboomers, M. R. Vos, N. A. Sommerdijk, R. J. Nolte, and J. A. Jansen. 2006. Cyto- and histocompatibility of multilayered DNA-coatings on titanium. *J Biomed Mater Res A* 77A:202-211.

10. van den Beucken, J. J. J. P., X. F. Walboomers, M. R. J. Vos, N. A. J. M. Sommerdijk, R. J. M. Nolte, and J. A. Jansen. Biological responses to multilayered DNA-coatings. *J Biomed Mater Res B*.

11. van den Beucken, J. J., X. F. Walboomers, O. C. Boerman, M. R. Vos, N. A. Sommerdijk, T. Hayakawa, T. Fukushima, Y. Okahata, R. J. Nolte, and J. A. Jansen. 2006. Functionalization of multilayered DNA-coatings with bone morphogenetic protein 2. *J Control Release* 113:63-72.

12. Decher G. Fuzzy Nanoassemblies: Toward Layered Polymeric Multicomposites. Science 277, 1232-1237. 97.

13. Yamamoto, M., Y. Ikada, and Y. Tabata. 2001. Controlled release of growth factors based on biodegradation of gelatin hydrogel. *J Biomater Sci Polym Ed* 12:77-88.

14. Kobayashi, H., N. Tsuruchi, K. Sugihara, T. Kaku, T. Saito, T. Kamura, N. Tsukamoto, H. Nakano, and S. Taniguchi. 1993. Expression of alpha-smooth muscle actin in benign or malignant ovarian tumors. *Gynecol Oncol* 48:308-13.

15. Parker, J. A., X. F. Walboomers, J. W. Von Den Hoff, J. C. Maltha, and J. A. Jansen. 2003. Soft tissue reaction to microgrooved poly-L-lactic acid implants loaded with transforming growth factor beta(3). *Tissue Eng* 9:117-26.

16. van den Beucken, J. J. J. P., X. F. Walboomers, M. R. J. Vos, N. J. A. M. Sommerdijk, R. J. M. Nolte, and J. A. Jansen. Macrophage behavior on multilayered DNA-coatings *in vitro*. *J Biomed Mater Res A*.

17. Rebai, O., J. Le Petit-Thevenin, N. Bruneau, D. Lombardo, and A. Verine. 2005. In vitro angiogenic effects of pancreatic bile salt-dependent lipase. *Arterioscler Thromb Vasc Biol* 25:359-64.

18. Steffens, G. C., C. Yao, P. Prevel, M. Markowicz, P. Schenck, E. M. Noah, and N. Pallua. 2004. Modulation of angiogenic potential of collagen matrices by covalent incorporation of heparin and loading with vascular endothelial growth factor. *Tissue Eng* 10:1502-9.

19. Ravin, A. G., K. C. Olbrich, L. S. Levin, A. L. Usala, and B. Klitzman. 2001. Long- and short-term effects of biological hydrogels on capsule microvascular density around implants in rats. *J Biomed Mater Res* 58:313-8.

20. Boura, C., P. Menu, E. Payan, C. Picart, J. C. Voegel, S. Muller, and J. F. Stoltz. 2003. Endothelial cells grown on thin polyelectrolyte mutlilayered films: an evaluation of a new versatile surface modification. *Biomaterials* 24:3521-30.

21. Boura, C., H. Kerdjoudj, V. Moby, D. Vautier, D. Dumas, P. Schaaf, J. C. Voegel, J. F. Stoltz, and P. Menu. 2006. Initial adhesion of endothelial cells on polyelectrolyte multilayer films. *Biomed Mater Eng* 16:S115-21.

22. Ruhe, P. Q., H. C. Kroese-Deutman, J. G. Wolke, P. H. Spauwen, and J. A. Jansen. 2004. Bone inductive properties of rhBMP-2 loaded porous calcium phosphate cement implants in cranial defects in rabbits. *Biomaterials* 25:2123-32.

23. Rucker, M., M. W. Laschke, D. Junker, C. Carvalho, A. Schramm, R. Mulhaupt, N. C. Gellrich, and M. D. Menger. 2006. Angiogenic and inflammatory response to biodegradable scaffolds in dorsal skinfold chambers of mice. *Biomaterials*.

24. Pike, D. B., S. Cai, K. R. Pomraning, M. A. Firpo, R. J. Fisher, X. Z. Shu, G. D. Prestwich, and R. A. Peattie. 2006. Heparin-regulated release of growth factors in vitro and angiogenic response in vivo to implanted hyaluronan hydrogels containing VEGF and bFGF. *Biomaterials* 27:5242-51.

25. Laschke, M. W., Y. Harder, M. Amon, I. Martin, J. Farhadi, A. Ring, N. Torio-Padron, R. Schramm, M. Rucker, D. Junker, J. M. Ha, C. Carvalho, M. Heberer, G. Germann, B. Vollmar, and M. D. Menger. 2006. Angiogenesis in Tissue Engineering: Breathing Life into Constructed Tissue Substitutes. *Tissue Eng*.

26. Ribatti, D., B. Nico, L. Morbidelli, S. Donnini, M. Ziche, A. Vacca, L. Roncali, and M. Presta. 2001. Cell-mediated delivery of fibroblast growth factor-2 and vascular endothelial growth factor onto the chick chorioallantoic membrane: endothelial fenestration and angiogenesis. *J Vasc Res* 38:389-97.

27. Kidd, K. R. and S. K. Williams. 2004. Laminin-5-enriched extracellular matrix accelerates angiogenesis and neovascularization in association with ePTFE. *J Biomed Mater Res A* 69:294-304.

28. Asahara, T., C. Bauters, L. P. Zheng, S. Takeshita, S. Bunting, N. Ferrara, J. F. Symes, and J. M. Isner. 1995. Synergistic effect of vascular endothelial growth factor and basic fibroblast growth factor on angiogenesis in vivo. *Circulation* 92:II365-71.

29. Peattie, R. A., E. R. Rieke, E. M. Hewett, R. J. Fisher, X. Z. Shu, and G. D. Prestwich. 2006. Dual growth factor-induced angiogenesis in vivo using hyaluronan hydrogel implants. *Biomaterials* 27:1868-75.

30. Garza, J. M., P. Schaaf, S. Muller, V. Ball, J. F. Stoltz, J. C. Voegel, and P. Lavalle. 2004. Multicompartment films made of alternate polyelectrolyte multilayers of exponential and linear growth. *Langmuir* 20:7298-302.

8

SUMMARY, ADDRESS TO THE AIMS, CLOSING REMARKS & FUTURE PERSPECTIVES

I SUMMARY AND ADDRESS TO THE AIMS

The growing world population in combination with the increasing life-expectancy make that the application of medical and dental implants will expand. The proper integration of these artificial devices relies greatly on the medical condition of the patient, the properties of the biomaterial device, and the interaction of the adjacent tissue with the biomaterial surface. Important biological and material aspects in the interaction of living tissue with artificial devices are described in the literature review as presented in **chapter 1**. Here it is described that improvements in the longevity of artificial devices are often sought in surface modifications and include topographical as well as chemical alterations. It needs to be emphasized that changes in surface chemistry commonly bring along changes in surface topography. Nevertheless, surface modification has demonstrated to be a powerful tool in controlling the processes at the interface between biomaterial and living tissue. In view of this, the general aim of the research described in this thesis was to evaluate the use of deoxyribonucleic acid (DNA) as a biomaterial coating. Irrespective of its genetic information, the structural properties of the vertebrate DNA molecule suggest that it can have beneficial effects on cell and tissue response with respect to immunology, drug-delivery, and apposition of bone mineral. The research on this subject was gradually approached, using experimental studies to answer specific research questions.

- **Fabrication and characterization of DNA-based coatings**

The initial research was focused on the fabrication of DNA-based coatings and their characterization. The use of DNA as a coating material is hampered by its water solubility and degradation by abundantly present nucleolytic enzymes. **Chapter 2** describes the fabrication of multilayered DNA-coatings using electrostatic self-assembly (ESA). This technique is based on the alternate deposition of cationic and anionic polyelectrolytes, by which a multilayered coating is fabricated. With the use of either poly-D-lysine (PDL) or poly(allylamine hydrochloride) (PAH) as the cationic component and DNA as the anionic counterpart, multilayered coatings consisting of 5 double-layers were fabricated on glass and titanium (assigned as $[PDL/DNA]_5$ and $[PAH/DNA]_5$). A progressive build up of both coatings was demonstrated from contact angle measurements, UV-measurements, and atomic force microscopy. Furthermore, a linear increase in the incorporation of DNA into the multilayered coatings was observed during build up, approximating 3 $\mu g/cm^2$ into each double-layer. Additionally, monitoring the surface morphology of the coatings by atomic force microscopy showed that the roughness of the coatings increased during build up. Finally, the coating constituents were checked for mutagenicity, and demonstrated to have no mutagenic effects on a mutant strain of *Salmonella typhimurium*. These results showed that with the ESA-technique it is feasible to fabricate DNA-coatings on glass and titanium whose constituents are safe.

- **Cyto- and histological responses to DNA-based coatings**

In **chapter 3**, cell and soft tissue responses to DNA-based coatings were evaluated and compared to non-coated controls. *In vitro* cell culture experiments with primary rat dermal fibroblasts demonstrated that both types of DNA-coatings ($[PDL/DNA]_5$ and $[PAH/DNA]_5$) did not affect cell viability and morphology compared to non-coated controls. However, cell proliferation on both types of DNA-coatings was increased compared to non-coated controls. Using an *in vivo* animal model, coated implants and non-coated controls were implanted subcutaneously for four and twelve weeks in the backs of rats. DNA-coatings demonstrated to induce no adverse reactions in terms of inflammation and wound healing. Furthermore, histological analysis showed that the soft tissue response to DNA-coated implants was similar to that of non-coated controls. The results of these studies demonstrated that DNA-coatings are cyto- as well as histocompatible.

- ***In vitro* macrophage response to DNA-based coatings**

Macrophages are regarded as the pivotal cell type in wound healing processes, including inflammation, tissue repair, and tissue remodeling. During these biological processes, macrophages orchestrate the

intensity and duration of these phases by producing a myriad of signaling molecules that control the behavior of other cell types involved in these processes. In **chapter 4**, the behavior of macrophages cultured on DNA-based coatings is described. To study macrophage behavior, two murine macrophage cell lines were used to evaluate cell attachment, viability, morphology, and cytokine secretion. For cytokine secretion, a group of four cytokines was selected, whose individual mode of action can be classified as pro- or anti-inflammatory, pro- or anti-wound healing, or a combination of these. Culture of macrophages on DNA-based coatings demonstrated to have no effect on cell attachment, viability, and morphology. However, a substrate-dependent cytokine secretion profile was observed, which showed that on DNA-based coatings the secretion of the major pro-inflammatory cytokine TNF-α was decreased. This observation indicates that the use of DNA-based coatings can decrease the inflammatory response and hence accelerate the total wound healing processes.

- **Effect of DNA-based coatings on the deposition of calcium phosphate and the behavior of bone-forming cells**

In addition to the beneficial low immunogenic properties of DNA-based coatings described above, it was hypothesized that the high phosphate content in the DNA-molecule could be beneficial for the deposition of calcium phosphate. It is known that for bone implants the direct apposition of bone tissue to the implant surface (without an intervening soft tissue capsule) is a prerequisite for fixation, and that the deposition of calcium phosphate from simulated body fluids is indicative for this property called bioactivity. Consequently, **chapter 5** describes *in vitro* immersion studies of DNA-based coatings in simulated body fluids, and the effect of DNA-based coatings on the behavior of bone-forming cells. These studies demonstrated that DNA-based coatings favored the deposition of calcium phosphate over non-coated titanium controls. Additionally, cell culture experiments with rat bone marrow-derived osteoblast-like cells showed that DNA-based coatings did not affect cell behavior. On the other hand, pre-treatment of DNA-based coatings in simulated body fluid affected cell differentiation, evidenced by an increased deposition of osteocalcin. These studies are indicative for bone-bonding capacities of DNA-based coatings, but conclusive evidence for the bioactivity of DNA-based coatings needs to be provided by *in vivo* animal experiments.

- **Functionalization of DNA-based coatings with the osteoinductive factor BMP-2**

Control over the behavior of cells and tissues in the direct vicinity of an implant is auxiliary to increase implant functionality. Powerful tools in this respect are factors that exhibit biological activity, such as growth factors and cytokines. In **chapter 6**, the functionalization of DNA-based coatings with the osteoinductive factor bone morphogenetic protein 2 (BMP-2) was assessed using three different loading modalities. Experiments with radiolabeled BMP-2 demonstrated the feasibility of DNA-based coatings to be functionalized with BMP-2 and showed a release pattern consisting of an initial burst release within 1 day followed by a sustained release up to 8 weeks. Additional cell culture experiments with rat bone marrow-derived osteoblast-like cells demonstrated that the incorporated factor remained biologically active, as evidenced by an accelerated mineralization of the extracellular matrix. From these experiments, it was concluded that DNA-based coatings are eligible for functionalization with biologically-active compounds, and hence can modulate cell response.

- **Angiogenic response to VEGF-functionalized DNA-based coatings**

Vascularization is regarded as an important issue in wound healing and essential for tissue ingrowth into porous tissue engineering matrices. Furthermore, the functionality of subcutaneously implanted biosensors is known to be dependent on peri-implant vascularization. In view of this, **chapter 7** describes a first exploration of the use of DNA-based coatings for optimization of peri-implant vascularization through their functionalization with the pro-angiogenic factor vascular endothelial growth factor (VEGF). *In vitro*, VEGF-functionalized DNA-based coatings demonstrated to increase the proliferation of endothelial cells. Additionally, released VEGF from these coatings was found to enhance

the migration of endothelial cells. In an *in vivo* animal model, subcutaneously implanted VEGF-functionalized DNA-based coatings showed to increase peri-implant vascularization. This study demonstrated that the functionalization of DNA-based coatings with biologically-active compounds is an effective means to modulate tissue response *in vivo*.

II CLOSING REMARKS & FUTURE PERSPECTIVES

The experiments described in this thesis concern the use of DNA as a coating material for implants. The idea to use DNA for this purpose arose from the structural properties of the DNA-molecule, which were hypothesized to beneficially affect several aspects of the biological processes that occur after the insertion of an implant. The homogeneity of DNA in vertebrate species rendered this material interesting from an immunological point of view. For hard tissue implants, the high phosphate content in DNA was hypothesized to facilitate the apposition of bone tissue. Additionally, the capacity of DNA to bind other compounds was hypothesized to allow the modulation of cell and tissue responses through drug-delivery at the site of implantation.

The first issue to address in this research was the fabrication of a coating containing DNA. Within the limited number of methods to fabricate DNA-based coatings, we have chosen for electrostatic self-assembly. This technique is inexpensive and simple, and has the advantage that it is applicable on many different materials without limitations regarding implant geometry. Although in our experiments all coatings were applied manually, several automated systems for the fabrication of coatings through electrostatic self-assembly are already commercially available. In view of the simplicity of the technique, the use of automated systems could rapidly upscale coating production for commercial exploitation.

For the fabrication of DNA-based coatings in our research, the number of double-layers (either [PDL/DNA] or [PAH/DNA]) used was limited to 5, since coating characterization methods indicated that 5 double-layers was sufficient to reach surface coverage. However, in view of the loading of DNA-based coatings, the number of double-layers could be increased to enlarge the total amount of biologically-active compound loaded into the DNA-based coatings. A point of concern remains the loading efficiency, which is relatively low due to necessary wash steps in case of non-terminal loading. An additional issue is the use of effective dosages (amount and release) of biologically-active compounds. Although a lot of effort has been put in elucidating application-dependent standards, more work needs to be done to unravel the requirements to optimize, both from a clinical and a cost-effective point of view, the use of biologically-active compounds in implantology.

In view of the eventual utilization of DNA-based coatings in a clinical setting, the first steps have been taken towards specific applications. In continuation of the results of the VEGF-functionalized DNA-based coatings on peri-implant tissue vascularization, the application of such coatings to optimize subcutaneously implanted biosensors (more specifically glucose-sensors) is currently under investigation. Furthermore, self-standing DNA-based films, consisting of DNA and chitosan, are being explored for their effects on the prevention of post-surgical adhesions.

A final issue in view of the eventual application of DNA-based coatings/material is the load enfolded in the abbreviation DNA. Although nature has provided us with many unique materials, including proteins, sugars, fats, and DNA, the latter rouses people to reluctance and anxiousness. To abandon or minimize such feelings, the general knowledge of people on DNA and its application(s) should be enlarged to give DNA a more common image.

9

SAMENVATTING, EVALUATIE VAN DE DOELSTELLINGEN, AFSLUITENDE OPMERKINGEN & TOEKOMSTVISIE

I SAMENVATTING EN EVALUATIE VAN DE DOELSTELLINGEN

Door de groei van de wereldbevolking en de toegenomen levensverwachting zal het toepassen van medische en tandheelkundige implantaten expanderen. Een adequate integratie van dit soort artificiele lichaamsdelen is afhankelijk van de medische conditie van de patient, de eigenschappen van het artificiele lichaamsdeel en de interactie van aangrenzend weefsel met het oppervlak van het implantaat. Belangrijke aspecten op het gebied van biologie en materiaalkunde in de interactie tussen levend weefsel en het oppervlak van biomaterialen staan beschreven in **hoofdstuk 1**. Dit hoofdstuk toont dat verbeteringen ter verlenging van de levensduur van kunstmatige lichaamsdelen vaak gezocht worden in oppervlakte-modificaties, welke zowel topografische als chemische veranderingen behelsen. Het dient te worden benadrukt dat chemische veranderingen veelal samengaan met veranderingen in oppervlakte-topografie. Niettemin, modificaties aan het implantaat-oppervlak hebben bewezen een krachtig middel te zijn om een bepaalde mate van controle op de processen op het scheidingsvlak tussen biomateriaal en levend weefsel uit te oefenen. Met dit in het achterhoofd was het algemene doel van het onderzoek beschreven in het onderhavige proefschrift de toepassing van deoxyribonucleine zuur (DNA) als coatings voor biomaterialen. Afgezien van de genetische informatie beschikt DNA van gewervelde organismen over een aantal structurele eigenschappen, welke mogelijk heilzame effecten zouden kunnen bewerkstelligen op de cel- en weefselreactie. Deze eigenschappen bieden mogelijkheden ten aanzien van ontstekingsreacties, drug-delivery en de afzetting van botmineraal. Het onderzoek naar deze mogelijkheden werd trapsgewijs aangepakt via meerdere experimentele studies ter beantwoording van specifieke onderzoeksvragen.

- **Productie en karakterisering van DNA-coatings**

Het initiele onderzoek was gericht op de productie van DNA-coatings en hun karakterisering. Het gebruik van DNA als coatingmateriaal wordt bemoeilijkt de oplosbaarheid van DNA in water en het gevaar van degradatie door door specifieke enzymes. **Hoofdstuk 2** beschrijft de productie-methode van gelaagde DNA-coatings middels electrostatic self-assembly (ESA). Deze techniek is gebaseerd op de beurtelingse afzetting van positief en negatief geladen polyelectrolyten, hetgeen leidt tot een gelaagde coating. Door gebruik te maken van poly-D-lysine (PDL) of poly(allylamine hydrochloride) (PAH) als positief polyelectrolyte en DNA als negatieve tegenhanger, werden gelaagde coatings bestaande uit 5 dubbellagen gemaakt op glas en titanium (aangegeven als $[PDL/DNA]_5$ en $[PAH/DNA]_5$). Door het meten van contacthoeken en UV-absorptie, en analyse middels atomic force microscopy werd aangetoond dat deze gelaagde coatings een progressieve opbouw vertonen. Verder werd aangetoond dat de incorporatie van DNA in deze gelaagde coatings een lineair verband vertoont met het aantal dubbellagen, overeenkomend met circa 3 $\mu g/cm^2$ in elke dubbellaag. Voorts werd middels atomic force microscopy aangetoond dat de ruwheid van de gelaagde coatings toenam gedurende hun opbouw. Tenslotte werden de bestanddelen van de gelaagde coatings onderzocht op mutageniteit middels een standaard mutageniteitstest, hetgeen toonde dat deze geen mutagene effecten op een stam van *Salmonella typhimurium* hebben. Samenvattend hebben deze experimenten bewezen dat middels ESA veilige, gelaagde coatings met DNA kunnen worden gemaakt op glas en titanium.

- **Cel- en weefselreactie op DNA-coatings**

In **Hoofdstuk 3** wordt de evaluatie van de zacht weefsel reactie op DNA-coatings beschreven en vergeleken met de reactie op ongecoate implantaten. Met behulp van *in vitro* celkweek experimenten met primaire fibroblasten werd aangetoond dat zowel $[PDL/DNA]_5$ als $[PAH/DNA]_5$ geen effect hebben op de levensvatbaarheid en morphologie van de cellen. Echter, op beide types DNA-coatings werd een vernelde groei van de primaire fibroblasten waargenomen vergeleken met de controles. In een *in vivo* diermodel werden implantaten met een DNA-coating en ongecoate controles onderhuids ingebracht in ratten. Na een periodes van 4 en 12 weken werden geen ongunstige weefselreacties waargenomen, zoals ontstekingsreacties of aangetaste wondgenezing. Deze observaties werden later ondersteund door de resultaten van de histologische analyse, waarin verder geen verschillen werden waargenomen

tussen de zacht weefsel reactie tegen implantaten mét of zonder DNA-coating. Op basis van deze resultaten werd geconcludeerd dat DNA-coatings zowel cel- als weefselcompatibel zijn.

- ***In vitro* reactie van macrofagen op DNA-coatings**

Macrofagen worden beschouwd als het belangrijkste celtype in de processen rond wondgenezing, zoals de ontstekingsreactie, weefselherstel, en weefsel remodeling. Tijdens het verloop van deze processen, bepalen macrofagen de intensiteit en duur van deze fases van de wondgenezing door hun productie van talloze signaalmoleculen, welke de activiteit van andere betrokken celtypen controleren. In **hoofdstuk 4** wordt het gedrag van macrofagen op beide types DNA-coatings beschreven. Hiertoe zijn 2 muizen-macrofaag cellijnen gebruikt, waarvan celhechting, levensvatbaarheid, morfologie en cytokine secretie zijn onderzocht na kweek op beide types DNA-coatings. De onderzochte cytokines werden geselcteerd op basis van hun rol in ontstekingsprocessen en wondgenezing. Beide types DNA-coatings bleken geen effect te hebben op celhechting, levensvatbaarheid en morfologie vergeleken met ongecoate controles. Wel werd een substraat-afhankelijke secretie van de geselecteerde cytokines waargenomen. Meest opvallend was hierbij dat op beide types DNA-coatings de secretie van TNF-α, het belangrijkste cytokine in ontstekingsreacties, verlaagd was. Deze waarneming duidt op een effect tot verlaging van de ontstekingsreactie door DNA-coatings, hetgeen zou kunnen leiden tot versnelde wondgenezing.

- **Effect van DNA-coatings op de afzetting van calcium fosfaat en het gedrag van botvormende cellen**

Naast de eerder beschreven gunstige effecten van DNA-coatings op ontstekingscellen, was een van de hyptheses dat gezien het hoge fosfaat-gehalte in DNA, dit materiaal de afzetting van calcium fosfaat positief zou kunnen beïnvloeden. Het is bekend dat voor bot-implantaten de directe afzetting van botmineraal (zonder een tussenliggende laag van zacht weefsel) een voorwaarde is voor stabiele fixatie, en dat de afzetting van calcium fosfaat vanuit lichaamsvloeistof-simulerende oplossingen indicatief is voor deze eigenschap, genaamd bioactiviteit, van materialen. Derhalve zijn experimenten uitgevoerd met lichaamsvloeistof-simulerende oplossingen en botvormende cellen, welke beschreven zijn in **hoofdstuk 5**. Deze experimenten tonen dat de afzetting van calcium fosfaat versneld plaatsvindt op beide types DNA-coatings in vergelijking met ongecoate titanium controles. Verder werd geen effect van DNA-coatings op het gedrag van (voorlopers van) botvormende cellen waargenomen. Echter, door gecoate substraten te incuberen in lichaamsvloeistof-simulerende oplossingen, en deze te vergelijken met ongecoate titanium controles, werd aangetoond dat deze voorbehandeling de ontwikkeling van botvormende cellen uit deze voorlopercellen stimuleert, blijkend uit een verhoogde depositie van het matrix-eiwit osteocalcine. Deze experimenten zijn indicatief voor de bot-bindende capaciteit van DNA-coatings, maar dienen te worden ondersteund door *in vivo* dier-experimenten om eensluidende uitspraken over de bioactiviteit van DNA-coatings te kunnen doen.

- **Functionaliseren van DNA-coatings met de osteoinductieve factor BMP-2**

Een bepaalde mate van controle op het gedrag van cellen en weefsels in de directe omgeving van een implantaat zou substantieel kunnen bijdragen aan de functionaliteit van het betreffende implantaat. In dit opzicht vormen stoffen met een bepaalde biologische activiteit, zoals groeifactoren en cytokines, een krachtig hulpmiddel. In **hoofdstuk 6** wordt de functionalisatie van DNA-coatings met de osteo-inductieve factor bone morphogenetic protein 2 (BMP-2; induceert de ontwikkeling van botvormende cellen uit voorlopers) beschreven, waarbij drie verschillende varianten van gefunctionaliseerde DNA-coatings werden vergeleken. Door BMP-2 radio-actief te labelen kon worden aangetoond dat DNA-coatings inderdaad te functionaliseren zijn met BMP-2, en dat het BMP-2 uit deze DNA-coatings vrijkomt via een initiële plotsklapse afgifte binnen een dag gevolgd door een geleidelijke afgifte gedurende minimaal acht weken. Daarnaast lieten celkweek experimenten met (voorlopers van) botvormende cellen zien dat het BMP-2 in de DNA-coatings zijn biologische activiteit behoudt, blijkend

uit een versnelde mineralisatie van de, door deze cellen gevormde, extracellulaire matrix. Op basis van deze resultaten werd geconcludeerd dat DNA-coatings te functionaliseren zijn met biologisch-aciteve stoffen, en op deze manier het gedrag van cellen kunnen beïnvloeden.

- **Effect van VEGF-gefunctionaliseerde DNA-coatings op de ontwikkeling van bloedvaten**

De ontwikkeling en aanwezigheid van bloedvaten wordt gezien als een belangrijk aspect van wondgenezing, en is essentieel voor het ingroeien van weefsel in poreuze tissue engineering constructen. Voorts is ook de functionaliteit van onderhuids geplaatste biosensoren afhankelijk van de ontwikkeling van bloedvaten in de directe nabijheid. Met dit in het achterhoofd beschrijft **hoofdstuk 7** de eerste stappen richting de toepassing van DNA-coatings ter optimalisatie van de bloedvatontwikkeling middels functionalisatie met de bloedvatontwikkeling-stimulerende stof vascular endothelial growth factor (VEGF). Door gebruik te maken van celkweek-modellen werd aangetoond dat functionalisatie van DNA-coatings de groei van bloedvatcellen versnelt. Daarnaast was uit de DNA-coatings vrijgekomen VEGF in staat om de mobiliteit van bloedvatcellen te vergroten. Met behulp van een diermodel, waarbij implantaten onderhuids werden geplaatst, werd aangetoond dat de ontwikkeling van bloedvaten in de directe omgeving van het implantaat werd gestimuleerd door functionalisatie van DNA-coatings met VEGF. Dit experiment laat zien dat functionalisatie van DNA-coatings een effectieve manier is om de weefselreactie te sturen.

II AFSLUITENDE OPMERKINGEN & TOEKOMSTVISIE

De experimenten beschreven in dit proefschrift zijn gerelateerd aan het gebruik van DNA als coatingsmateriaal voor implantaten. Het idee om DNA voor dit doel te gebruiken kwam voort uit de structurele eigenschappen van DNA, waarvan verondersteld werd dat deze een gunstige bijdrage kunnen leveren ten aanzien van verschillende aspecten van de biologische processen die plaatsvinden na het plaatsen van een implantaat. Vanwege de homogeniteit van DNA binnen gwervelde organismen is dit materiaal interessant vanuit immunologisch oogpunt. Daarnaast zou het hoge gehalte aan fosfaat in het DNA gunstig kunnen zijn voor de afzetting van botmineraal op bot-implantaten. Tenslotte werd aangenomen dat de capaciteit van DNA om andere stoffen te binden aangewend zou kunnen worden om middels drug-delivery het gedrag van cellen en weefsels te kunnen beïnvloeden.

Het eerste dat gedaan moest worden om het onderzoek naar DNA-coatings voor implantaten van de grond te kunnen krijgen, was het maken van DNA-coatings. Binnen de beperkte mogelijkheden om coatings met DNA te kunnen maken, hebben we gekozen voor electrostatic self-assembly (ESA). Dit is een goedkope en eenvoudige methode, en heeft als voordeel dat het toepasbaar is op vele materialen zonder beperking ten opzichte van de vorm van het implantaat. Hoewel voor onze experimenten alle DNA-coatings handmatig gemaakt zijn, had dit ook gedaan kunnen worden middels commercieel verkrijgbare, geautomatiseerde systemen. Gezien de eenvoud van deze methode, zou het gebruik van geautomatiseerde systemen eventuele commerciële uitbuiting kunnen doen versnellen.

In het in dit proefschrift beschreven onderzoek is gebruik gemaakt van DNA-coatings bestaande uit 5 dubbellagen (hetzij [PDL/DNA] of [PAH/DNA]) omdat de karakterisering van deze DNA-coatings aantoonde dat dit aantal dubbellagen voldoende was om het oppervlak van een substraat te bedekken. Voor het functionaliseren van DNA-coatings kan echter het aantal dubbellagen eenvoudig verhoogd worden, waardoor er meer biologisch-actieve stof in de DNA-coatings kan worden opgenomen. Een aandachtspunt hierbij blijft de opname-efficiëntie van de stof in de DNA-coatings, welke relatief laag is vanwege de benodigde wasstappen bij het functionaliseren van andere dubbellagen dan de laatste. Daarbij komt ook nog het belang van het gebruik van effectieve doseringen (hoeveelheid en afgifte-patroon) van de ingebrachte biologisch-actieve stof. Hoewel reeds veel energie is gestoken in het vinden van toepassingsafhankelijke standaarden voor effectiviteit van dit soort stoffen, is nog altijd meer onderzoek noodzakelijk om de vereisten op te helderen, zowel vanuit klinisch als financieel oogpunt, ten aanzien van het gebruik van biologisch-actieve stoffen in de implantologie.

Momenteel zijn de eerste stappen gezet om de resultaten van het in dit proefschrift beschreven onderzoek klinisch te toetsen. Aan de hand van de resultaten van het experiment waarin DNA-coatings werden gefunctionaliseerd met VEGF ten behoeve van het stimuleren van de ontwikkeling van bloedvaten rond een implantaat, is onderzoek naar de toepassing van DNA-coatings voor onderhuids geplaatste biosensoren (zoals een glucose-sensor voor diabetici) gepland. Daarnaast is een onderzoek gestart naar het gebruik van vliesjes bestaande uit DNA en chitosan, ter preventie van post-operatieve verklevingen.

Een laatste punt ten aanzien van het gebruik van op DNA gebaseerde coatings en materialen is de lading die de afkorting DNA met zich meedraagt. Hoewel 'moedertje Natuur' ons vele unieke materialen heeft gegeven, zoals eiwitten, suikers, vetten, en ook DNA, roept voornamelijk DNA nog altijd terughoudendheid en angst op bij mensen. Om dit gevoel uit te roeien of te minimaliseren dient de kennis van mensen over DNA en de bijbehorende toepassingen ervan te worden vergroot, waardoor het image van DNA minder abnormaal wordt.

10

DANKWOORD

Bij de start van het onderzoeksproject, dat als basis diende voor dit proefschrift, was mij niet duidelijk hoe groot de betrokkenheid van mensen zou zijn bij de totstandkoming van het uiteindelijke proefschrift. De lijst van mensen, welke hieronder bedankt worden voor hun bijdrage, is al aardig qua omvang, maar waarschijnlijk niet volledig. Ontbreken in onderstaand overzicht wil echter zeker niet zeggen dat de geleverde bijdrage niet gewaardeerd is…
Allereerst wil ik benadrukken dat ik een prima tijd heb gehad op de afdeling Parodontologie & Biomaterialen, zowel inhoudelijk als sociaal. Meteen vanaf het begin was de sfeer prima, en ondanks meerdere veranderingen in het personeelsbestand bleef deze uitstekend. Het type onderzoek dat gedaan wordt, is boeiend en blijft toenemen in belang door vraag van de samenleving, waardoor de link met het praktisch nut duidelijk in zicht blijft.

Prof. dr. JA Jansen – Beste John, ongelooflijk bedankt voor alles wat je me geleerd hebt. Dat dit verder gaat dan zuiver inhoudelijke kennis op het gebied van implantologie moge duidelijk zijn! Bewonderenswaardig is de wijze waarop je overzicht houdt op vrijwel al het relevante op wetenschappelijk gebied, en zeker hoe je dit weet te vertalen naar gebruik in eigen onderzoekslijnen. Wat me echter het meest heeft weten te raken, is de open manier van communiceren, het doelgericht werken, en je snelheid van werken. Dit werd vooral duidelijk tijdens onze eerste (hoofdstuk 1) en laatste publicatie (hoofdstuk 7) in dit project. Door jouw openheid zijn we er uiteindelijk 'samen' achter gekomen hoe we de proof konden openen, en door jouw snelheid van werken (de turbo erop!) hebben we razendsnel het laatste manuscript kunnen indienen. Uit dit alles blijkt dat je gedreven en doelgericht bent, zonder te vergeten met beide benen op de grond te blijven staan. Dit was al een voorbeeld voor me en zal dat ook blijven. Bedankt!!!
Prof. dr. RJM Nolte – Beste Roeland, inspirerend was de wijze waarop je tijdens gezamenlijke bijeenkomsten van de leden van het DNA-project altijd op zoek was naar oplossingen voor problemen bij lopende zaken. Mijn waardering is groot voor je immer optimistische visie en oplossingsgerichte bijdrage aan dit proefschrift. Het meest zal me bijblijven de charme waarmee je sturend optreedt: dat is een buitengewoon bijzondere kwaliteit!
Dr. XF Walboomers – Beste Frank, met plezier denk ik terug aan onze samenwerking. Ik waardeer de mate van vrijheid en vertrouwen, welke je me gaf in je dagelijkse begeleiding. Naast je inhoudelijke kennis ben je een persoon met een fantastische humor. De meest eenvoudige opmerking van jou kan voldoende zijn voor een halve dag plezier voor mij! Ook ons bezoek aan het domein van 'the King' was een hoogtepunt. Ik heb zelden een zo overweldigende busreis (van 2 minuten!) gehad… Merci voor je hulp en focus op *TCB* (Taking Care of Business)!
Dr. NAJM Sommerdijk – Beste Nico, ik ken weinig mensen met een vrijwel onbeperkt ruime visie op onderzoeksgebied, maar jij beschikt hierover! Het echte verrassende aan jou is echter dat je deze breedte weet te combineren met diepte. Dit bleek vooral tijdens de vele meetings en uit je kritische blik bij de totstandkoming van de publicaties. Ongetwijfeld heeft jouw inbreng geleid tot een toename in de kwaliteit van het onderzoek. Merci hiervoor!
Dr. MRJ Vos – Beste Matthijn, in 2002 zijn we samen ingestapt in het onderzoek naar DNA-coatings voor implantaten. Met jouw chemische achtergrond heb je de basis gelegd voor de volledig gelaagde coatings en de mogelijkheid tot functionalisatie van het niet-DNA gedeelte van de coating. Bedankt voor je didactische uiteenzetting van de chemische wereld: het heeft mijn inzicht in deze materie enorm vergroot! Succes met je baan bij het NKI in Amsterdam!
Dr. T Hayakawa, dr. T Fukushima & prof. dr. Y Okahata – Dear Tohru, Tadao, and Yoshio, the three of you have been of great help in 2003, when we were exploring the possibilities to fabricate DNA-based coatings. It was a privilege for me to work with you! Tohru, thank you very much for your kindness during my stay. As DNA as a biomaterial will remain a research topic in the next years, I think we will definitely meet again. Tadao, I have really appreciated your help with preparing DNA-lipid complexes. Evidently, your gift (the year of the monkey) has helped, although it was not 2004 when our first success in DNA-based coatings worked out! Yoshio, thanks for your contribution to our work. It was definitely of added value for our research!
Dr. OC Boerman, dr. TH van Kuppevelt, drs. STM Nillesen – Beste Otto, hartelijk dank voor je snelle bereidheid tot meewerken aan het BMP-artikel: het gemak waarmee deze samenwerking gepaard ging is fantastisch!! Beste Toin en Suzan, hartelijk dank voor jullie bijdrage aan het VEGF-artikel. Dit artikel was het laatste uit dit project, maar ik zou wensen dat het als voorbeeld had kunnen dienen voor de andere publicaties uit dit project! Dank voor jullie bijdrage!

Prof. dr. LH Koole – Beste Leo, ik waardeer je openheid en bereidheid tot meewerken aan onze ideeën enorm. Helaas heeft onze samenwerking niet geleid tot bruikbare resultaten voor in een publicatie voor dit project. Echter, ik verwacht zeker dat deze vruchtbare basis van samenwerking haar vruchten zal gaan afwerpen. Merci voor alles!

Behalve bovengenoemde personen, is er een groot aantal anderen waaraan ik dank verschuldigd ben. In eerste instantie de directe (ex-)collega's van de afdeling Parodontologie & Biomaterialen: Anne, Afsheen, Corinne, Daniel, Dennis, Diederik, Dimitris, Edwin Ooms, Edwin vd Wal, Esther, Fang, Harry, Henriette, Hongbin, Jacky, Joop, Juliet vd Dolder, Juliet Moeljoredjo, Jurgen, Lise, Manal, Martijn, Marijke, Meike, Natasja, Olga, Peter, Quinten, Remco, Sander, Vincent, Walter, Weibo, Wouter, Xuechao en Yonggang. Zonder jullie aanwezigheid was promoveren zeker niet zo leuk (lees: gezellig!!!) geweest. Van deze groep mensen verdient een aantal een speciale vermelding. Allereerst Anja en Joop, fantastische steun heb ik aan jullie gehad, zowel inhoudelijk als relativerend. Kenmerk daarbij was 'recht voor z'n raap', wat ik zeer zeker weet te waarderen – dank hiervoor! Dan Marijke, steun en toeverlaat in bange tijden. Dank voor je gezelligheid en ordentelijkheid – dit heeft me enorm geholpen, al had mijn buro vaker mogen worden opgeruimd… Speciale dank ook aan de mede-leden van de club van vier: Diederik, Sander en Quinten. Het was prettig om met jullie te kunnen genieten van de geneugten des levens in het Nijmeegse. Hopelijk zal de traditie van op z'n tijd lekker eten met mekaar worden voortgezet, zeker nu Q weer op het oude nest terugkomt! En (the award-winning) Sander, chapeau voor jouw inzet voor zowel werk als vriendschap!! Tot slot Corinne, Dennis en Lise: mede dankzij jullie initiatief voor borrels (vooral van de dames, sorry Dennis!) en vermakelijke verhalen (nu doe je wel mee, Dennis!) is de laatste fase van mijn promotie een feest geweest! Laten we proberen ook deze traditie in stand te houden…
Ook indirecte (ex-)collega's zijn belangrijk geweest. De groupies van Orthopedie – Chris, Gerjon, Luc en René – zijn waardige partners gebleken voor het vieren van een feestje, maar ook voor een goed gesprek. Verder was het jaarlijkse treffen met Erik van de Mesjtreechter Universiteit altijd een goede Lunterse afsluiting van het jaar – merci hiervoor! Ook een woord van dank aan de mensen die het Centraal Dieren Lab (CDL) gezicht geven: Debby, Geert, Ilona, Alex en Jeroen. Zonder jullie back-up is uitvoering van dierexperimenten in Nijmegen onmogelijk!
Tijdens mijn promotie-onderzoek heb ik verder verschillende studenten begeleid, welke ik wil bedanken voor hun inzet voor en bijdrage aan mijn onderzoek. Joost, Martijn & Erik, Guido & Iraj en Ellen & Noortje: merci!
Tevens wil ik graag mensen bedanken die dan wel inhoudelijk geen bijdrage hebben geleverd, maar zeker broodnodig waren! De vrienden- en vriendinnengroep uit Kessel en Maasbree (en inmiddels omstreken) – dank voor jullie gezelligheid! Verder de vakantievriendinnen – Yvonne en Judith – tijdens de vakanties in de villa's in Spanje. Heerlijk om daar met jullie te relaxen en genieten van tapas, zon, zee & strand! Tevens bedankt voor jullie bijdrage aan mijn introductie in ski-vakanties!
Tot slot wellicht de belangrijkste personen. Mijn ouders – Harrie en Corrie – wil ik ongelooflijk bedanken voor hun onvoorwaardelijke steun tijdens mijn eerste drie decennia in deze wereld. Jullie weten dat ik dat waardeer, maar ik kan het nooit voldoende benadrukken!! De waarde die jullie voor mij vertegenwoordigen is nergens in uit te drukken. Ik ben ontzettend blij met jullie als ouders en mede-uitoefenaars van onze gezamenlijke hobby. Mijn zus – Saskia – wil ik bedanken voor haar steun: ik heb me altijd afgevraagd (en doe dat nog steeds!) hoe het kan dat elf maanden leeftijdsverschil zo'n meerwaarde aan levenservaring kan opleveren!! En als allerlaatste – zeker onterecht! – Rian. Chapeau voor de manier waarop jij me steunt en er altijd voor me bent. Dit is onbeschrijflijk belangrijk voor me en zorgt voor de perfecte uitvalsbasis: merci en x.

11

RÉSUMÉ

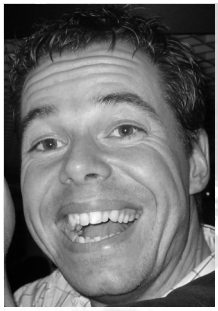

Jeroen van den Beucken – born on March 21st 1975 in Kessel-Eik – followed elementary and high school in Kessel-Eik and attended higher secundary education (atheneum) at the Bouwens van der Boije College in Helden-Panningen. Subsequently, he succesfully graduated from Den Bosch University for Applied Agricultural Sciences (animal husbandry and health) in 1998. During this education period, he was a trainee at KI Zuid-Nederland (artificial insemination facility currently known as CR Delta) and Intervet International BV (Department of Antibiotics; veterinary-pharmaceutical company). His trainee-ship at Intervet International BV resulted in a position as a part-time research associate at the same department. In 1998, he continued education at the Radboud University Nijmegen (medical biology) and graduated in 2002. Within the compass of this education, he was a trainee at the Department of Tumor Immunology (prof. dr. C.G. Figdor) of the Nijmegen Center for Molecular Life Sciences (NCMLS) studying the effect of substrate properties on the expression of adhesion molecules by endothelial cells and the subsequent adhesion of leucocytes. Additionally, he was a trainee at Future Diagnostics BV developing a point-of-care (POC) test for the detection of brain damage.

In that same year, he started working as a PhD-student at the Department of Periodontology & Biomaterials (prof. dr. J.A. Jansen and dr. X.F. Walboomers) of Radboud University Nijmegen Medical Center. The results of the experiments performed as part of the research project entitled 'DNA-lipid films for tailor-made implant surfaces', in collaboration with the Laboratory for Macromolecular & Organic Chemistry of the Eindhoven University of Technology (prof. dr. R.J.M. Nolte and dr. N.A.J.M. Sommerdijk) are described in this thesis. Within the compass of this research, he worked at the Department of Dental Materials (Nihon University School of Dentistry at Matsudo, Japan), where he collaborated with resident researchers dr. T. Hayakawa, dr. T. Fukushima (Fukuoka Dental College, Japan), and prof. dr. Y. Okahata (Tokyo Institute of Technology, Japan). Furthermore, he presented his work at 5 (inter)national conferences, including the 2006 conference of the European Society for Biomaterials in Nantes (France), at which his presentation was awarded with the 'Best Oral Presentation Award'. Currently, he is employed as scientific researcher at the Department of Periodontology & Biomaterials at the Radboud University Nijmegen Medical Center.

12

LIST OF PUBLICATIONS

1. JJJP van den Beucken, XF Walboomers, JA Jansen. Implants and prostheses, *in:* **Biomedical Nanotechnology** (NH Malsch, ed.), CRC Press, Taylor & Francis Group, Boca Raton, US, 2005

2. Fabrication, characterization, and biological assessment of multilayered DNA-coatings for biomaterial purposes
   JJJP van den Beucken, MRJ Vos, PC Thüne, T Hayakawa, T Fukushima, Y Okahata, XF Walboomers, NAJM Sommerdijk, RJM Nolte, JA Jansen
   Biomaterials 27: 691-701 (2006)

3. Cyto- and histocompatibility of multilayered DNA-coatings on titanium
   JJJP van den Beucken, XF Walboomers, MRJ Vos, NAJM Sommerdijk, RJM Nolte, JA Jansen
   J Biomed Mater Res Part A 77(1): 202-211 (2006)

4. Biological responses to multilayered DNA-coatings
   JJJP van den Beucken, XF Walboomers, MRJ Vos, NAJM Sommerdijk, RJM Nolte, JA Jansen
   J Biomed Mater Res Part B: in press (2006)

5. Macrophage behavior on multilayered DNA-coatings *in vitro*
   JJJP van den Beucken, XF Walboomers, MRJ Vos, NAJM Sommerdijk, RJM Nolte, JA Jansen
   J Biomed Mater Res Part A: in press (2006)

6. Multilayered DNA-coatings: *in vitro* bioactivity studies and osteoblast-like cell behavior
   JJJP van den Beucken, XF Walboomers, SCG Leeuwenburgh, MRJ Vos, NAJM Sommerdijk, RJM Nolte, JA Jansen
   Acta Biomaterialia: in press (2006)

7. Functionalization of multilayered DNA-coatings with bone morphogenetic protein 2
   JJJP van den Beucken, XF Walboomers, OC Boerman, MRJ Vos, NAJM Sommerdijk, T Hayakawa, T Fukushima, Y Okahata, RJM Nolte, JA Jansen
   J Control Release 113(1): 63-72 (2006)

8. *In vitro* and *in vivo* effects of DNA-based coatings functionalized with vascular endothelial growth factor (VEGF)
   JJJP van den Beucken, XF Walboomers, STM Nillesen, MRJ Vos, NAJM Sommerdijk, TH van Kuppevelt, RJM Nolte, JA Jansen
   Tissue Eng: in press (2006)

9. Nanobiomaterial applications in orthopaedics
   EM Christenson, KS Anseth, JJJP van den Beucken, CK Chan, B Ercan, JA Jansen, CT Laurencin, W-J Li, R Murugan, LS Nair, S Ramakrishna, RS Tuan, TJ Webster, AG Mikos
   J Ortho Res: in press (2006)

10. DNA-based coatings for implants (patent application WO2006088368)
    JA Jansen, RJM Nolte, NAJM Sommerdijk, XF Walboomers, MRJ Vos, JJJP van den Beucken